



Development of a mini-tablet-in-capsule dosage form for macromolecular drug delivery

L Bodenstein

 **orcid.org/0000-0003-1147-0764**

Dissertation accepted in fulfilment of the requirements for the degree Masters of Science in Pharmaceutics at the North-West University

Supervisor: Prof JH Steenekamp

Co-supervisor: Prof JH Hamman

Graduation: May 2020

Student number: 22784136

ACKNOWLEDGEMENTS

Firstly, to God all glory. Without Him, I would not have been able to pull this off. He empowered me and blessed me with the mental capacity to climb this mountain and the strength not to give up.

To Professor Jan Steenekamp my study leader and mentor, thank you so much for taking me on for this post-graduate study. Thank you for taking a chance on me even though I took much more time to complete my bachelor's degree. Thank you for always making time to help and guide me through the struggles and for teaching me to always sit back and see the bigger picture. Without you, this would never have been possible.

To Professor Sias Hamman, thank you for being an important part in my study. Thank you for providing me with your expertise in the field of pharmaceuticals and for taking the time to guide me and to help me make a success of this study.

My parents James and Elmarié Bodenstein, mom and dad, thank you for your support through my study career and thank you for not giving up on me. During my bachelor's degree, I fell many times but you both were always by my side to pick me up and motivate me to keep on pushing through. This is for you. We made it.

My brother James Bodenstein, thank you for always supporting me and for the motivational calls. You always believed in me.

Esté du Plessis. Thank you for your love, support and motivation. Thank you for always making sure that I had something to eat when the days turned into nights inside the laboratory. Thank you for always listening to me although it never made any sense to you.

My friends Niël de Beer, Safiyyah Malek and Jannes van der Merwe, thank you for the role each of you played in my post-grad and in my life. Niël, for always showing care, bringing snack packs when I needed it most and for the late night venting sessions I thank you. Safs, for always lending me your ear when I needed to talk and the late night venting sessions I thank you. Jannes, for sharing your experience and knowledge with me and your willingness to always lend me a helping hand I thank you.

My lab partner and colleagues Vilise Lemmer, Carli and Tinka Berry, thank you for your support through the rough times as well as the great times. It was especially an honour working with the three of you. Thank you for always listening to me and motivating me. The coffee was always worthwhile.

Lastly, to Kampus pharmacy for providing me with a place to work during my academic internship, thank you all very much.

ABSTRACT

Oral delivery of protein and peptide drugs faces immense challenges, partially due to the inherent unfavourable characteristics of the molecules and partially due to the unfavourable gastrointestinal environment. These barriers to oral protein drug delivery include the large molecular size, enzymatic degradation and hydrophilic nature of protein drugs, which lead to their low oral bioavailability (1 – 2%). Protein drugs (i.e. insulin) are therefore primarily administered via the parenteral route (i.e. subcutaneous injections), which lead to a decrease in patient adherence. Advancements in biotechnology have made it possible for improving oral delivery of protein and peptide drugs. One such advancement is the inclusion of safe and effective absorption enhancers in the formulation of oral dosage forms. Previous studies have shown that the inclusion of *A. vera* gel and whole leaf materials as well as *N*-trimethyl chitosan chloride (TMC) can increase the intestinal membrane permeability of protein drugs after application to *in vitro* and *ex vivo* models.

The purpose of this study was to develop and evaluate a mini-tablet-in-capsule dosage form by means of developing different sized bead formulations (i.e. 0.5 mm, 0.75 mm, 1.0 mm and 1.5 mm in diameter) containing the model compound fluorescein isothiocyanate (FITC)-dextran 4000 (FD4) and compacting these beads into mini-tablets containing different absorption enhancers (*A. vera* gel, *A. vera* whole leaf extract and TMC) in the tablet matrix, which were then filled into hard gelatine capsules. The beads were evaluated with regards to morphology and internal structure, size and FD4 content. Mini-tablets produced were evaluated (BP specifications) with regards to disintegration, friability and mass variation. The delivery of FD4 from the mini-tablet dosage forms across excised pig intestinal tissues was evaluated using a modified Sweetana-Grass diffusion apparatus.

All the mini-tablets complied with the specifications for physical evaluation of tablets namely mass variation, hardness and friability. The results of the *ex vivo* transport studies showed that all three absorption enhancers incorporated into the mini-tablets caused increased FD4 transport across the excised pig intestinal tissues. The effect of the size of the beads used to produce the mini-tablets on FD4 transport was clearly visible; and in general the smaller beads (0.5 mm and 0.75 mm in diameter) showed faster initial, and the highest cumulative FD4 transport in comparison to the larger bead sizes (1.0 mm and 1.5 mm in diameter). Mini-tablets containing *A. vera* gel exhibited the highest increase in transport, followed by mini-tablets containing *A. vera* whole leaf extracts and TMC, respectively.

This study has shown that absorption enhancers incorporated as part of the matrix in mini-tablet-in-capsule dosage forms can significantly ($p < 0.05$) increase the transport of a macromolecular model compound across excised pig intestinal tissues in an *ex vivo* model.

Key words: FITC-Dextran, *Aloe vera*, *N*-trimethyl chitosan chloride, beads, mini-tablets

CONTENTS

1.1	Background and justification	1
1.1.1	Protein and peptide drugs and their delivery limitations	1
1.1.2	Drug absorption enhancement.....	2
1.1.3	Preparation of beads (pellets) as delivery system	3
1.1.4	Possible models to be used for permeation studies	4
1.2	Research problem	4
1.3	Aims and objectives	5
1.3.1	General aim.....	5
1.3.2	Objectives of the study	5
1.4	Ethics regarding research.....	5
1.5	Layout of the dissertation	6
2.1	Introduction	7
2.2	Drug absorption mechanisms from the gastrointestinal tract	8
2.2.1	Passive transcellular diffusion.....	9
2.3	Barriers to delivery	12
2.3.1	The chemical barriers	13
2.3.2	The physical barriers	14
2.4	Approaches to improve delivery	16
2.4.1	Chemical modification.....	16
2.4.2	Formulation approaches	18
2.4.3	Particulate delivery systems	23

2.5	Summary	29
3.1	Introduction	30
3.2	Materials.....	31
3.2.1	Materials used for analytical method validation.....	31
3.2.2	Materials used for bead formulation.....	31
3.2.3	Materials used for mini tablet production.....	31
3.2.4	Materials used for particle size analysis.....	31
3.2.5	Materials used for proton nuclear magnetic resonance.....	31
3.2.6	Materials used for dissolution studies	32
3.2.7	Materials used for <i>ex vivo</i> transport studies	32
3.3	Validation of analytical methods	32
3.3.1	Linearity.....	33
3.3.2	Limit of detection	34
3.3.3	Limit of quantification	35
3.3.4	Precision.....	35
3.3.5	Specificity	36
3.3.6	Accuracy.....	36
3.4	Bead formulation composition	37
3.4.1	Bead preparation method	37
3.5	Evaluation of beads.....	38
3.5.1	Assay	39
3.5.2	Flow properties of the beads.....	39
3.5.3	Particle size analysis	41

3.5.4	Bead structure and morphology	41
3.6	Chemical characterisation of <i>N</i>-trimethyl chitosan chloride with proton nuclear magnetic resonance	42
3.7	Formulation and preparation of mini-tablets	42
3.7.1	Mini-tablet production	42
3.7.2	Evaluation of the mini-tablets.....	44
3.8	Dissolution studies.....	45
3.9	<i>Ex-vivo</i> transport studies.....	46
3.9.1	Preparation of buffer	46
3.9.2	Procurement and preparation of pig intestinal tissue	46
3.9.3	Determining membrane integrity using Lucifer yellow	48
3.9.4	Transport studies across the mounted pig intestinal tissues	48
3.9.5	Statistical analysis	49
4.1	Introduction	50
4.2	Fluorescence spectrometry method validation.....	51
4.2.1	Linearity.....	51
4.2.2	Precision.....	54
4.2.3	Limit of detection and limit of quantification.....	57
4.2.4	Specificity	59
4.2.5	Accuracy.....	59
4.2.6	Validation result summary	61
4.3	Bead evaluation	62
4.3.1	Assay	62

4.3.2	Flow properties of the beads.....	62
4.3.3	Particle size analysis	65
4.3.4	Bead morphology and internal structure	70
4.4	Chemical characterization of <i>N</i>-trimethyl chitosan chloride with proton nuclear magnetic resonance	71
4.5	Evaluation of mini-tablets	72
4.5.1	Mass variation	72
4.5.2	Friability	73
4.5.3	Disintegration	73
4.6	Dissolution studies.....	74
4.6.1	Dissolution studies conducted on the mini-tablet-in-capsule formulations containing 0.5 mm bead mini-tablets	76
4.6.2	Dissolution studies conducted on the mini-tablet-in-capsule formulations containing 0.75 mm bead mini-tablets	78
4.6.3	Dissolution studies conducted on the mini-tablet-in-capsule formulations containing 1.0 mm bead mini-tablets	79
4.6.4	Dissolution studies conducted on the mini-tablet-in-capsule formulations containing 1.5 mm bead mini-tablets	81
4.6.5	Effect of bead size on dissolution.....	82
4.6.6	Dissolution study conclusion.....	83
4.7	<i>Ex vivo</i> transport studies	83
4.7.1	Determination of membrane integrity by means of Lucifer Yellow	83
4.7.2	Comparison of FITC-dextran 4000 delivery (FD4) across excised pig intestinal tissues from the mini-tablet formulations	84
4.8	Conclusion.....	90

5.1 Final conclusions 92

5.2 Future recommendations..... 94

REFERENCES..... 95

ADDENDUM A..... 104

ADDENDUM B..... 118

ADDENDUM C..... 120

ADDENDUM D..... 122

ADDENDUM E 123

ADDENDUM F 125

ADDENDUM G 150

LIST OF TABLES

Table 2.1:	A list of different chemical substances known to increase the absorption of hydrophilic drugs (Hamman <i>et al.</i> , 2005; Beneke <i>et al.</i> , 2012, Tegos <i>et al.</i> , 2011).....	19
Table 2.2:	Types of extruders and their different features (Sinha <i>et al.</i> , 2009)	27
Table 3.1:	The concentrations of both the FITC-dextran 4000 and LY solutions used to construct a standard curve for evaluation of linearity	34
Table 3.2:	Concentrations of the respective samples used to determine FITC-dextran 4000 and Lucifer Yellow recovery as a measurement of accuracy	36
Table 3.3:	Composition of all the bead formulations.....	37
Table 3.4:	Rotation speeds of the extruder for the respective aperture sizes during extrudate preparation and for the spheroniser during spheronisation.	38
Table 3.5:	Composition of the different bead mixtures for mini-tablet production	43
Table 4.1:	Mean fluorescent values of FITC-dextran 4000 (FD4) over a predetermined concentration range.....	52
Table 4.2:	Mean fluorescent values of Lucifer Yellow (LY) over a predetermined concentration range	53
Table 4.3:	Fluorescence values of FITC-dextran 4000 (FD4) obtained during the intra-day precision measurements, as well as standard deviation and percentage relative standard deviation (%RSD) values.....	54
Table 4.4:	Fluorescence values of Lucifer Yellow (LY) obtained during the intra-day precision measurements, as well as standard deviation and percentage relative standard deviation (%RSD) values	55
Table 4.5:	Fluorescence values of FITC-dextran 4000 (FD4) obtained during the inter-day precision measurements, as well as standard deviation and percentage relative standard deviation (%RSD) values.....	56

Table 4.6:	Fluorescence values of Lucifer Yellow (LY) obtained during the inter-day precision measurements, as well as standard deviation and percentage relative standard deviation (%RSD) values	57
Table 4.7:	Background noise fluorescence values for FITC-dextran 4000 (FD4)	58
Table 4.8:	Background noise fluorescence values for Lucifer Yellow (LY)	58
Table 4.9:	Percentage recovery as an indication of the accuracy of the FITC-dextran 4000 (FD4) fluorometric analytical method	60
Table 4.10:	Percentage recovery as an indication of accuracy of the Lucifer Yellow (LY) fluorometric analytical method	61
Table 4.11:	Average percentage of FITC-dextran 4000 (FD4) in each respective bead formulation	62
Table 4.12:	Bulk and tapped density values of the bead formulations	63
Table 4.13:	Carr's index and Hausner ratio of the bead formulations	64
Table 4.14:	Flow rates of the bead formulations	64
Table 4.15:	The particle size analysis results of the different bead formulations	65
Table 4.16:	Average mass and standard deviation of the different mini-tablet formulations containing FITC-dextran 4000 (FD4) and different absorption enhancers.....	72
Table 4.17:	Percentage friability of the mini-tablet formulations	73
Table 4.18:	Average disintegration time of the various mini-tablet-in-capsule formulations	74
Table 4.19:	Area under curve (AUC) and mean dissolution time (MDT) of all the mini-tablet-in-capsule systems	75
Table 4.20:	Apparent permeability (P_{app}) values for the different multiple-unit dosage forms (MUDFs)	90

LIST OF FIGURES

Figure 2.1:	A schematic illustration depicting the possible mechanisms of transport across the gastrointestinal tract epithelium: A, transcellular passive diffusion; B, carrier mediated transcellular diffusion; C, paracellular diffusion; D, endocytosis; E, diffusion and incorporation into lipid particles; F, paracellular transport with tight junction modulation; G, polarized efflux system (Zhu <i>et al.</i> , 2017).....	9
Figure 2.2:	Schematic illustration of carrier-mediated transport across the lipid double-layer (Zhu <i>et al.</i> , 2017).	10
Figure 2.3:	The presentation of different PEGylation strategies (Pfister & Morbidelli 2014).....	17
Figure 2.4:	Different factors affecting mucoadhesion (adapted from Mansuri <i>et al.</i> , 2016).....	22
Figure 2.5:	The different steps involved during bead preparation by means of extrusion-spheronisation (Sirisha <i>et al.</i> , 2013).....	28
Figure 3.1:	Photographs illustrating A) the removal of the serosa from excised jejunum pulled over a glass tube, B) cutting of the jejunum along the mesenteric border, C) removal and placement of the tissue onto wetted filter paper, D) cutting of flattened tissue into equally sized pieces, E) mounting of the tissue pieces on the half-cells with the spikes visible and filter paper on the basolateral side facing up, F) the assembled half-cells with the sir-clips holding the half-cells together and G) the assembled half-cells placed in the diffusion apparatus with Krebs Ringer Bicarbonate buffer in the chambers connected to the O ₂ /CO ₂ supply.	47
Figure 4.1:	Standard curve and regression data for FITC-dextran 4000.....	51
Figure 4.2:	Standard curve and regression data for Lucifer Yellow	53
Figure 4.3:	Calibration curve for FITC-dextran 4000 (FD4) in the presence of Ac-Di-Sol [®] , Kollidon [®] VA 64, Pharmacel [®] 101, magnesium stearate, <i>Aloe vera</i> whole leaf extract, <i>Aloe vera</i> gel, <i>N</i> -trimethyl chitosan chloride and Avicel [®] PH 200.....	59

Figure 4.4:	Typical percentage frequency distribution plot of the particle size distribution of the bead (0.5 mm) formulation containing FITC-dextran 4000.....	66
Figure 4.5:	Typical percentage frequency distribution plot of the particle size distribution of the bead (0.75 mm) formulation containing FITC-dextran 4000.....	67
Figure 4.6:	Typical percentage frequency distribution plot of the particle size distribution of the bead (1.0 mm) formulation containing FITC-dextran 4000.....	68
Figure 4.7:	Typical percentage frequency distribution plot of the particle size distribution of the bead (1.5 mm) formulation containing FITC-dextran 4000.....	69
Figure 4.8:	Micrographs illustrating the morphology and internal structures of the various bead formulations produced by means of extrusion-spheronisation; A) 0.5 mm bead morphology, B) 0.5 mm bead internal structure, C) 0.75 mm morphology, D) 0.75 mm internal structure, E) 1.0 mm bead morphology, F) 1.0 mm bead internal structure, G) 1.5 mm bead morphology and H) 1.5 mm bead internal structure	70
Figure 4.9:	¹ H-NMR spectrum of <i>N</i> -trimethyl chitosan chloride.....	71
Figure 4.10:	Percentage dissolution of FITC-dextran 4000 from the mini-tablet-in-capsule formulations containing 0.5 mm bead mini-tablets with no absorption enhancer (Control), <i>Aloe vera</i> gel (AVG), <i>Aloe vera</i> whole leaf extract (AVW) and <i>N</i> -trimethyl chitosan chloride (TMC).....	76
Figure 4.11:	Percentage dissolution of FITC-dextran 4000 from the multiple unit dosage forms containing 0.75 mm bead mini-tablets with no absorption enhancer (Control), <i>Aloe vera</i> gel (AVG), <i>Aloe vera</i> whole leaf extract (AVW) and <i>N</i> -trimethyl chitosan chloride (TMC).....	78
Figure 4.12:	Percentage dissolution of FITC-dextran 4000 from the multiple unit dosage forms containing 1.0 mm bead mini-tablets with no absorption enhancer (Control), <i>Aloe vera</i> gel (AVG), <i>Aloe vera</i> whole leaf extract (AVW) and <i>N</i> -trimethyl chitosan chloride (TMC).....	79

Figure 4.13:	Percentage dissolution of FITC-dextran 4000 from the multiple unit dosage forms containing 1.5 mm bead mini-tablets with no absorption enhancer (Control), <i>Aloe vera</i> gel (AVG), <i>Aloe vera</i> whole leaf extract (AVW) and <i>N</i> -trimethyl chitosan chloride (TMC).....	81
Figure 4.14:	Average percentage Lucifer Yellow transport across excised pig intestinal tissues mounted in a Sweetana-Grass diffusion chamber apparatus.....	83
Figure 4.15:	Cumulative percentage FITC-dextran 4000 transport from the mini-tablets without absorption enhancers (control) prepared from different sized beads.....	84
Figure 4.16:	Cumulative percentage FITC-dextran 4000 transport from the mini-tablets prepared from the different sized beads containing <i>A. vera</i> gel.....	85
Figure 4.17:	Cumulative percentage FITC-dextran 4000 transport from the mini-tablets prepared from the different sized beads containing <i>A. vera</i> whole leaf extract	87
Figure 4.18:	Cumulative percentage FITC-dextran 4000 transport from the mini-tablets prepared from the different sized beads containing <i>N</i> -trimethyl chitosan chloride	88
Figure 4.19:	Apparent permeability (P_{app}) values for the different multiple-unit dosage forms (MUDFs)	89

CHAPTER 1

INTRODUCTION

1.1 Background and justification

1.1.1 Protein and peptide drugs and their delivery limitations

The history of peptide and protein drug usage dates back to the 1920's when the treatment of diabetes mellitus (DM) with bovine and porcine insulin commenced (Renukuntla *et al.*, 2013). Insulin was soon identified as an essential drug for the control of type 1 DM (Banting *et al.*, 1921). Compared to conventional drugs, protein and peptide therapeutics have the advantage of high activity, high specificity, low toxicity and minimal drug-drug interactions (Renukuntla *et al.*, 2013).

The oral route of drug administration remains the preferred way for patients to take drugs, which is associated with improved compliance and ease of administration (Lebitsa *et al.*, 2012). There are, however, limitations to the administration of proteins and peptides via the oral route, which can be attributed to poor absorption from the gastrointestinal tract as a result of their unfavourable physicochemical properties (Crowley & Martini, 2004). These unfavourable properties include the hydrophilic nature and large molecular weight of peptide drugs (Beneke *et al.*, 2012). Oral bioavailability of protein and peptide drugs rarely exceeds 1 — 2% (Renukuntla *et al.*, 2013). One of the greatest challenges in modern pharmaceuticals remains the effective delivery of peptide and protein drugs (e.g. insulin) after oral administration (Niu *et al.*, 2014). Poor bioavailability after oral administration of peptide and protein therapeutics is also aggravated by extensive hydrolysis by the proteolytic enzymes in the gastrointestinal (GI) tract (Hamman *et al.*, 2005). Due to poor oral bioavailability, the administration of insulin is currently limited to the parenteral route of administration (e.g. subcutaneous injections) (Jalali *et al.*, 2014).

Possible strategies or approaches that may be employed to improve the poor absorption and bioavailability of orally administered peptide and protein therapeutics include the co-administration of absorption enhancing agents, chemical modification of the molecules or pro-drug formation (Beneke *et al.*, 2012; Salama *et al.*, 2006).

The GI epithelium can be seen as a physical barrier that separates the interior of the body from the exterior and maintains distinct compartments within the body. Furthermore, it acts as a barrier to passive transcellular diffusion of macromolecular drugs (Beneke *et al.*, 2012; Renukuntla *et al.*, 2013). Protein and peptide drugs are usually not recognised by active transporter systems (excluding drugs that are recognised by the di-/tri-peptide transporter system in the GI tract) (Renukuntla *et al.*, 2013). With regards to paracellular transport, the transport of protein and peptide drugs via intercellular spaces is restricted by tight junctions (Salama *et al.*, 2006). On the other hand, tight junctions are dynamic structures, which can be regulated by several substances that can lead to increased paracellular permeability (Hamman *et al.*, 2005). Different proteolytic enzymes, namely pepsin, trypsin and chymotrypsin, throughout the GI tract represent a chemical barrier that degrades peptide and protein drugs (Choonara *et al.*, 2013; Dane & Hänninen, 2015). This degradation can occur in several places, such as in the lumen, at the brush border or intracellularly in the cytosol of the enterocytes (Banga, 2006).

To overcome these barriers, different strategies can be employed such as the modification of the physicochemical properties of drug molecules, the addition of novel functionalism (improving cell permeability or receptor recognition), addition of absorption enhancers or bio-adhesive polymers; or development of carrier systems (Mahajan *et al.*, 2014).

1.1.2 Drug absorption enhancement

Absorption enhancers are substances that increase the absorption of peptide and protein drugs by reversibly altering or temporarily disrupting the intestinal barrier with minimum tissue damage, thus allowing enhanced drug penetration into the circulatory system (Aungst, 2011). There are different mechanisms by which this can be achieved, namely increasing membrane fluidity; opening tight junctions; temporarily disrupting the structural integrity of the intestinal barrier and decreasing mucus viscosity (Renukuntla *et al.*, 2013). Absorption enhancers are frequently investigated as functional excipients in novel dosage forms to increase the absorption of hydrophilic macromolecules, including insulin (Park *et al.*, 2010). Unfortunately, the most effective absorption enhancers often cause damage and/or irritate the intestinal mucosal membrane. Consequently, there is an increased need for more effective and less toxic drug absorption enhancers (Salamat-Miller & Johnston, 2005).

Aloe vera gel, *Aloe vera* whole leaf extract and TMC are examples of absorption enhancing agents. *A. vera* gel has previously shown the ability to increase the bioavailability of both vitamin C and E in humans (Vinson *et al.*, 2005). *In vitro* studies on *A. vera* gel as well as whole leaf extract have shown a significant reduction in the transepithelial electrical resistance (TEER) of Caco-2 cell monolayers, thus showing the ability to open tight junctions (Chen *et al.*, 2009; Haasbroek *et al.*, 2019). *Aloe vera* gel and whole leaf materials on their own, and in combination with other absorption enhancers, exhibited the ability to increase intestinal drug transport *in vitro* and bioavailability *in vivo* (Lebitsa *et al.*, 2012; Du Toit *et al.*, 2016; Wallis *et al.*, 2016).

The development and synthesis of *N*-trimethyl chitosan chloride (TMC), was inspired by the unfavourable solubility characteristics of chitosan. Chitosan is practically insoluble in neutral and alkaline environments such as those found in the small intestine (Mourya & Inamdar, 2009). TMC, a derivative of chitosan, is soluble in acidic, alkaline and neutral media (pH 1-9) (Mourya & Inamdar, 2009). Similar to chitosan, TMC also opens tight junctions between intestinal epithelial cells without damaging cell membranes as depicted by a reduction in TEER as well as an increase in the transport of hydrophilic and macromolecular drugs (Thanou *et al.*, 2000; Mourya & Inamdar, 2009).

1.1.3 Preparation of beads (pellets) as delivery system

Pelletisation is an agglomeration process that converts fine powders and/or granules of bulk drugs and excipients into small, spherical or semi-spherical free flowing pellets, also referred to as beads. In general, pharmaceutical bead sizes vary from 0.5 mm to 1.5 mm, although other sizes can be produced depending on the production method. Beads are receiving more attention due to their ability to extend, or control drug release in different dosage forms (Vikash *et al.*, 2011; Hamman *et al.*, 2017).

Beads can be used to produce mini-tablets or to fill hard capsules, though there is a significant difference in cost (Vikash *et al.*, 2011). There are different ways in which beads can be prepared, for example drug layering, freeze pelletisation, cryopelletisation, extrusion-spheronisation, compression, spray drying and spray congealing, balling and fluid bed pelletising technologies (Hamman *et al.*, 2017). Extrusion-spheronisation is, however, a very popular technique due to ease and mild processing conditions. There are different reasons for producing beads in the pharmaceutical industry, which include the reduction of dust formation (in comparison with conventional tablets), the prevention of segregation of co-agglomerated components, the increase of bulk density and the decrease of bulk volume and the control of drug release in oral dosage forms (Hirjau *et al.*, 2011).

1.1.4 Possible models to be used for permeation studies

The experimental models available for membrane permeation studies and efficacy of absorption enhancers can be divided into the following classes:

- *In vivo* models (e.g. an experiment in live animals such as rats);
- *In vitro* models (e.g. cell culture monolayers on a membrane such as the Caco-2 cell line);
- *Ex vivo* models (e.g. on excised animal tissue such as pig intestines);
- *In silico* models (e.g. software ran simulations on computers).

Ex vivo drug permeation experiments will be conducted in this study on excised pig intestines. The pigs are slaughtered at the abattoir for food purposes thus eliminating unnecessary sacrifice of animals. Excised pig intestinal tissues can be mounted in a diffusion apparatus between two half-cells, and then connected to a heating block whilst gas is bubbled through the liquid medium. Pig intestines show anatomical and physiological similarities to that of human intestinal tissue and are therefore an acceptable surrogate for human intestinal tissues (Patterson *et al.*, 2008).

1.2 Research problem

Peptide and protein drugs are in general very potent with low toxicity (Renukuntla *et al.*, 2013). The problem, however, is that peptide and protein drugs (e.g. insulin) exhibit significantly low bioavailability when administered by means of the oral route of drug administration. Due to parenteral administration (e.g. sub-cutaneous injections), patients are less likely to comply with the treatment regime mainly due to a fear of needles, pain and discomfort.

The most convenient route of administration for drugs, especially for chronic drug treatment regimes, remains the oral route of administration. If the barriers of poor permeation across the gastrointestinal epithelial cells can be overcome by dosage forms containing absorption enhancers (e.g. *Aloe vera* gel, *Aloe vera* whole leaf extract and TMC), orally administered peptides will achieve improved therapeutic outcomes. This will also contribute to dosage forms containing lower doses that can be prepared at lower production costs.

1.3 Aims and objectives

1.3.1 General aim

The aim of this study is to develop and evaluate a mini-tablet-in-capsule drug delivery system intended for the effective peroral delivery of macromolecular drugs by means of incorporating drug absorption enhancers as functional excipients. The aim is to prepare the mini-tablets from beads with different sizes in order to obtain mini-matrix type multiple-unit pellet systems (MUPS).

1.3.2 Objectives of the study

- To validate a fluorometric analysis method for fluorescein isothiocyanate (FITC)-Dextran 4000 (FD4) in terms of linearity, precision, accuracy and selectivity.
- To prepare beads by using different extrusion sieve aperture sizes (i.e. 0.5 mm, 0.75 mm, 1.0 mm and 1.5 mm in diameter) by means of extrusion-spheronisation containing FD4 as model compound.
- To evaluate the physico-chemical properties of the prepared beads, including assay for active ingredient content, particle size, size distribution and morphology.
- To produce bead containing mini-tablets (5 mm in diameter) from the respective bead formulations (i.e. beads with different sizes) containing each of the selected drug absorption enhancers (i.e. *Aloe vera* gel, *Aloe vera* whole leaf extract and TMC) together with FD4 as model compound.
- To evaluate each of the mini-tablet formulations with respect to disintegration, friability, content assay, dissolution and uniformity of mass.
- To conduct *ex vivo* FD4 delivery studies for each mini-tablet formulation across excised pig intestinal tissues in a modified Sweetana-Grass diffusion chamber apparatus.

1.4 Ethics regarding research

Ethics approval for experimental work on excised pig intestinal tissue was approved by the AnimCare Ethics Committee (approval number: NWU00579-19-A5) to utilise the excised tissues from slaughtered pigs in permeation experiments (i.e. category 0, low risk study).

Biological waste was disposed in accordance with the NWU standard operating procedure (SOP) for pig intestinal waste disposal (Pharmacn_SOP001_v02_Biological waste management) which is approved by the Ethics committee (NWU-00369-16-A1).

1.5 Layout of the dissertation

A short introduction, the aims and objectives and the motivation as to why this study was undertaken is provided in chapter 1. Chapter 2 contains the background and literature study relevant to this study. The scientific methods that were followed in this study are described in chapter 3. Chapter 4 contains the results and the discussion thereof. A final conclusion of the study and future recommendations are contained in chapter 5.

CHAPTER 2

LITERATURE REVIEW ON PROTEIN AND PEPTIDE DRUG DELIVERY

2.1 Introduction

Protein and peptide drugs are used in the treatment of a wide variety of human diseases (e.g. treatment of type 1 diabetes mellitus with insulin), although the more successful route of delivery is by means of parenteral injections (Shaji & Patole, 2008). Due to the invasive nature of injections as a means to administer the majority of peptide drugs, there is a substantial drop in patient compliance and thus often less than optimal therapeutic outcomes (Buckley *et al.*, 2016). Advances in biotechnology have created an increased need for the successful oral delivery of protein and peptide drugs due to an increase in development of effective therapeutic compounds (Shaji & Patole, 2008). Compared to conventional drugs, peptide and protein therapeutics have the advantage of high activity and high specificity, while having low toxicity and minimal drug-drug interactions (Morishita & Peppas, 2006). Oral delivery of peptide and protein drugs, however, remains a challenge due to their large molecular structures and hydrophilicity, contributing to their low bioavailability of 1% or less (Renukuntla *et al.*, 2013; Shaji & Patole, 2008).

Approaches to improve the oral bioavailability of peptide and protein therapeutics have already received considerable interest. These approaches include chemical modification, structural modification and formulation strategies (Hamman *et al.*, 2005). A promising way to improve the absorption of peptide and protein drugs from the gastro-intestinal tract is to include a permeation enhancer or absorption enhancing agent in a dosage form. There are different types of absorption enhancers, which can be divided in synthetic (e.g. *N*-trimethyl chitosan chloride) and natural (e.g. *Aloe vera* gel and whole leaf materials as natural examples) compounds. Absorption enhancers are substances that increase the absorption of peptide and protein drugs by reversibly altering or temporarily disrupting the intestinal barrier with minimum tissue damage, thus allowing improved drug penetration into the circulatory system (Aungst, 2011). There are different mechanisms by which this can be achieved, namely increasing membrane fluidity; opening of tight junctions; temporarily disrupting the structural integrity of the intestinal barrier, and decreasing mucus viscosity (Renukuntla *et al.*, 2013).

Absorption enhancing agents are incorporated as functional excipients into the dosage form, such as matrix systems in multiple-unit dosage forms (MUDFs). MUDFs consist of different components, each containing a portion of the dose such as beads (also referred to as pellets) or mini-tablets that are combined into a single delivery system, such as a tablet or hard gelatine capsule (Hamman *et al.*, 2017). Research on the development and evaluation of MUDFs, dates back to as early as the 1950's (Vikash *et al.*, 2011). Mini-tablets are produced either by wet granulation or direct compression (of powders or prepared beads mixed together with excipients). Mini-tablets can be filled into hard gelatine capsules, as alternative to pellets, or compressed into larger tablets to serve as sub-units in MUDFs (Gaber *et al.*, 2015). MUDFs were designed to control the release of drugs and have many advantages over single-unit dosage forms (Vikash *et al.*, 2011; Hamman *et al.*, 2017).

Advantages of MUDFs include less inter- and intra-subject variability; less risk of dose dumping; more predictable drug release; offers a high drug load and a high degree of drug dispersion in the GIT. Different types of mini-tablets can be characterised based on the target area for drug delivery, method of manufacturing and patient needs. Different types of mini-tablets include paediatric, gastro-retentive, bio-adhesive, pH-responsive and biphasic type tablets (Ranjith & Mahalaxmi, 2015).

Specialised mini-tablet formulations such as biphasic mini-tablets are employed in mini-tablet-in-capsule systems in order to achieve the fast release of certain components (i.e. the first phase) and the slow release of other components (i.e. the second phase). For example, the fast release of functional excipients in the first phase and then the slow release of the active ingredient in the second phase (De Bruyn *et al.*, 2018). In the case where components (such as the drug) in the mini-tablets are sensitive to degradation due to pH differences between the stomach and the small intestine, it can be enteric coated or encapsulated to protect the mini-tablets against the initial exposure of the acidic environment of the stomach (Ranjith & Mahalaxmi, 2015).

2.2 Drug absorption mechanisms from the gastrointestinal tract

Absorption can be defined as the process of transferring substances from the GI tract through its wall into the blood circulation draining the GI tract. There are different mechanisms of transport that vary in absorption rate depending on the location in the GI tract, e.g. the degree of passive diffusion decreases further down the GI tract (Vertzoni *et al.*, 2019). Drug absorption depends on physicochemical factors, which include drug (i.e. solubility and lipophilicity) and biological factors (i.e. membrane permeability and stomach emptying rate).

The two main pathways of drug transport across the GI epithelium are transcellular (i.e., across cells) and paracellular (i.e., between cells) (Zhu *et al.*, 2017). Figure 2.1 illustrates the different absorption pathways across the cell membrane.

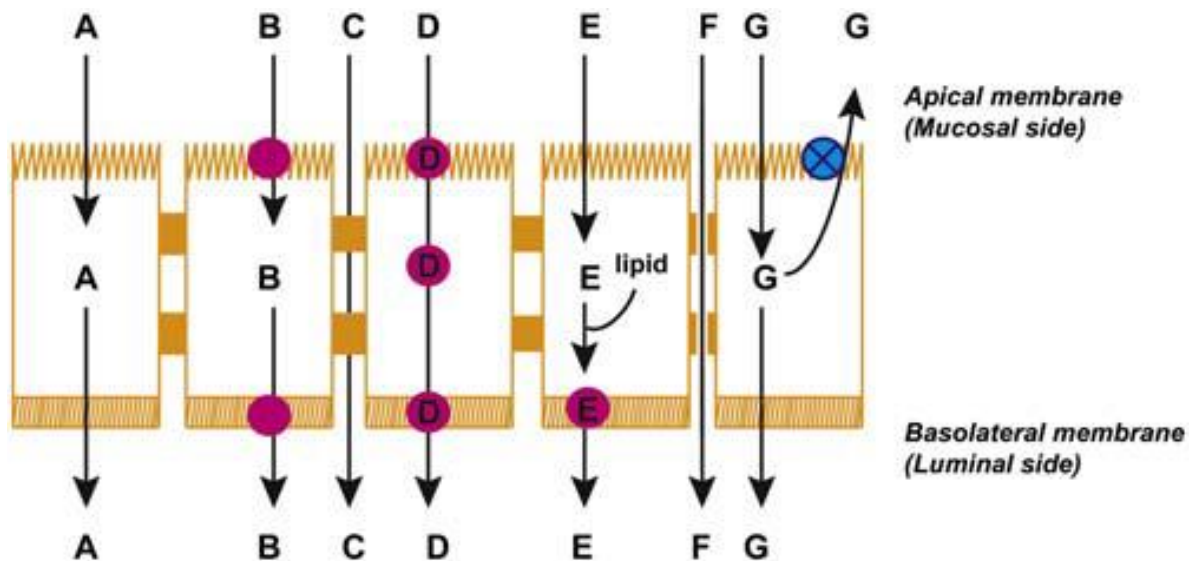


Figure 2.1: A schematic illustration depicting the possible mechanisms of transport across the gastrointestinal tract epithelium: A, transcellular passive diffusion; B, carrier mediated transcellular diffusion; C, paracellular diffusion; D, endocytosis; E, diffusion and incorporation into lipid particles; F, paracellular transport with tight junction modulation; G, polarized efflux system (Zhu *et al.*, 2017).

2.2.1 Passive transcellular diffusion

The passive transcellular absorption pathway is still regarded as the most important pathway for drug absorption. Passive transcellular transport involves the movement of materials across the cells from the apical to the basolateral side. For transport via the passive transcellular route to be possible, it is a prerequisite that solutes permeate the apical cell membrane. This movement is made possible by a concentration difference (movement occurs from an area with a high concentration, e.g. the intestinal fluid, to an area with a low concentration, e.g. the blood) between the apical and basolateral sides of the membrane, which doesn't require any external energy. It is generally accepted that the apical membrane has a lower permeability than the basolateral membrane, thus the apical membrane is the rate limiting barrier to passive transcellular drug transport (Vertzoni *et al.*, 2019; Zhu *et al.*, 2017). The transcellular pathway can be further divided into different mechanisms, such as carrier mediated transport (active transport and facilitated diffusion) and endocytosis (pinocytosis, phagocytosis, receptor mediated endocytosis and transcytosis) (Artursson *et al.*, 2001; Zhu *et al.*, 2017). These will be discussed in subsequent sections.

2.2.1.1 Carrier-mediated transport

There are numerous carrier-mediated transport systems which can be divided into two basic groups, namely active and passive carrier-mediated transport. Active carrier-mediated transport is usually Na^+ or H^+ linked with bifunctional carriers, as shown in Figure 2.2. This process can transport material against the concentration gradient (active carrier-mediated transport) which requires metabolic energy (Zhu *et al.*, 2017).

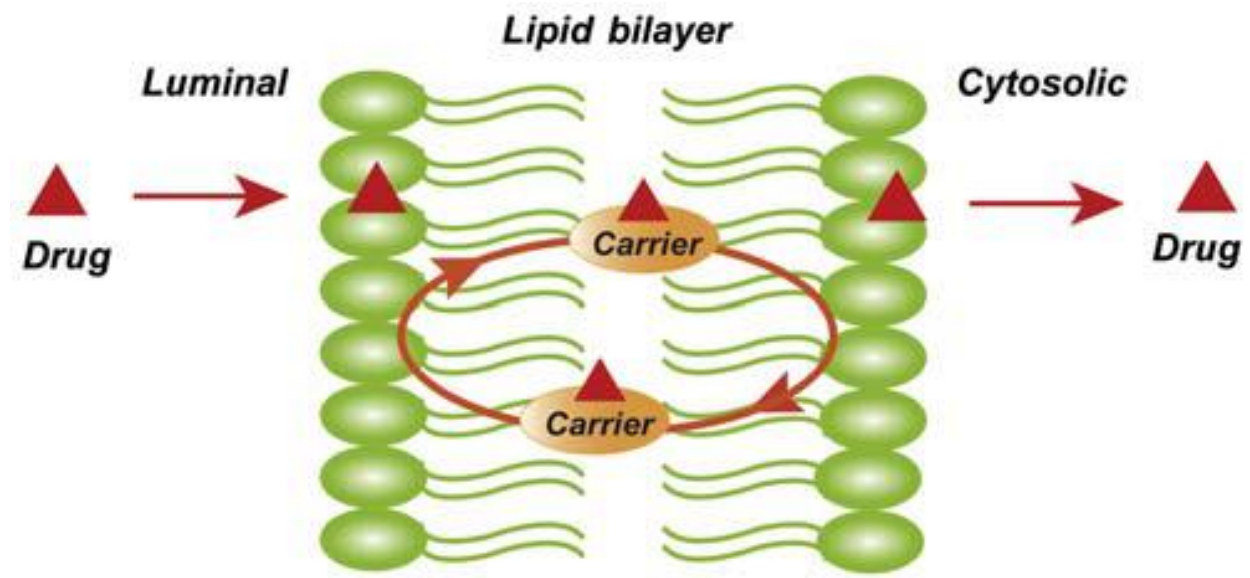


Figure 2.2: Schematic illustration of carrier-mediated transport across the lipid double-layer (Zhu *et al.*, 2017).

In contrast to active carrier-mediated transport, passive carrier-mediated transport does not require metabolic energy to function, but is rather driven by the concentration gradient of the substrate (Zhu *et al.*, 2017).

2.2.1.1.1 Active transport and facilitated diffusion

Active transport is an energy consuming process that can move materials against the concentration gradient, thus from an area with low concentration (e.g. the blood) to an area with high concentration (e.g. the intestinal fluid) (Ashford, 2018; Zhu *et al.*, 2017). The energy needed for this process is generated by the hydrolysis of adenosine triphosphate (ATP) and/or the transmembrane ion gradient. This process has a limiting step in that the carriers can become saturated and thus reaches a point where no further increase in transport can take place (Ashford, 2018).

Facilitated diffusion is a transport mechanism that is also carrier mediated, like active transport, but differs from it in that facilitated transport does not carry a substance against the concentration gradient. Therefore, facilitated transport doesn't require energy in order to transport a substance, but does require a concentration gradient as driving force similar to passive diffusion (Ashford, 2018). Similar to active transport, facilitated diffusion can also become saturated due to the fact that carriers are used as transport vessels (Zhu *et al.*, 2017).

2.2.1.2 Endocytosis

Endocytosis is the process by which the plasma membrane takes up particles or molecules from the surrounding area or medium by means of engulfment, and then budding off into vesicles containing the ingested particles, and thus be transported into the cell. The uptake process is energy dependent (Ashford, 2018). Endocytosis can further be divided into different sub mechanisms of transport.

2.2.1.2.1 Pinocytosis

Pinocytosis, a form of endocytosis, is the process where the membrane engulfs small droplets of extracellular fluid by means of small vesicles. The vesicles engulfed via pinocytosis are notably smaller than that of phagocytosis. This process has a very low efficiency with respect to drug transport (Ashford, 2018).

2.2.1.2.2 Phagocytosis

As previously mentioned, phagocytosis is a form of endocytosis where the membrane engulfs particles to form vesicles. During this process, cells can engulf large particles (>500 nm) that can include debris, bacteria and even whole cells (Lancaster *et al.*, 2018).

2.2.1.2.3 Receptor-mediated endocytosis

This process can roughly be defined as the movement of bound ligands from the cell surface to the cell interior (Wileman *et al.*, 1985). Within the vesicles, the ligands usually dissociate from their respective receptors. Many of these receptors are then recycled back to the surface of the plasma membrane to be available to transport another ligand (Ashford, 2018).

2.2.1.2.4 Transcytosis

Transcytosis, like endocytosis, engulfs materials and particles; and transports it through the cell secreting it on the opposite side (Ashford, 2018; Di Pasquale & Chiorini, 2005). This process is one of the main mechanisms by which bacteria penetrate cells (Di Pasquale & Chiorini, 2005).

2.2.1.3 Paracellular transport

The paracellular pathway differs from all other absorption pathways in the sense that materials move through the aqueous intercellular spaces between the cells rather than across the cells (Mahato *et al.*, 2003). Transport via the intercellular aqueous spaces is restricted on the apical side by structures, named tight junctions (Buckley *et al.*, 2016; Ashford, 2018). The absorptive epithelia, such as those situated in the small intestine, tend to leak more through the intercellular spaces than other epithelial cells (due to the tight junctions not being packed as close together) and the permeability of these cells decrease further down the intestinal tract (Daugherty & Mrsny, 1999).

In terms of macromolecular drugs, like protein and peptide therapeutics, the most viable pathway for absorption to occur throughout the GIT is via the paracellular pathway. When compared to conventional drugs, protein and peptide therapeutics show higher activity, higher specificity, less toxicity and less drug-drug interactions. In addition to this, these are the drugs of choice when it comes to treatment of patients with enzyme deficiency, degenerative diseases and protein dysfunction (Renukuntla *et al.*, 2013). Protein and peptide drugs are hydrophilic and polar, thus absorption via the conventional pathways, like passive transcellular diffusion, is restricted (Tang & Goodenough, 2003).

2.3 Barriers to delivery

Peptide and protein drugs have some barriers (which include physical, biological and chemical in the GI tract) that need to be overcome in order to be successfully delivered into the systemic circulation after oral administration. The low pH of the stomach environment and enzymes (e.g. protease enzymes) that break down peptides and proteins into essential amino acids for absorption contribute to the chemical barrier. The physical barrier, on the other hand, can be divided into the two main transport pathways. Absorption via the transcellular pathway is hindered by the epithelial cell layer, whereas absorption via the paracellular pathway is hindered by the tight junctions (Renukuntla *et al.*, 2013). The unstirred water layer further contributes to the physical barrier. The presence of certain micro-organisms facilitates the breakdown of peptides into amino acids via the release of peptide metabolizing enzymes directly contributing to the biological barrier (Yin *et al.*, 2014).

2.3.1 The chemical barriers

Protein and peptide drugs are susceptible to enzymatic degradation and breakdown as well as denaturation in acidic environments. This is seen as chemical barriers that hinder the successful oral delivery of protein and peptide drugs (Renukuntla *et al.*, 2013).

2.3.1.1 pH

The stomach is an acidic area within the GIT that is normally responsible for the digestion and break down of orally ingested materials. This is, however, a problem for protein and peptide drugs that are taken orally (Bruno *et al.*, 2013). The acidic nature of the stomach area thus poses a problem for the effective absorption and delivery of these drugs. The low pH within the stomach (normally between 1 and 3) is responsible for the breakdown of proteins through the acquisition of similar internal charges that cause repulsion and the unfolding of the protein structures (Choonara *et al.*, 2013).

2.3.1.2 Enzymes

There are enzymes within the GIT that specifically target the degradation of proteins and peptides, e.g. proteases and peptidases. These enzymes can be divided into more specific groups and can be found at different areas within the GIT, but are broadly classified into five groups, namely serine, cysteine, threonine, aspartic and metallo proteases (Bruno *et al.*, 2013). Pancreatic enzymes include trypsin, chymotrypsin and carboxy-peptidase. These enzymes are secreted into the intestines, more specifically the duodenum, and are responsible for roughly 20% of the degradation and the breakdown of proteins and peptides into non-essential amino acids (Choonara *et al.*, 2013).

Pepsin, an endopeptidase, is one of the most important enzymes that break down proteins into smaller peptides and amino acids. It is only active in environments with a low pH, like namely the stomach (pH 1 – 2). It is produced in the stomach and is one of the main digestive enzymes in the digestive system. Pepsin is one of the three main proteases in the human digestive system (the other being trypsin and chymotrypsin). During the breakdown of proteins in the stomach, these enzymes targets proteins, severing links between amino acids and producing peptides and amino acids, respectively (Choonara *et al.*, 2013). Pepsin is most efficient in cleaving peptide bonds between hydrophobic and aromatic amino acids, including phenylalanine, tryptophan and tyrosine (Choonara *et al.*, 2013; Bruno *et al.*, 2013).

2.3.2 The physical barriers

In addition to the chemical barriers, there are physical barriers that hinder the absorption of orally administered protein and peptide based drugs. The physical barriers include the unstirred water layer, the mucus layer on the epithelial membrane, efflux, and the extent by which the tight junctions can open (Bruno *et al.*, 2013; Lundquist & Artursson, 2016).

2.3.2.1 The mucus barrier

The mucus barrier can be seen as the first physical barrier to absorption in the GIT after oral ingestion. It can be defined as a hydrogel layer composed mostly of large glycoproteins, predominantly from the mucin family. Mucin is mainly secreted by goblet cells. In the small intestine, mucin 2 is the main mucin secreted. In the average person, mucus production is on average 1 kg/day in adults. The thickness of the mucus layer in an average adult human ranges from 10 to 100 – 200 μm (jejunum to colon) and consists of an outer, loose layer and an inner, strongly adherent layer (Lundquist & Artursson, 2016).

The mucus layer binds nanoparticles and proteins via hydrophobic interactions. Interactions between charged mucin proteins and polar molecules, like protein drugs, also occur and immobilize the molecules in the mucus, thus hindering the uptake thereof (Lundquist & Artursson, 2016). The adhesion of drugs to the mucus layer can be taken advantage of for certain drug delivery systems. In the case where certain permeation enhancers are used to improve drug delivery, mucoadhesion is necessary to prolong drug residence time. Proteins are an example of polypeptide molecules, due to its structure comprising out of natural polymers made from various amino acid monomer units. Thus, in this case the factor prolonging the residence time is the molecular weight and chain length of the polymer, which increase the residence time as both respective factors increase (Pandey *et al.*, 2017).

2.3.2.2 Unstirred water layer

Epithelial cells are covered by a stagnant, aqueous layer, which consists of water, glycoproteins, electrolytes, proteins and nucleic acids. This is called the unstirred water layer (UWL), which is bound to the apical cell surface by the glycocalyx (a form of glycoprotein) (Hamman & Steenekamp 2011). During the process of dissolution and absorption through a membrane, a concentration gradient can form close to the vicinity of the surface of the mucosal membrane. As shown in a study conducted by Korjamo *et al.* in 2009, the diffusion rate is much slower next to the surface of the membrane, due to the stagnant water layer that acts as a

barrier, than that of the bulk solution, which is due to incomplete mixing of the luminal fluids. Consequently, the rapidly moving molecules released from the dosage form have to move through the stagnant layer by diffusion rather than by convection. This is seen as a permeability barrier during absorption (Korjamo *et al.*, 2009; Lennernäs, 1998).

2.3.2.3 Efflux

Efflux can loosely be defined as the active movement of solutes out of the epithelial cells back to the luminal area of the GI tract by means of efflux transporters (Hamman & Steenekamp 2011). These efflux transporters are principally adenosine tri-phosphate (ATP) binding cassette (ABC) proteins such as P-glycoprotein (Pgp) and multidrug resistance-associated protein (MRP2). The efflux system proteins are located on the apical side of the membrane which protects the host from absorption of possible toxic compounds. Pgp-like mechanisms have been implicated in the intestinal secretion of certain drugs, including peptide drugs, and consequently contributed to the low bioavailability of these, and other drugs (Chan *et al.*, 2003). Examples of drugs being targeted by efflux transporters are statins, macrolide antibiotics and angiotensin receptor blockers, where the efflux transporters are known to affect the exposure and clearance of these drugs (Mitchell & Thompson, 2013).

2.3.2.4 Tight junctions

As previously discussed, paracellular transport is the movement of polar solutes through small openings between adjacent epithelial cells within the small intestine. The permeability for these small openings is managed by tight junctional complexes which can be divided into three groups, namely tight junctions (or zonula occludens), adherens junctions and desmosomes. The adherens junctions and desmosomes are believed to contribute mainly to the mechanical linkage of the epithelial cells (Lemmer & Hamman 2013).

Tight junctions (TJs) are responsible for the regulation of the paracellular transport of solutes. These openings consist of proteins, from which more than 40 different types of transmembrane proteins were identified (Anderson & Van Itallie 2009). The most important transmembrane protein responsible for the ion selectivity of TJs is that from the claudin family (Schneeberger & Lynch 2004). TJs are seen as a barrier to drug absorption due the fact that without any modulation, transport of solutes exceeding a molecule radii of 15 Å is excluded (Lemmer & Hamman 2013).

2.4 Approaches to improve delivery

Due to the barriers and problems associated with oral administration of protein and peptide compounds, different strategies pertaining to the successful delivery thereof have been under investigation. Several promising strategies or approaches to improve delivery of protein and peptide drugs have been investigated with different degrees of success.

These strategies or approaches include chemical modification of proteins or peptide molecules, following different formulation approaches and developing particulate delivery systems (Yin *et al.*, 2009; Dulal 2010; Renukuntla *et al.*, 2013).

2.4.1 Chemical modification

Chemical modifications to peptide and protein drugs are but one of the ways by which absorption and bioavailability can be increased in order to facilitate a therapeutic effect. In order to chemically modify a protein or peptide, the native structure is tailored to provide a more efficient uptake across the epithelial membrane in the GIT. This is possible due to a variety of methods as discussed below (Yin *et al.*, 2009; Buckley *et al.*, 2016).

2.4.1.1 PEGylation (PEG)

Poly (ethylene glycol) (PEG) is a polymer that was investigated for properties by which it can enhance the absorption and bioavailability of orally administered protein and peptide drugs. PEGylation is the process by which PEG chains are conjugated to the structure of a peptide based drug in order to enhance the absorption thereof, without altering the pharmacodynamics to a significant extent (Pfister & Morbidelli 2014). PEGylation (e.g. amine-, thiol- and carboxyl PEGylation) became the method of choice as it increases the proteins' half-life in circulation. This is achieved, in part, by protecting the peptide drug against proteolytic degradation and increasing the molecular size, which in turn decreases renal filtration. Contributing factors that affect the aforementioned are the number of PEG chains attached to the peptide, the weight and structure of the attached PEG chains, the site where the PEG chains are attached and the chemistry that is used to attach the PEG chains (Roberts *et al.*, 2012). The different mechanisms of PEGylation are depicted in Figure 2.3.

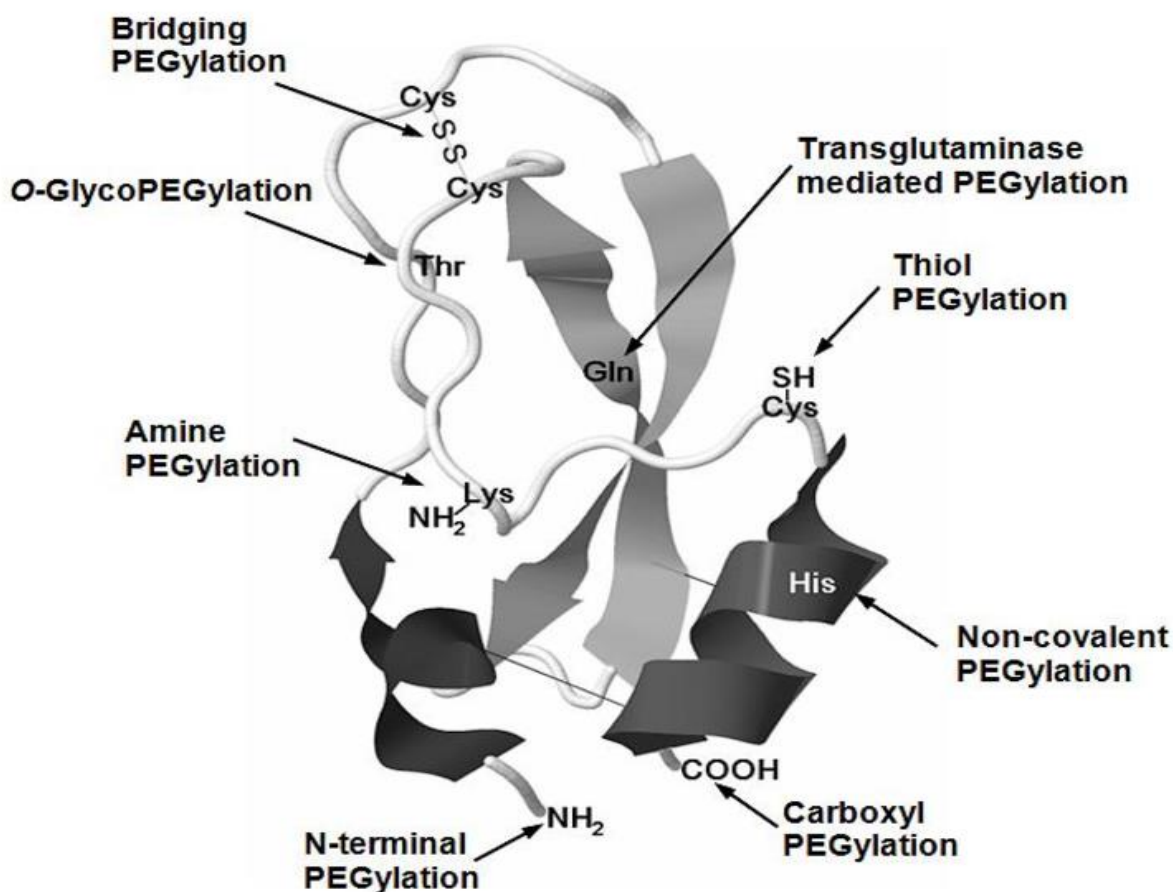


Figure 2.3: The presentation of different PEGylation strategies (Pfister & Morbidelli 2014).

2.4.1.2 Prodrugs

Prodrugs are another method of chemical modification in order to improve the absorption and bioavailability of compounds and/or drugs. A prodrug is a drug conjugated or combined with a chemically inactive substance to ultimately improve the absorption or mask any undesirable properties the drug might have after being activated by drug metabolism, i.e. low solubility, low membrane permeation, chemical instability or low target selectivity (Zawilska *et al.*, 2013). About 5 – 7% of all worldwide approved drugs can be classified as prodrugs. Some of the most common functional groups that are used in prodrug design are carboxylic, amine, ester, hydroxyl and phosphate groups (Rautio *et al.*, 2008). This approach has, however, been limited for protein and peptide drugs due to structural complexity, lack of methodology for synthesis and poor stability during synthesis (Renukuntla *et al.*, 2013).

2.4.1.3 Cell penetrating peptides and reverse aqueous lipidisation

Cell penetrating peptides (CPPs) are short, positively charged or amphiphilic chains consisting of 5 – 30 amino acids that can penetrate and transport micro- or macromolecules across biological membranes (Derakhshankhah & Jafari 2018). This penetration is possible either due to perturbation of the lipid bi-layer or due to endocytosis (Renukuntla *et al.*, 2013). CPPs can be seen as “cargo” delivering methods, as they deliver the drug intracellularly. Conjugation of CPPs to these cargo molecules can be done either by binding the molecules covalently or non-covalently to the peptide. Covalent bonding is a time consuming process and requires binding each cargo molecule individually. Non-covalent bonding of the CPP to the molecule is achieved by electrostatic interaction binding between the two molecules. This method is very flexible and is suited for a wide range of delivery molecules, especially in delivering fluorescent compounds for imaging during diagnostics (Derakhshankhah & Jafari 2018). Reverse aqueous lipidisation, another method, is a chemical modification method by which fatty acids are conjugated to a protein or peptide in order to render the drug more lipophilic and thus increase membrane permeation and bioavailability (Trabulo *et al.*, 2012; Chen *et al.*, 2012; Renukuntla *et al.*, 2013).

2.4.2 Formulation approaches

The rising interest and research on how to overcome the low solubility and absorption of orally administered protein and peptide drugs also include various formulation approaches. Formulation approaches consist of methods to improve the absorption and bioavailability of these drugs by either inhibiting enzymatic degradation, delivering a substance to a specific target, implementing carrier type drug delivery systems, adding a substance that can assist with the absorption process, or increasing the residence of the drug in a specific area of the GI tract.

2.4.2.1 Absorption enhancers

Absorption enhancers are substances that increase the absorption of peptide and protein drugs by reversibly altering or temporarily disrupting the intestinal barrier with minimum tissue damage, thus allowing improved drug penetration into the circulatory system (Aungst, 2011). There are different mechanisms by which these substances render enhanced absorption, namely increasing membrane fluidity; opening tight junctions; temporarily disrupting the structural integrity of the intestinal barrier and decreasing mucus viscosity (Renukuntla *et al.*, 2013). Absorption enhancers are frequently investigated as functional excipients in novel dosage forms to increase the absorption of hydrophilic macromolecules, such as insulin (Park *et al.*, 2010).

Unfortunately, some absorption enhancers often cause damage and/or irritate the intestinal mucosal membrane. Consequently, there is an increased need for more effective and less toxic drug absorption enhancers (Salamat-Miller & Johnston, 2005). In Table 2.1, different chemical substances that showed potential to increase the absorption or increase the membrane permeability of hydrophilic molecules are listed.

Table 2.1: A list of different chemical substances known to increase the absorption of hydrophilic drugs (Hamman *et al.*, 2005; Beneke *et al.*, 2012, Tegos *et al.*, 2011).

Absorption enhancers	Examples	Mechanism of action
Anionic polymers	Poly(acylic acid) derivatives	Combination action of calcium depletion and enzyme inhibition
Bile salts	Sodium glycocholate, sodium taurodeoxycholate, sodium taurohydrofusidate	Membrane integrity disruption by means of phospholipid solubilisation. Reduction in mucus viscosity
Cationic polymers	Chitosan salts, N-trimethyl chitosan chloride	Opening of tight junctions by ionic interaction with cell membrane in combination with mucoadhesive properties
Chelating agents	Ethylene-diamine-tetraacetic acid (EDTA), ethylene-glycoltetraacetic acid (EGTA)	Complexation of calcium and magnesium (tight junction opening)
Complexation	Cyclodextrins	Increases drug solubility and dissolution rate
Efflux pump inhibitors	First, second and third generation (reserpine, biricodar, timcodar)	Altering cell membrane integrity, blocking drug binding site on P21 glycoprotein (Pgp) and interfering with adenosine triphosphate (ATP) hydrolysis
Fatty acids	Medium chain glycerides, long chain fatty acid esters (palmitoylcarnitine)	Paracellular (dilation of tight junctions) and transcellular (epithelial cell damage or disruption of cell membranes)

Plant materials	Aloe vera gel and whole leaf Piperine Naringin (flavonoid glycoside in grapefruit)	Significantly reduces transepithelial electrical resistance (TEER) and opens tight junctions to allow paracellular transport. Inhibits drug metabolising enzymes, stimulates gut amino acid transporters, inhibits drug efflux and inhibits intestinal production of glucuronic acid. Inhibits human cytochrome P450 metabolising enzymes and inhibits efflux transport by inhibiting P-glycoprotein.
Salicylates	Sodium salicylate, salicylate ion	Increasing cell membrane fluidity, decreasing concentration of non-protein thiols
Surfactants	Sodium dodecyl sulfate, nonylphenoxy (polyoxyethylene), sodium dioctyl sulfosuccinate	Membrane damage by extracting membrane proteins or lipids, phospholipid acyl chain perturbation
Toxins and venom extracts	Zonula occludens toxin (ZOT), melittin (bee venom extract)	Interaction with the zonulin surface receptor induces tight junction opening, α -helix ion channel formation, bilayer micellisation and fusion

In the subsequent section, specific focus will be given on the discussion of *Aloe vera* (both whole leaf extract and gel) and TMC, as it is the absorption enhancers that pertain to this study.

2.4.2.1.1 *Aloe vera*

Aloe vera gel is a clear, viscous substance obtained from the parenchymatous cells in fresh *A. vera* leaves (WHO, 1999:43). *Aloe vera* (L) Burm. F (Xanthorrhoeaceae) gel has previously shown the ability to increase the bioavailability of both vitamin C and E in humans. In this study, the results showed that, when compared to the control (ascorbic acid without any absorption enhancers), the addition of the *A. vera* whole leaf extract didn't make a significant difference. However, when of *A. vera* gel was co-administered with ascorbic acid, it caused a three-fold increase in the bioavailability of vitamin C (Vinson *et al.*, 2005). *In vitro* studies on *A. vera* gel as well as whole leaf extract have shown a significant reduction in the transepithelial electrical resistance (TEER) of Caco-2 cell monolayers, thus, displaying the ability to open tight junctions between adjacent cells (Chen *et al.*, 2009).

Absorption enhancement by means of *A. vera* gel and whole leaf materials of the FITC-dextran via the paracellular pathway across Caco-2 cell monolayers has been confirmed by confocal laser scanning microscopy. F-actin filament redistribution also indicated tight junction modulation by *A. vera* leaf materials (Haasbroek *et al.*, 2019). This effect of tight junction modulation when using *A. vera* gel or whole leaf extract is completely reversible after removing it from the membranes (Lemmer & Hamman, 2013). *Aloe vera* gel and whole leaf materials on their own, and in combination with other absorption enhancers showed the ability to increase intestinal drug transport of protein drugs *in vitro* as well as enhance bioavailability *in vivo* (Lebitsa *et al.*, 2012; Du Toit *et al.*, 2016; Wallis *et al.*, 2016).

2.4.2.1.2 *N*-trimethyl chitosan

The development and synthesis of *N*-trimethyl chitosan chloride (TMC), was inspired by the unfavourable solubility characteristics of chitosan. Chitosan is practically insoluble in neutral and alkaline environments such as those found in the small intestine (Mourya & Inamdar, 2009). TMC, a derivative of chitosan, is soluble in acidic, neutral and alkaline media (pH 1 – 9) (Mourya & Inamdar, 2009). Similar to chitosan, TMC also opens tight junctions between intestinal epithelial cells without damaging cell membranes as shown by a reduction in TEER as well as an increase in the transport of hydrophilic and macromolecular drugs (Thanou *et al.*, 1999; Mourya & Inamdar, 2009).

2.4.2.2 Enzyme inhibition

To overcome biological barriers, one has to understand how these barriers affect the drugs that are being administered. Protein and peptide drugs are prone to enzymatic degradation; either due to hydrolysis of the peptide bonds by endopeptidases or exopeptidases, or by proteolytic enzymes. The area most notable for the degradation of protein and peptide drugs are within the duodenum, where gram quantities of peptidases are present. The second biggest enzymatic barrier is the enzymes present in the brush-border membrane of the epithelial cells (Mahato *et al.*, 2003). Theoretically, inhibiting these types of enzymes should improve the absorption and consequently, the bioavailability of orally delivered protein and peptide drugs (Yamamoto *et al.*, 1998).

The co-administration of enzyme inhibitors with protein and peptide drugs aims to eliminate specific enzymes that hinder the stability and successful delivery of the drugs. Research shows that polycarbophil and carbopol 934P are strong inhibitors of the proteolytic enzymes trypsin, carboxypeptidase A and α -chymotrypsin (Lueßen *et al.*, 1998).

This approach of co-administering enzyme inhibitors, however, has some challenges that have caused research in this field to decrease drastically. One such challenge is negative feedback that stimulates higher secretion of enzymes (Berg *et al.*, 2015).

2.4.2.3 Mucoadhesive systems

Mucoadhesive systems comprise of synthetic polymers that bind substances to intestinal mucosal membranes in order to increase the retention time in the GI tract. This increases the amount of drug available at the site of absorption (Renukuntla *et al.*, 2013). There are many different mechanistic theories to mucoadhesion, including the wettability; adsorption; electrostatic; fracture; diffusion interlocking; and mechanical theory (Mansuri *et al.*, 2016). Mucoadhesion is dependent on different factors, which are shown in Figure 2.4.

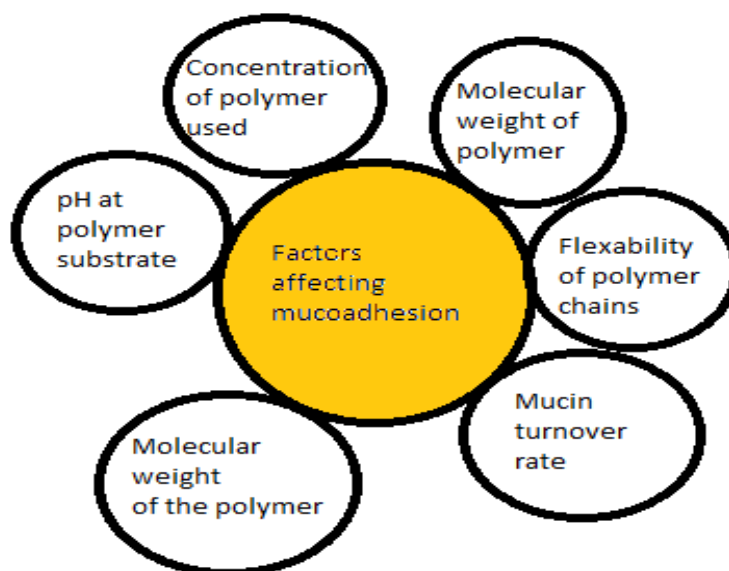


Figure 2.4: Different factors affecting mucoadhesion (adapted from Mansuri *et al.*, 2016)

2.4.2.4 Site specific drug delivery

Due to a high concentration of proteolytic enzymes present in the small intestines that degrade protein and peptides, alternative methods of drug delivery have been sought. Site specific drug delivery is one such alternative method, which targets the colon as delivery area due to a lower concentration of degrading enzymes (Renukuntla *et al.*, 2013).

Currently, this specific method is being exploited for the successful delivery of non-steroidal anti-inflammatory drugs (NSAIDs) for long term treatment of irritable bowel diseases, such as Crohn's disease and ulcerative colitis (Friend 2005; Maroni *et al.*, 2012).

2.4.3 Particulate delivery systems

Particulate drug delivery systems exist in different forms, i.e. nano- and micro particulate systems as well as MUPS, where particle sizes range from 1 nm for nanoparticles to 1.5 mm for beads. These systems were developed for more successful delivery of protein and peptide based drugs, amongst others (Marais *et al.*, 2013).

Nanoparticles are considered as colloidal drug carriers with particle sizes ranging from 1 to 1000 nm. These nanoparticles are broadly classified into two categories, namely nanospheres and nanocapsules. Nanospheres are matrix systems in which the drug is physically uniformly dispersed, whereas nanocapsules are vesicles wherein the drug molecules are encapsulated. This, in turn, helps to protect protein and peptide drugs against degradation from protease enzymes (Ranjit & Baquee 2013; Renukuntla *et al.*, 2013).

The formulation of nanoparticle drug delivery systems has gained significant interest in recent years, especially in the oral treatment of type 1 diabetic patients with insulin (Su *et al.*, 2011). The advantages of oral delivery of insulin include better patient compliance due to the more convenient administration route. This will also mimic the endogenous route of insulin after secretion, which allows first pass metabolism in the liver to break down some of the insulin and consequently lowers the chances of hypoglycaemic episodes (Fonte *et al.*, 2015; Wallis *et al.*, 2014).

Particulate delivery systems (or drug carrier systems) offer different ways to deliver macromolecules successfully by means of coupling the drug to a carrier system, such as microspheres. These microspheres haven't shown noteworthy success due to their lack of residence time. This can be improved by giving the microspheres bio-adhesive properties, resulting in the delivery system referred to as bio-adhesive microspheres (Vasir *et al.*, 2003). According to a study conducted by Marais *et al.* (2013), this delivery method has shown promise as there was a statistical improvement of insulin delivery across excised rat intestinal tissue due to the inclusion of TMC in the microspheres when compared to the control, from which TMC was excluded (Marais *et al.*, 2013).

Liposomes are another method by which macromolecules can be successfully delivered. Liposomes can be defined as micro vesicles composed of one, or more phospholipid bilayer membranes up to 10 µm in size. These lipid-based delivery systems offer some degree of protection for protein and peptide based drugs in the GIT (Renukuntla *et al.*, 2013).

2.4.3.1 Beads and pellets

Pelletisation is an agglomeration process that converts fine powders and/or granules of bulk drugs and excipients into small, spherical or semi-spherical free flowing pellets, also referred to as beads. In general, pharmaceutical bead sizes vary from 0.5 mm to 1.5 mm, although other sizes can be produced depending on the production method. Beads are receiving more attention due to their ability to extend or control drug release in different dosage forms (Vikash *et al.*, 2011).

Beads can be used to produce mini-tablets or to be filled into hard gelatine capsules, though there is a significant difference in cost (Vikash *et al.*, 2011). There are different ways in which beads can be prepared, for example drug layering, freeze pelletisation, cryopelletisation, extrusion-spheronisation, compression method, spray drying and spray congealing, balling method and fluid bed pelletising technologies (Hamman *et al.*, 2017), which will be discussed in the following sections.

2.4.3.1.1 Drug layering

Drug layering, or powder layering, is a bead (or pellet) preparation technique, which layers a suspension or solution of a drug onto a seed material in order to produce beads that are uniform in size and possess good morphology. This method involves the disposition of drug solution/suspension layers and binder on starter seeds that may be inert materials or granules of the drug that are being formulated into beads. In the initial stages of bead preparation, the drug particles are bound to the seeds with the help of liquid bridges, which are obtained from the sprayed product. Eventually, the liquid bridges are replaced by solid bridges derived from either the binder or any other particle that can dissolve in the liquid (Hamman *et al.*, 2017). This process of layering of the binder and drugs is continued until the desired bead size is obtained. It is of utmost importance that the powder is delivered accurately to the core seed and in such a manner that the delivery of the drug and binder is in equilibrium. If this is not done correctly, the quality of beads will not be sufficient and the yield of the bead formulations will be negatively affected (Gupta *et al.*, 2015).

2.4.3.1.2 Freeze pelletisation

Freeze pelletisation is used to prepare spherical beads for pharmaceutical use where a molten-solid carrier along with the dispersed active ingredient is introduced as droplets into an inert column of liquid in which the molten solid is insoluble (Cheboyina *et al.*, 2004). The column is divided into two parts, one maintaining the molten solid carrier at a temperature between 20 to 100°C and the other, where droplet solidification takes place, maintains a temperature of 0 to -40°C by means of a dry ice and acetone mixture (Hamman *et al.*, 2017; Sirisha *et al.*, 2013). Dispersions are created by mixing the active ingredient and other excipients with molten carriers. The dispersion or solution droplets are then introduced into the chamber where the droplets can move up or down in the liquid of the column depending on the density of the droplets with respect to the liquid of the column. If the density of the molten solid carriers is higher than the liquid of the column, the droplets are introduced from the upper portion of the column where the carriers will move downward and solidify. However, if the density of the molten solid carriers is lower than that of the liquid used in the column, the molten solid carriers are introduced in the lower part of the column, where the molten solid carriers move upward and solidifies (Cheboyina *et al.*, 2004; Hamman *et al.*, 2017).

2.4.3.1.3 Cryopelletisation

In this technique, freeze dried or lyophilised pellets are formed by instant freezing liquid formulations using liquid nitrogen. This method was initially used for lyophilising of viscous bacterial suspensions, but was later adapted and used to produce uniform beads by instantaneously freezing drug loaded suspensions (Gupta *et al.*, 2015; Sirisha *et al.*, 2013). The outer morphology of the beads is uniform in nature due to the rapid heat transfer between the droplets and the liquid nitrogen. The frozen pellets are transported to a storage container (-60°C) after which it is dried in a freeze dryer to remove any water or organic solvents (Hamman *et al.*, 2017).

2.4.3.1.4 Compression method

Compression is a pelletisation technique in which mixtures of active ingredients and excipients are compacted under pressure in order to produce beads of definite shape and size. When categorised, these beads exhibit a narrow particle size distribution and are normally used to fill capsules (Hamman *et al.*, 2017; Sirisha *et al.*, 2013).

2.4.3.1.5 Spray drying and spray congealing

During the process of spray drying, a suspended or dissolved drug (without any excipients) is sprayed into a hot air in order to produce dry, spherical particles. The droplet size during this process is kept small to maximise the evaporation rate or congealing. The size of the pellets produced with this method is usually small. As the atomised particles come into contact with the hot air, the solvent in the solution starts to evaporate (in a series of stages) and the viscosity of the droplets constantly increases until the entire solvent medium is evaporated and solid particles are formed (Gupta *et al.*, 2015).

2.4.3.1.6 Balling (spherical agglomeration method)

This method consists of bead formulation from powder mixtures by means of continuous rolling or tumbling in discs, drums or pans. This takes place with the addition of liquid or with exposure to high temperatures. Finely divided particles are formed into spherical particles upon the addition of the appropriate amounts of liquid whilst applying physical forces by the rotating drum (Hamman *et al.*, 2017).

2.4.3.1.7 Fluid bed pelletising technology

Fluid bed pelletising techniques can be divided into three sub groups, among others, which include the Controlled Release Pelletising (CPS™), Fluidised Bed MicroPx™ and ProCell™ (Hamman *et al.*, 2017; Srivastava & Mishra, 2010).

- CPS™ is a direct, continuous pelletisation process which produces matrix type pellets (Srivastava & Mishra, 2010). During this method, advanced fluid bed rotor technology, incorporating a conical shape rotating disk is utilised. Basic excipients are used as starting material, which are wetted with either water or organic solvents. This is followed in by a rolling movement (i.e. spheronisation), which yields spherical beads that are then dried in the CPS™ or in a classical fluid bed dryer (Hamman *et al.*, 2017; Srivastava & Mishra, 2010). This technique is normally used with low dose, high potency drugs.
- MicroPx™ technology is a continuous fluid bed agglomeration process yielding matrix type beads. This process, like CPS™, negates the use of starting cores. It produces small pellets (< 400 µm) and yields high drug loading (typically 95%); and it exhibits a narrow particle size distribution (Srivastava & Mishra, 2010).
- ProCell™ technology is a spouted-bed type process used for the preparation of highly concentrated pellets. In this process, no additional excipients are used, thus pellets containing pure active ingredients are produced. The pellets yield a very high (up to 100%) drug load (Srivastava & Mishra, 2010).

2.4.3.1.8 Extrusion-spheronisation

Extrusion-spheronisation is a multi-step process involving dry mixing; wetting of a mixture of excipients and active ingredient; extrusion of the wetted powder mass; spheronisation of extrudates; freezing of spheronised particles; and drying of frozen pellets under vacuum. During the first step of this process, the dry excipients and active ingredient are mixed together to produce a homogenous mixture (Sirisha *et al.*, 2013). The powder mixture is then wetted by either distilled water or a mixture of distilled water and ethanol. This is done by constantly mixing the powder mass, while adding the wetting agent in appropriate amounts until a grainy consistency is reached. The wetted powder mass is added to the extrusion chamber, which forces the wetted powder mixture through a sieve aperture in order to produce long extrudates with a definite diameter equal to the aperture size. These long extrudates are transferred to the bowl of a spheroniser, which breaks the spaghetti shaped extrudates into smaller pieces, rounding them to ultimately produce spherical beads (Gupta *et al.*, 2015; Hamman *et al.*, 2017, Vervaet *et al.*, 1995).

Extrusion is an integral part of the overall spheronisation process in which the wet powder mass is forced through a sieve ranging between 0.5 mm and 2.0 mm, but is rarely less than 500 μm . There are different types of extruders employed to produce the extrudates used in spheronisation. These different types of extruders control the extrudate and subsequently the final pellet properties. Table 2.2 shows the different types of extruders and the different features each possesses.

Table 2.2: Types of extruders and their different features (Sinha *et al.*, 2009)

Type of extruder	Features
1) Screw extruders	Consists of one or two screens feeding the wetted mass to an axial or radial extrusion screen
Axial type	Screen is placed at the end of the screw, perpendicular to the axis of the screw
Radial type	Die is placed around the screw, discharging the extrudate perpendicular to the axis of the screw
2) Sieve extruder	Granulate is fed by a screw into the extrusion chamber where a rotating or oscillating device pushes the wetted mass through the screen. The screen is positioned at the bottom of the extrusion chamber.
3) Basket extruder	Similar to sieve extruder, only differing in that the granulate is fed by gravity into the extrusion chamber

4) Roll extruders	
With one perforated roll	Contains two contra-rotating wheels, of which only one is perforated
With two perforated rolls	Both contra-rotating wheels are perforated
With the extrusion screen rotating around the rollers	Contains a perforated cylinder rotating around the rollers, discharging the material outside the cylinder
5) Ram extruder	Based on a piston which pushes the wet mass through a screen situated at the end of a barrel

Figure 2.5 illustrates the different steps during the extrusion-spheronisation technique of bead preparation. This process is unique in the sense that it is not only used to produce pellets with high drug loading, but it can also produce extended-release pellets in certain situations (Gupta *et al.*, 2015). Extrusion-spheronisation is a widely used technique to produce beads owing to the fact that it is a more cost effective method when compared to other preparation methods (Sinha *et al.*, 2009).

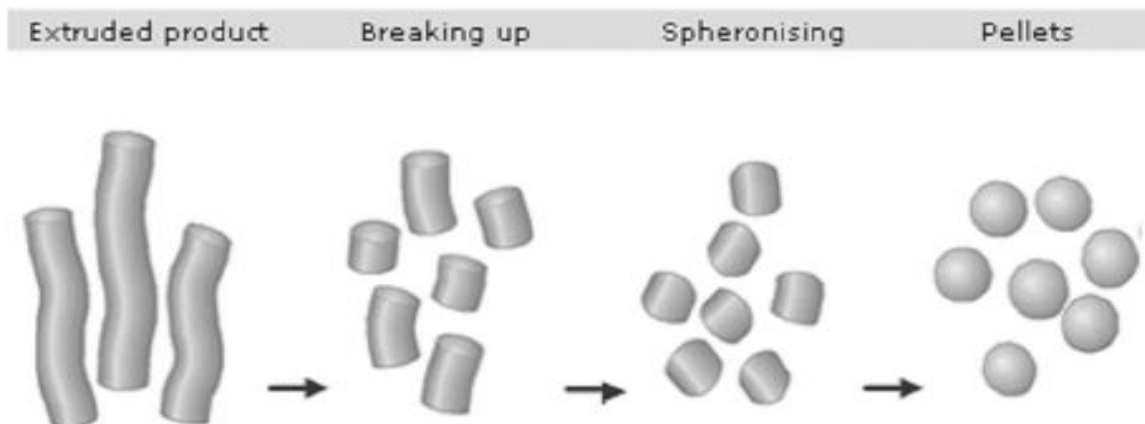


Figure 2.5: The different steps involved during bead preparation by means of extrusion-spheronisation (Sirisha *et al.*, 2013)

There are different reasons for producing beads in the pharmaceutical industry, which include the reduction of dust formation (in comparison with conventional tablets), the prevention of segregation of co-agglomerated components, higher drug dose loading, the increase of bulk density and the decrease in bulk volume, and the control of drug release in oral dosage forms (Srivastava & Mishra, 2010; Hirjau *et al.*, 2011).

A study conducted by de Bruyn *et al.* (2018) showed that insulin (a peptide drug) incorporated into beads — along with absorption enhancers incorporated into separate beads — filled into a hard gelatine capsule; facilitated transport of insulin across excised pig intestinal tissue.

The use of beads in a multiple-unit double phase dosage form showed an increase of up to 14.77% in insulin transport when compared to the control, which contained no absorption enhancers (de Bruyn *et al.*, 2018). This shows promise for the transport and delivery of protein based drugs by means of beads as a delivery system.

2.5 Summary

It is generally accepted that the oral delivery of protein and peptide drugs is problematic. Protein and peptide drugs are hydrophilic in nature and usually consist of macromolecular, polypeptide structures. Due to these characteristics, protein and peptide drugs cannot be delivered to the circulatory system by means of passive diffusion, thus, alternative means of delivery must be investigated. There have been significant technical advances in respect to protein and peptide drug delivery. Several promising strategies or approaches to improve delivery of protein and peptide drugs have been investigated with varying degrees of success.

These strategies or approaches include chemical modification of proteins or peptide molecules and following different formulation approaches. Examples of chemical modification of protein and peptide molecules include PEGylation, prodrug development and linking to cell penetrating peptides. Different formulation approaches that can be followed to improve protein and peptide drug delivery include enzyme inhibition, muco-adhesive systems, site specific drug delivery, particulate delivery systems, addition of absorption enhancers and incorporating beads into multiple-unit dosage forms. The latter two, in combination, will be investigated in this research project.

CHAPTER 3

METHODS AND MATERIALS

3.1 Introduction

In this chapter the materials and methods applicable to the research conducted in this project are described. The experimental work included formulation of beads, the preparation of mini-tablets from these bead formulations as well as the evaluation of the beads and mini-tablets in terms of content assay, physical properties, dissolution behaviour and delivery of the model compound across excised epithelial tissues. Four different bead formulations with different sizes (i.e. 0.5 mm, 0.75 mm, 1.0 mm and 1.5 mm, respectively) were produced by extrusion spherulisation, each containing the model compound FITC-dextran 4000 (FD4), Pharmacel[®] 101 as filler, Kollidon[®] VA 64 as binder and Ac-Di-Sol[®] as disintegrant. All bead formulations were evaluated with regard to particle size, content (assay) and morphology. Validation of fluorometric analytical methods to quantify Lucifer yellow (LY) and FD4 was performed. The analytical methods were validated with respect to accuracy, linearity; specificity and precision prior to the commencement of the formulation studies.

The different sized bead formulations were consequently used to produce three different batches of matrix-type mini-tablets (5 mm diameter), which contained in addition to the beads also the selected absorption enhancers (i.e. *A. vera* gel, *A. vera* whole leaf extract and TMC). Mini-tablets that did not contain any absorption enhancers were also produced to serve as a control group. Ten mini-tablets were carefully loaded into a size 0 hard gelatine capsule to produce the final dosage form, namely a multiple-unit dosage form (MUDF) known as a mini-tablet-in-capsule drug delivery system. All the mini-tablet formulations were subjected to physical evaluation as specified by the BP for tablets, which included mass variation, friability and disintegration (BP, 2019).

The rationale for producing the specific mini-tablet-in-capsule formulations was to facilitate different stages of release of the functional excipients and the active ingredient, respectively. The objective was to render release of the functional excipients during the first phase followed by the release of the FD4 (model compound) during the second phase.

The intention of the first phase-release is to successfully deliver the absorption enhancers to the mucus membrane to facilitate improved membrane permeability (e.g. by tight junction opening) before bead disintegration and the subsequent release of FD4 to become available for delivery

across the intestinal membrane. To test this idea, delivery of the FD4 released from mini-tablets was tested across excised pig intestinal tissues mounted in a modified Sweetana-Grass diffusion apparatus.

3.2 Materials

3.2.1 Materials used for analytical method validation

- LY was purchased from Sigma-Aldrich (Johannesburg, South Africa).

3.2.2 Materials used for bead formulation

- Fluorescein isothiocyanate (FITC)-dextran with an average molecular weight of 4000 Da (FD4) was purchased from Sigma-Aldrich (Johannesburg, South Africa).
- Pharmacel[®] 101 (microcrystalline cellulose) was purchased from DB Fine chemicals (Johannesburg, South Africa).
- Kollidon[®] VA 64 (vinylpyrrolidone-vinyl acetate copolymer) was purchased from DB Fine chemicals (Johannesburg, South Africa).
- Ac-Di-Sol[®] (croscarmellose sodium) was purchased from DB Fine chemicals (Johannesburg, South Africa).

3.2.3 Materials used for mini tablet production

- *Aloe vera* gel and *Aloe vera* whole leaf extract were donated by Improve USA, Inc. (Texas, USA).
- *N*-trimethyl chitosan was synthesised by Dr. Righard Lemmer at the North West University (Potchefstroom, South Africa).
- Avicel[®] PH 200 was purchased from DB Fine chemicals (Johannesburg, South Africa).
- Magnesium stearate was purchased from DB Fine chemicals (Johannesburg, South Africa).

3.2.4 Materials used for particle size analysis

- Ethanol (99.5% v/v) was purchased from ACE chemicals (Johannesburg, South Africa).

3.2.5 Materials used for proton nuclear magnetic resonance

- Deuterium oxide (D₂O) was purchased from Sigma-Aldrich (Johannesburg, South Africa).

3.2.6 Materials used for dissolution studies

- Sodium hydroxide was purchased from ACE chemicals (Johannesburg, South Africa).
- Potassium dihydrogen orthophosphate was purchased from ACE chemicals (Johannesburg, South Africa).
- Hydrochloric acid was purchased from ACE chemicals (Johannesburg, South Africa).

3.2.7 Materials used for *ex vivo* transport studies

- Corning® Costar® Black 96-well plates were purchased from The Scientific Group (Johannesburg, South Africa).
- Krebs-Ringer bicarbonate (KRB) buffer mixture was purchased from Sigma-Aldrich (Johannesburg, South Africa).
- Pig proximal jejunum tissue was collected from a local abattoir (Potchefstroom, South Africa).
- Sodium bicarbonate was purchased from Sigma-Aldrich (Johannesburg, South Africa).
- Syringe filters (0.45 µm) were purchased from Stargate Scientific (Johannesburg, South Africa).
- Syringes (2 ml) were purchased from B Braum (Sandton, South Africa).

3.3 Validation of analytical methods

To ensure that the analytical method produced reliable, accurate and reproducible results during the analysis and quantification of the model compound, the method or procedure must comply with certain standards. FD4, which was quantified in the transport samples, and LY that was used for determining membrane integrity, were quantified by means of a fluorometric analytical method using a SpectraMax Paradigm® plate reader. Both analytical methods were validated with respect to accuracy, linearity, specificity and precision prior to the commencement of the formulation studies.

3.3.1 Linearity

The linearity of an analytical method refers to the ability to obtain detection values that are directly proportional to the concentration of the analyte within a certain given range. A stock solution was prepared by dissolving 1.25 mg FD4 in KRB buffer that was consequently made up to volume (100 ml) to produce a concentration of 12.5 µg/ml. A series of dilutions was prepared from the FD4 stock solution as shown in Table 3.1. Samples of these dilutions were transferred to a Costar® Black 96-well plate in triplicate.

Fluorescence values of these samples were measured with the SpectraMax Paradigm® plate reader and processed to plot fluorescence values as a function of FD4 concentration. Linear regression was performed on this data using Microsoft Excel®. In order for the analytical method to be acceptable and usable, a correlation coefficient (R^2) value of ≥ 0.999 (Green, 1996) should be obtained. The straight line of the standard curve is described by Equation 3.1:

$$y = mx + c \qquad \text{Equation 3.1}$$

Where y is the fluorescence value of the FD4 sample, m is the slope, x is the concentration of the analyte (FD4) samples, and c is the y-intercept.

Linearity for LY was determined by mixing the contents of 5 aliquots LY (500 µg/ml each) and KRB and filling the volume up to 50 ml in a volumetric flask with KRB, thereby yielding a stock solution with a concentration of 50 µg/ml. A range of dilutions were prepared from this LY stock solution as shown in Table 3.1. Samples from the respective dilutions were transferred to a Costar® Black 96-well plate in triplicate. Fluorescence values of these samples were measured with the SpectraMax Paradigm® plate reader, which were processed and plotted as a function of LY concentration. Linear regression was consequently applied to the data using Microsoft Excel®.

In order for the analytical method to be acceptable and usable, a correlation coefficient (R^2) value of ≥ 0.999 should be obtained. The straight line obtained from the standard curve is described by Equation 3.1, where y is the fluorescence obtained from the LY solution, m is the slope, x is the concentration of the analyte (LY) and c is the y-intercept.

Table 3.1: The concentrations of both the FITC-dextran 4000 and LY solutions used to construct a standard curve for evaluation of linearity

Solution	Concentration FD4 (µg/ml)	Concentration LY (µg/ml)
1	12.5	50
2	6.25	25
3	3.125	12.5
4	1.56	6.25
5	0.781	3.125
6	0.39	1.563
7	0.195	0.781
8	0.097	0.391
9	0.0488	0.195

3.3.2 Limit of detection

The limit of detection (LOD) is the lowest concentration of a substance or analyte that is detectable in an analytical sample, but that cannot necessarily be reliably quantified (Singh, 2013). Equation 3.2 was used to determine the LOD for FD4 and LY with the fluorometric analytical method:

$$\text{LOD} = 3.3 \times \frac{\text{SD}}{\text{S}} \quad \text{Equation 3.2}$$

Where LOD is limit of detection, SD is the standard deviation of the response of a blank (background noise) and S is the slope of the standard curve obtained for FD4 and LY, respectively.

3.3.3 Limit of quantification

Limit of quantification (LOQ) is the lowest concentration of an analyte that can be quantitatively determined with acceptable accuracy and precision in the specific experimental conditions (Singh, 2013). Equation 3.3 was used to determine the LOQ for FD4 and LY, respectively:

$$\text{LOQ} = 10 \times \frac{\text{SD}}{\text{S}} \quad \text{Equation 3.3}$$

Where LOQ is the limit of quantification, SD is the standard deviation of the response of a blank (background noise) and S is the slope of the standard curve obtained for FD4 and LY, respectively.

3.3.4 Precision

Precision of an analytical procedure is seen as the ability to produce results that are consistent when multiple samples of the same solution are subjected to repeated measurements. This procedure can be split into two different categories, which is intra-day precision and inter-day precision (Singh, 2013).

3.3.4.1 Intra-day precision

Intra-day precision or intra-day repeatability is a measurement of precision determined on different times over a short time period under the same conditions. The intra-day precision was obtained via fluorometric analysis by analysing samples (with different concentrations) of FD4 and LY respectively, in triplicate on the same day. The concentrations of the samples used, were 12.5 µg/ml, 6.25 µg/ml and 3.125 µg/ml for FD4; and 50 µg/ml, 25 µg/ml and 12.5 µg/ml for LY. These measurements were taken at 09:00, 12:00 and 15:00 on the same day. For intra-day precision to be acceptable, the %RSD should be ≤ 5% (Shabir, 2004).

3.3.4.2 Inter-day precision

Inter-day precision or inter-day repeatability was determined by analysing samples with three different concentrations (usually a high, intermediate and low concentration) on three consecutive days. The concentrations of the samples used, were 12.5 µg/ml, 6.25 µg/ml and 3.125 µg/ml for FD4; and 50 µg/ml, 25 µg/ml and 12.5 µg/ml for LY. For inter-day precision to be acceptable, the %RSD should be ≤ 5% (Shabir, 2004).

3.3.5 Specificity

Specificity is the ability of an analytical method to detect the analyte without interference in the presence of other compounds, which may be present and that can possibly interfere with the detection process (Singh, 2013). In order to determine if there was any interference involved with the analysis of FD4, a solution was prepared containing FD4 and all the other compounds (Ac-Di-Sol[®], Kollidon[®] VA 64, Pharmacel[®] 101, Magnesium stearate, *Aloe vera* whole leaf extract, *Aloe vera* gel, *N*-trimethyl chitosan chloride and Avicel[®] PH 200) that were used in the formulation process. The obtained fluorescence values were used to construct a standard curve, which in turn was utilised to calculate the FD4 concentrations in the presence of all the other excipients.

3.3.6 Accuracy

Accuracy can be defined as the closeness of the measured quantity to that of the real quantity (Singh, 2013). During this study, accuracy was determined in terms of the percentage recovery, using nine different samples with three different concentrations. In order to be acceptable in terms of accuracy, a mean recovery of $100 \pm 2\%$ should be obtained (Shabir, 2004).

Nine different samples of FD4 and LY solutions, respectively, were diluted from the original stock solutions to produce three different concentration values as shown in Table 3.2 (three concentrations were prepared in triplicate). These samples were subsequently analysed using a SpectraMax Paradigm[®] plate reader. The values obtained from the fluorometric plate reader were used to calculate the percentage recovery for FD4 and LY, respectively.

Table 3.2: Concentrations of the respective samples used to determine FITC-dextran 4000 and Lucifer Yellow recovery as a measurement of accuracy

Analyte	Concentration ($\mu\text{g/ml}$)		
FD4	12.5	6.25	3.125
LY	50	25	12.5

3.4 Bead formulation composition

Four different bead sizes (0.5 mm, 0.75 mm, 1.0 mm and 1.5 mm, respectively) were prepared by means of extrusion-spheronisation. Table 3.3 indicates the composition of the different bead formulations. The wetting agent used during bead preparation was a mixture of 80% distilled water and 20% ethanol (99.5% v/v).

Table 3.3: Composition of all the bead formulations

Bead size (mm)	Model compound (0.3% w/w)	Diluent (95% w/w)	Binding agent (3% w/w)	Disintegrant (1.7% w/w)	Wetting agent (water and ethanol) in ml
0.5	Fluorescein isothiocyanate-dextran 4000	Pharmacel® 101	Kollidon® VA 64	Ac-Di-Sol®	121 ml
0.75	Fluorescein isothiocyanate-dextran 4000	Pharmacel® 101	Kollidon® VA 64	Ac-Di-Sol®	112 ml
1	Fluorescein isothiocyanate-dextran 4000	Pharmacel® 101	Kollidon® VA 64	Ac-Di-Sol®	109 ml
1.5	Fluorescein isothiocyanate-dextran 4000	Pharmacel® 101	Kollidon® VA 64	Ac-Di-Sol®	112 ml

3.4.1 Bead preparation method

The excipients corresponding to the concentrations indicated in Table 3.3 were weighed individually to produce a total mass of 100 g. Firstly, half of the diluent was added to a mixing vessel, followed by the binding agent, model compound and disintegrant, which was then followed by the remaining filling agent. The mixing vessel was then closed, placed in a Turbula T2B (WA Bachofen Maschinenfabrik, Germany) mixer; and mixed for 5 min at 69 rpm. After mixing, the mixing vessels' contents were emptied into a large pestle for bead preparation.

A 100 ml burette, containing a mixture of 80 ml distilled water and 20 ml ethanol (99.5% v/v), was used to dispense the wetting agent whilst mixing the powder by hand in a mortar. The wetted powder mass was then transferred to a Type 20 Caleva[®] extruder (Caleva[®] Process Solutions, Sturminster Newton, England) where it was passed through the respective sieves with different size apertures corresponding with the bead sizes, at the respective rotation speeds shown in Table 3.4, to produce long extrudates (Addendum F).

The extrudates were transferred to the bowl of a Caleva[®] spheroniser (Caleva[®] Process Solutions, Sturminster Newton, England), which was operated at different rotation speeds and times for the respective extrudates (Table 3.4). The formed beads were then subsequently frozen in a -80°C freezer for 24 h after which it was dried under a vacuum using a Virtis[®] Sentry 2.0 (Virtis[®], Gardiner N.Y. USA) lyophiliser for a further 24 h.

Table 3.4: Rotation speeds of the extruder for the respective aperture sizes during extrudate preparation and for the spheroniser during spheronisation.

Aperture size of extruder	Rotation speed of extruder (rpm)	Rotation speed of spheroniser (rpm)	Spheronisation time
0.5 mm	35	1800	7 min
0.75 mm	35	1900	4 min
1.0 mm	35	1800	2 min
1.5 mm	35	1975	3 min 30 s

3.5 Evaluation of beads

All the prepared bead formulations were submitted to a series of tests in order to evaluate the quality of the beads' structure as well as the content of the beads as discussed in the following sections.

3.5.1 Assay

Assays were conducted on all the bead formulations in order to determine the quantity of FD4 that was contained within each respective bead formulation. A sample of 500 mg of each respective bead formulation was weighed, after which the sample was crushed in a mortar with a pestle. The crushed beads of each respective formulation was transferred to separate 200 ml volumetric flasks and suspended in KRB. The suspensions were then stirred for 30 min on a magnetic stirrer before it was made up to volume to produce a theoretical FD4 concentration of 7.5 µg/ml. A volume of 1 ml of each suspension was withdrawn and filtered through a 0.45 µm syringe filter (in duplicate) for each respective bead formulation.

A volume of 180 µl of each separate bead formulation sample was then transferred to a Costar® Black 96-well plate in triplicate. The samples was then analysed using a SpectraMax Paradigm® plate reader from which the fluorometric values were used to calculate the experimental concentration of FD4 within each respective bead formulation using the constructed standard curve. To construct a standard curve, a series of dilutions was created using FD4 dissolved in KRB. The solution series contained FD4 in concentrations from 0.0488 µg/ml to 12.5 µg/ml. Samples of this series were transferred to the wells of a Costar® Black 96-well plate in triplicate and analysed fluorometrically and the values used to prepare a standard curve.

The experimental values obtained for the FD4 quantity within each bead formulation were compared to the theoretical value (7.5 µg/ml) in order to express the FD4 content as a percentage of the intended dose (i.e. % FD4 content) by using the following equation:

$$\% \text{ Content} = \frac{\text{Experimental value FD4}}{\text{Theoretical value FD4}} \times 100 \quad \text{Equation 3.4}$$

3.5.2 Flow properties of the beads

In order to determine the flow properties of the prepared beads, a series of parameters or tests were determined, including bulk density, tapped density, Hausner ratio, Carr's index and flow rate.

3.5.2.1 Bulk and tapped density

To determine the bead sample density, a sample (50 g) from each of the bead formulations was placed in a 250 ml graduated measuring cylinder. The bulk volume (V_0) was noted. The cylinder containing the beads was then placed on an Erweka[®] powder density apparatus (Type SVM 223, Erweka GmbH, Heusenstamm, Germany). The machine tapped the beads for 180 s intervals until the volume change was less than 2%. Upon completion, the tapped volume (V_{tap}) was noted. The respective densities (bulk density, (ρ_{bulk}) and tapped density, (ρ_{tap})) were calculated using equations 3.5 and 3.6, respectively (Aulton, 2018:192).

$$\rho_{\text{bulk}} = \frac{M}{V_0} \quad (\text{Equation 3.5})$$

Where ρ_{bulk} is the bulk density of the bead sample, M the mass of the bead sample and V_0 the bulk volume of the bead sample.

$$\rho_{\text{tap}} = \frac{M}{V_{\text{tap}}} \quad (\text{Equation 3.6})$$

Where ρ_{tap} is the tapped density of the bead formulation, M the mass of the beads and V_{tap} the tapped volume of the beads.

3.5.2.2 Hausner ratio

The Hausner ratio is an indirect method, which describes the inter-particulate friction between powder particles. Powder with more friction between the particles will show poor flow, while powder with less friction between the particles will show better flow (Aulton, 2018:198).

The Hausner ratio for the bead formulations was calculated using equation 3.7 (Aulton, 2018:198):

$$\text{Hausner ratio} = \frac{\rho_{\text{tap}}}{\rho_{\text{bulk}}} \quad (\text{Equation 3.7})$$

3.5.2.3 Carr's index

Carr's index (or compressibility) is also an indirect method of determining the flowability of a powder. Equation 3.8 was used to calculate Carr's index for the bead formulations (Aulton, 2018:198).

$$\% \text{ Compressibility} = \frac{\rho_{\text{tap}} - \rho_{\text{bulk}}}{\rho_{\text{tap}}} \times 100 \quad (\text{Equation 3.8})$$

3.5.2.4 Flow rate

The flow rate of the bead formulations was calculated using an Erweka[®] powder and granulate flow test apparatus (Type GTL, Erweka GmbH, Heusenstamm, Germany). The funnel was filled with 50 g of each bead formulation and allowed to flow through a 10 mm opening, noting the time until there was no sample left. The test was repeated three times for each bead formulation.

3.5.3 Particle size analysis

Particle size analysis was conducted with a Malvern Mastersizer 2000 instrument fitted with a Hydro 2000 MU dispersion unit (Malvern Instruments, Malvern, UK). As dispersant, 99.5% v/v ethanol was used at a stirring speed of 1750 rpm. The Hydro 2000 MU dispersion unit was flushed twice with ethanol prior to analyses. The unit was then filled with 500 ml 99.5% v/v ethanol and a background measurement was taken in order to compensate for electrical interference as well as possible interference from the dispersion medium. Upon completion of the background measurement, a sufficient quantity of sample of the respective bead formulation (0.5 mm, 0.75 mm, 1.0 mm and 1.5 mm respectively) was added to the dispersion unit in order to obtain an obscuration of between 5 and 10%. After obtaining a suitable obscuration, the particle size measurement followed consisting of 12 000 sweeps. The particle size distribution of the bead sample was measured in triplicate. The average particle size and distribution parameters were calculated by means of Malvern Software (Malvern Instruments, Malvern, UK).

3.5.4 Bead structure and morphology

To investigate the surface morphology and the internal structure of the beads, scanning electron microscope images were taken with an FEI Quanta 200 environmental scanning electron microscope (ESEM) (FEI Company, Netherlands). To expose the internal structures of the beads, a scalpel was used to produce a cross section of a single, isolated bead from each of the formulations.

Before the microscope images could be captured, all the bead formulations (the whole beads as well as the cross sections) were mounted on small aluminium mounts and coated with carbon, while under vacuum. Following this, the carbon coated beads were then sputter-coated by gold-palladium to minimise the surface charge of the beads.

3.6 Chemical characterisation of *N*-trimethyl chitosan chloride with proton nuclear magnetic resonance

The chemical characterisation of TMC was done by means of proton nuclear magnetic resonance (¹H-NMR) spectroscopy utilising an Avance III 600 Hz NMR spectrometer (Bruker BioSpin Corporation, Rheinstetten, Germany). A 100 mg sample of TMC was dissolved in 2 ml of D₂O and analysed in the NMR spectrometer at 80°C with suppression of the water peak. The degree of quarternisation was calculated from the ¹H-NMR spectra (equation 3.9), by using the integral of the H-1 peak at δ 5.2-6.2 ppm (Hamman & Kotzé, 2001):

$$\% \text{ } N,N,N\text{-Trimethylation} = \left[\frac{[\text{N}(\text{CH}_3)_3]}{[\text{H-1}]} \times \frac{1}{9} \times 100 \right] \quad (\text{Equation 3.9})$$

Where $[\text{N}(\text{CH}_3)_3]$ is the integral of *N,N,N*-trimethyl-amino (3.2 ppm) singlet peak. The integral of H-1 represents one proton. The degree of quarternisation was expressed as the percentage trimethylation (Hamman & Kotzé, 2001; Rúnarsson *et al.*, 2007).

3.7 Formulation and preparation of mini-tablets

3.7.1 Mini-tablet production

In order to produce the mini-tablets, the different sizes of the beads were weighed and divided into four smaller quantities, for each bead size, in order to produce a batch of mini-tablets for each of the selected absorption enhancers and a control group (see Table 3.5). Each of these smaller batches of beads were then mixed with a binding agent, a lubricant and each of the different absorption enhancers using a Turbula[®] T2B mixer at 33 rpm for 2 min. The slower mixing speed was chosen to prevent changes to the bead structure during mixing. The respective batches of bead mixtures were produced as to reflect the composition as shown in Table 3.5.

Table 3.5: Composition of the different bead mixtures for mini-tablet production

Bead size (mm)	Diluent (25% w/w)	Lubricant (0.5% w/w)	Absorption enhancing agent (1% w/w)
0.5	Avicel® PH 200	Magnesium stearate	Aloe vera gel
0.5	Avicel® PH 200	Magnesium stearate	Aloe vera whole leaf extract
0.5	Avicel® PH 200	Magnesium stearate	TMC
0.5	Avicel® PH 200	Magnesium stearate	None (Control)
0.75	Avicel® PH 200	Magnesium stearate	Aloe vera gel
0.75	Avicel® PH 200	Magnesium stearate	Aloe vera whole leaf extract
0.75	Avicel® PH 200	Magnesium stearate	TMC
0.75	Avicel® PH 200	Magnesium stearate	None (Control)
1	Avicel® PH 200	Magnesium stearate	Aloe vera gel
1	Avicel® PH 200	Magnesium stearate	Aloe vera whole leaf extract
1	Avicel® PH 200	Magnesium stearate	TMC
1	Avicel® PH 200	Magnesium stearate	None (Control)
1.5	Avicel® PH 200	Magnesium stearate	Aloe vera gel
1.5	Avicel® PH 200	Magnesium stearate	Aloe vera whole leaf extract
1.5	Avicel® PH 200	Magnesium stearate	TMC
1.5	Avicel® PH 200	Magnesium stearate	None (Control)

After the preparation of the bead mixtures, a Korsch® XP1 single station tablet press was set up to produce mini-tablets weighing 50 mg using a 5 mm punch and die set. Each bead mixture was then separately used to produce the mini-tablets, testing hardness, disintegration and consistency in process during the tableting process. A batch of 120 tablets was produced as per each bead mixture.

3.7.2 Evaluation of the mini-tablets

The mini-tablets were evaluated to determine if they were viable for further use in this research project. Official BP tests were conducted (BP, 2019). Evaluation tests included mass variation, friability and disintegration. Furthermore, the unofficial test of crushing strength was also conducted.

3.7.2.1 Mass variation

In this case, 10 mini-tablets were taken at random to be weighed individually contrary to 20 tablets as specified in the BP. The rationale for this deviation was based on the design of the multiple-unit dosage form in this study. Each multiple-unit dosage form (a sized 0 capsule) comprised of 10 mini-tablets filled into a size 0 capsule. According to the BP, if the produced tablets weigh less than 80 mg, the mass may not deviate more than 10% from the average tablet mass. The ten mini-tablets were weighed individually and the mass of each mini-tablet was compared to the average mass of the mini-tablets.

3.7.2.2 Friability

The friability of the mini-tablet formulations was determined using an Erweka® friabilator (Type TAR 220, Erweka GmbH, Heusenstamm, Germany). Ten mini-tablets were randomly selected from each formulation respectively and tested for friability. The rationale for using 10 tablets was the same as for mass variation. Before starting the test, the mini-tablets were dusted properly and weighed together (W_1). The tablets were placed in the friabilator, which was then operated at 25 rpm for 4 min. Upon completion of the rotation cycle, the tablets were dusted again and weighed (W_2). The friability was then calculated using equation 3.10:

$$\%F = \frac{W_1 - W_2}{W_1} \times 100 \quad \text{Equation 3.10}$$

Where %F is the percentage friability, W_1 is the weight of the tablets before the test was done, and W_2 is the weight of the tablets after the test was concluded.

3.7.2.3 Disintegration

Disintegration behaviour of the mini-tablets was evaluated using an Erweka[®] disintegration apparatus (Type ZT 323, Erweka GmbH, Heusenstamm, Germany). Before any testing commenced, the temperature of the disintegration medium (in this case distilled water) was adjusted to, and kept at $37 \pm 2^\circ\text{C}$. It is important to note that this test was conducted using the complete multiple unit dosage form (MUDF), consisting of 10 mini-tablets stacked carefully into size 0 gelatine capsules, as that was one of the objectives pertaining to this study. This test was conducted using three of the MUDFs (i.e. mini-tablet-in-capsule system). A precautionary measure was taken to prevent the mini-tablet-in-capsule formulations from floating by using wired weights attached to the capsules. According to BP standards, to pass the test, the mini-tablet-in-capsule formulations should be fully disintegrated within 15 minutes (BP, 2019). Three mini-tablet-in-capsule formulations were put into the disintegration apparatus and the time was noted at the moment when no debris was left on the sieve at the bottom of the disintegration chamber.

3.8 Dissolution studies

The dissolution medium was prepared by mixing 1 750 ml of 0.2 M potassium dihydrogen orthophosphate solution with 2 753.8 ml of 0.1 M sodium hydroxide which was made up to volume with distilled water to produce 7 L in total of phosphate buffer (BP, 2019). The pH of the abovementioned buffer was adjusted to 7.4 by adding sufficient hydrochloric acid (0.1 M HCl).

The release and dissolution behaviour of FD4 from the mini-tablet-in-capsule formulations was determined by placing the capsule containing 10 mini-tablets in each of the baskets of a six vessel dissolution apparatus (Distek 2500 dissolution apparatus, North Brunswick, NJ, USA). The height was adjusted so that the basket was completely submerged (37 ± 3 mm from the bottom of the chamber) (BP, 2019) in 900 ml of dissolution medium. All dissolution experiments were done in triplicate. After submerging the baskets containing the mini-tablet-in-capsule dosage forms, a steady stirring rate of 50 rpm was employed while maintaining a constant temperature of $37 \pm 0.5^\circ\text{C}$. Using 2 ml syringes, 2 ml samples were withdrawn and filtered through a $0.45 \mu\text{m}$ filter. Samples were withdrawn at time intervals of 5, 10, 15, 30, 60, 90, 120, 150, 180 and 240 min, respectively. Filtration of the samples ensured that no possible suspended particles from the mini-tablet-in-capsule formulations would be present in the samples that were analysed for FD4 content. After each withdrawal, the sample volume was immediately replaced with fresh buffer solution of the same volume that was also kept at $37 \pm 0.5^\circ\text{C}$.

Once the last sample was withdrawn, the rotation speed of the baskets was increased to 250 rpm for 15 min after which a final sample was withdrawn. This last sample was taken to obtain the value for 100% of the FD4 released from the mini-tablet-in-capsule formulations. All the samples were then transferred to a Costar® Black 96-well plate to be analysed using a SpectraMax® Paradigm® reader in order to determine the concentration of FD4 released at each pre-determined time point.

3.9 Ex-vivo transport studies

There are a wide variety of techniques used to evaluate drug permeability across the intestinal epithelium. In this particular study, a modified Sweetana Grass diffusion chamber was used to perform unidirectional transport studies across excised pig intestinal tissue. This study was conducted in order to evaluate the transport of FD4 (as model compound) from different mini-tablet formulations.

3.9.1 Preparation of buffer

The transport medium used during this study was Krebs-ringer bicarbonate buffer (KRB) at pH 7.4. To prepare this buffer, 1.26 g of sodium bicarbonate along with the contents of an entire KRB buffer mixture container (Sigma-Aldrich, Johannesburg, South Africa) was added to a 1 L volumetric flask and made up to volume with distilled water. The buffer solution was then stirred for 5 min using a magnetic stirrer and stored in a refrigerator until needed for the experiments.

3.9.2 Procurement and preparation of pig intestinal tissue

Ethics approval was granted by the Animal Ethics Committee at North-West University under the ethics approval number NWU-00579-19-A5 for experimental procedures on excised pig intestinal tissue (Addendum B). Pig proximal jejunum was collected from the local abattoir (Potchefstroom, South Africa) immediately after the slaughtering of the pigs. A piece of jejunum, approximately 30 – 40 cm in length, was excised and rinsed out with ice cold KRB, after which the tissue was stored and transported in ice cold KRB to the laboratory.

Upon arrival in the laboratory, the excised piece of pig jejunum tissue was pulled over a glass tube and positioned such that the mesenteric border was visible. The tissue was constantly kept moist with KRB while the serosa was removed by means of blunt dissection (Figure 3.1 A). Once the serosa was removed, an incision was made along the mesenteric border (Figure 3.1 B).

After the incision was made, the tissue was removed from the glass tube and placed on wetted filter paper (Figure 3.1 C). The tissue was subsequently cut into equal sized sections (Figure 3.1 D) and mounted between the Sweetana-Grass diffusion chamber half-cells (Figure 3.1 E).

The tissue was mounted in the half-cells in such a manner that the apical side of the tissue faced the pins of the chamber (Figure 3.1 E). If any Payer's patches were found on the excised pig jejunum, it was removed and not used for this experiment. Once the half-cells were assembled and mounted (Figure 3.1 F), the cells were filled with transport medium (KRB) and connected to the O₂/CO₂ supply (Figure 3.1 G).

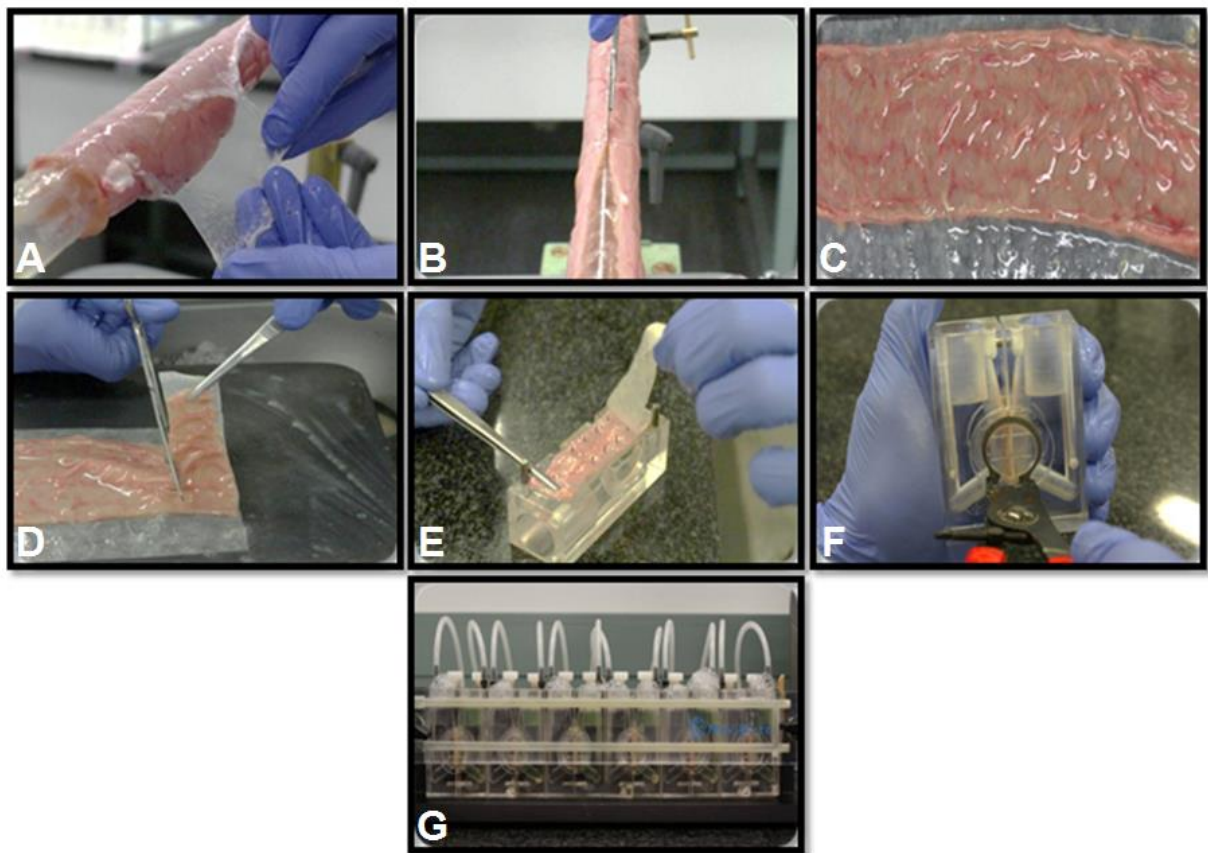


Figure 3.1: Photographs illustrating A) the removal of the serosa from excised jejunum pulled over a glass tube, B) cutting of the jejunum along the mesenteric border, C) removal and placement of the tissue onto wetted filter paper, D) cutting of flattened tissue into equally sized pieces, E) mounting of the tissue pieces on the half-cells with the spikes visible and filter paper on the basolateral side facing up, F) the assembled half-cells with the sir-clips holding the half-cells together and G) the assembled half-cells placed in the diffusion apparatus with Krebs Ringer Bicarbonate buffer in the chambers connected to the O₂/CO₂ supply.

3.9.3 Determining membrane integrity using Lucifer yellow

Lucifer yellow (LY) was used to determine the integrity of the excised pig intestinal tissues. A concentration of 50 µg/ml was applied to the apical chamber of the diffusion chamber. Samples of 200 µl were withdrawn from the basolateral chamber every 20 min over a 2 h period and immediately replaced with the same volume of pre-heated (37°C) KRB buffer solution. The samples were transferred to a Costar® Black 96-well plate and analysed with a validated fluorescence method. The percentage LY transported was then plotted as a function of time to produce a transport graph.

3.9.4 Transport studies across the mounted pig intestinal tissues

Transport of the FD4 (contained within the mini-tablets) across the excised pig jejunum was determined in the apical-to-basolateral direction (intestinal lumen toward the circulatory system) after being exposed to the FD4-containing mini-tablets. The half-cells were filled with 7 ml of KRB (preheated to 37°C to simulate normal human core temperature) after the excised pig intestinal tissues were being mounted on the diffusion apparatus, whilst a mixture of 95% O₂ and 5% CO₂ was allowed to bubble through the buffer allowing the intestinal tissue time to adjust to the new environment (Grass & Sweetana, 1988).

Ten mini-tablets from a specific formulation were placed into the respective apical chambers of the half-cells. Samples (200 µl) were withdrawn from the basolateral chambers of the half-cell block every 20 min over a period of 2 h which was immediately replaced after each withdrawal with KRB buffer solution of the same volume pre-heated to 37°C. The concentration FD4 in each transport sample withdrawn was determined by means of a validated fluorometric analysis method using a SpectraMax® Paradigm® plate reader.

The percentage of FD4 transported across the membranes was plotted as a function of time. Equation 3.11 was utilised to calculate the apparent permeability coefficient values (Hellum & Nilsen, 2008):

$$P_{app} = \frac{dQ}{dt} \times \frac{1}{A \cdot C_0 \cdot 60} \quad (\text{Equation 3.11})$$

P_{app} represents the apparent permeability coefficient (cm/s); $\frac{dQ}{dt}$ (µg/s) represents the increase in the amount of drug in the receiver chamber within a given time period; A (cm²) represents the surface area of the excised tissue and C_0 (µg/ml) the initial FD4 concentration.

3.9.5 Statistical analysis

Data analyses on the transport results were outsourced to Statistical Consultation Services at the North-West University in Potchefstroom. A two-way analysis of variance (ANOVA) was conducted. Based on the presence of 32 degrees of freedom for the data set, ANOVA was deemed suitable for statistical analysis. The F test is robust to violations of normality of variables (provided that there are no outliers) if there are at least 20 degrees of freedom for error in univariate ANOVA (Tabachnick & Fidell, 2001). A Tukey post-hoc test was conducted to determine statistically significant differences between the different treatment groups. Statistically significant differences were accepted when $p < 0.05$.

CHAPTER 4

RESULTS AND DISCUSSION

4.1 Introduction

In this study, a model macromolecular compound (i.e. fluorescein isothiocyanate (FITC)-dextran with an average molecular weight of 4000 Da, FD4) was incorporated into different bead formulations (0.5 mm, 0.75 mm, 1.0 mm and 1.5 mm in diameter, respectively) together with selected absorption enhancers in a matrix system where the beads were compressed into mini-tablets that were loaded into hard gelatine capsules to form multiple-unit drug formulations (MUDFs). The effects of these selected absorption enhancers (i.e. *Aloe vera* gel, *Aloe vera* whole leaf extract and *N*-trimethyl chitosan chloride) were then evaluated in these mini-tablet-in-capsule formulations to ascertain the effects on *ex vivo* drug transport. The beads were prepared by means of extrusion-spheronisation and the produced beads were evaluated with regard to size, morphology and FD4 content and then compressed into mini-tablets. The mini-tablets were evaluated with respect to mass variation, disintegration and friability as well as dissolution and FD4 delivery across excised pig intestinal tissues.

Although the physical properties of the beads and mini-tablets were evaluated and could give some important information regarding the dosage form, it was important to measure the different mini-tablet-in-capsule formulation's ability to deliver a macromolecular model compound (FD4) across excised pig intestinal tissues (proximal jejunum) utilising a Sweetana-Grass diffusion apparatus. The percentage of FD4 transported across the excised intestinal tissue was plotted as a function of time and the apparent permeability coefficient (P_{app}) values were calculated. This could be used as an indication of the effectiveness of the selected drug absorption enhancers as functional excipients in the formulated mini-tablet-in-capsule systems.

4.2 Fluorescence spectrometry method validation

Analyses of LY and FD4 concentrations in assay and transport samples were done by means of fluorescence spectrometry using a SpectraMax® Paradigm® plate reader. In order to validate these analytical methods for these two model compounds, the linearity, accuracy, precision, limit of detection (LOD), limit of quantification (LOQ) and specificity were determined for each model compound.

4.2.1 Linearity

4.2.1.1 Linearity of FITC-dextran 4000 fluorometric analytical method

Figure 4.1 illustrates the standard curve and regression data obtained from the fluorescent values plotted as a function of FD4 concentration.

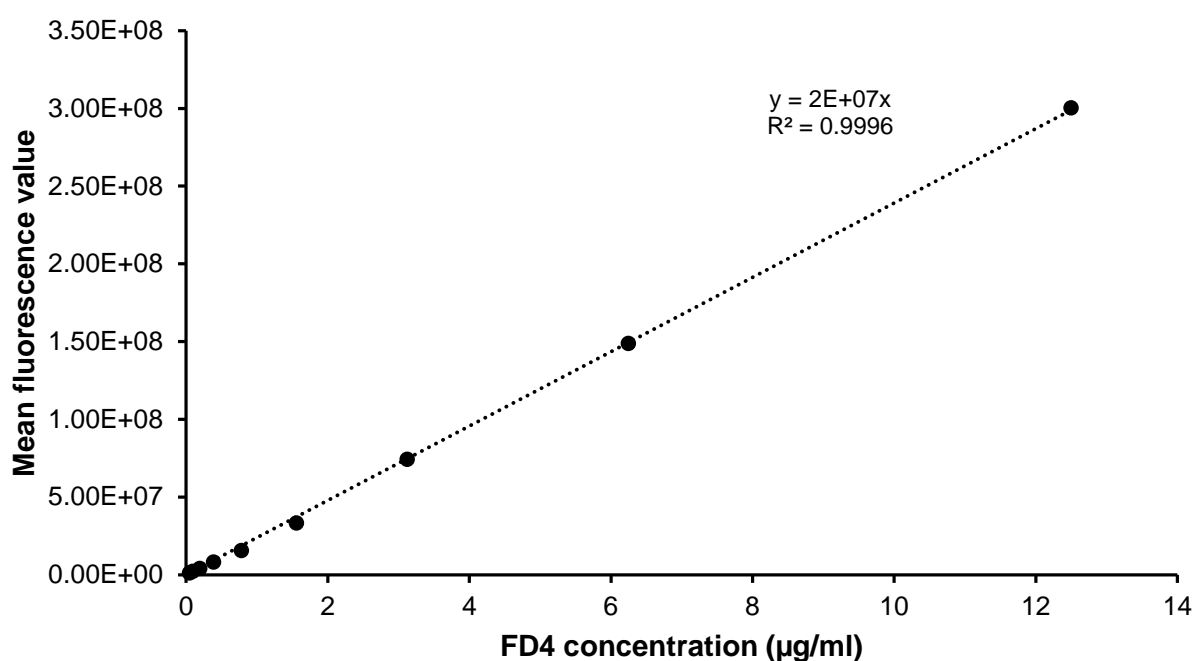


Figure 4.1: Standard curve and regression data for FITC-dextran 4000

The typical fluorescence values as a function of FD4 concentration that were obtained for a standard curve are given in Table 4.1.

Table 4.1: Mean fluorescent values of FITC-dextran 4000 (FD4) over a predetermined concentration range

Concentration FD4 ($\mu\text{g/ml}$)	Mean fluorescent value \pm SD*
0.0488	1004553.96 \pm 17572.55
0.097	2001820.96 \pm 115809.17
0.195	3980940.96 \pm 521376.70
0.39	8000668.29 \pm 322209.92
0.781	15543869.29 \pm 56427.33
1.56	33211844.63 \pm 1033862.33
3.125	74237507.96 \pm 2527519.08
6.25	148665012.00 \pm 746490.75
12.5	300123678.6 \pm 6122970.73

*SD = standard deviation

From Figure 4.1 and Table 4.1, it is clear that the analytical method for FD4 met the requirements as measured for linearity by means of the correlation coefficient (R^2) of the standard curve. The obtained R^2 of 0.9996 is greater than the requirement of ≥ 0.999 and shows that a linear relationship between the fluorescence values and concentration of FD4 exists, as measured by the SpectraMax[®] Paradigm[®] plate reader (Shabir 2004, Singh, 2013).

4.2.1.2 Linearity of Lucifer Yellow (LY) fluorometric analytical method

Figure 4.2 illustrates the standard curve and regression data obtained for LY which depicts the fluorescent values plotted as a function of LY concentration.

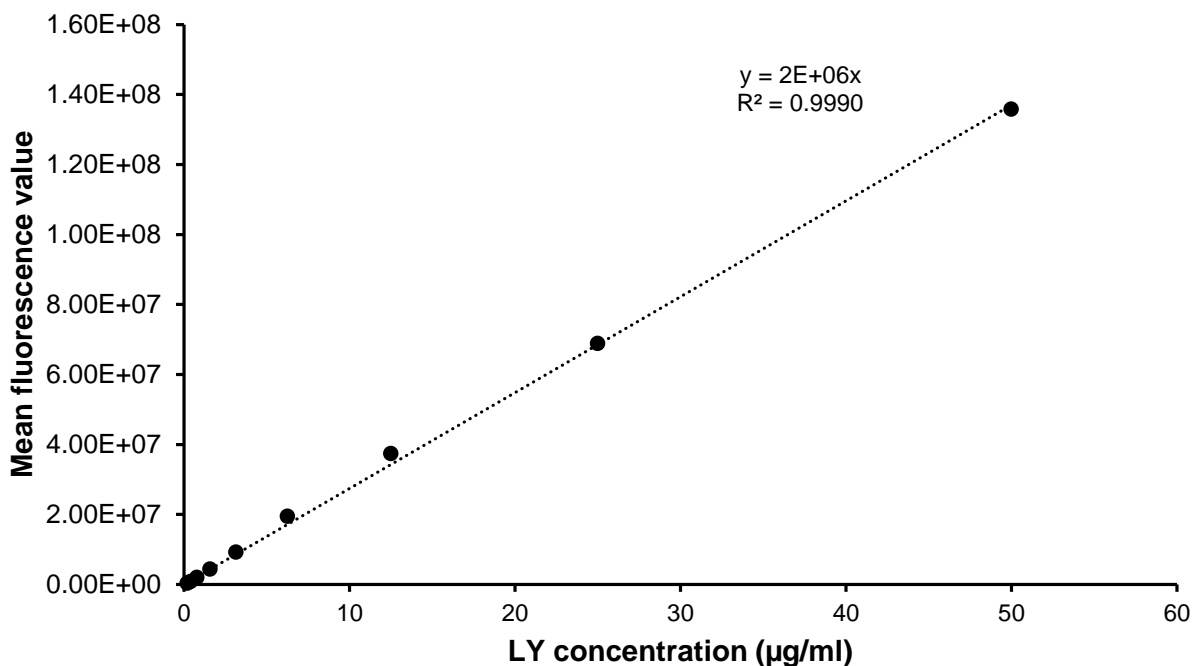


Figure 4.2: Standard curve and regression data for Lucifer Yellow

The typical fluorescence values as a function of LY concentration that were obtained for the standard curve are given in Table 4.2.

Table 4.2: Mean fluorescent values of Lucifer Yellow (LY) over a predetermined concentration range

Concentration LY (µg/ml)	Mean fluorescent value ± SD*
0.195	327615.33 ± 29581.70
0.391	746356.67 ± 102962.97
0.781	1924821.33 ± 187700.28
1.563	4377482.00 ± 184906.84
3.125	9177793.67 ± 886106.88
6.25	19391592.00 ± 1385777.37
12.5	37326864.33 ± 1063908.45
25	68862637.33 ± 2988074.90
50	135735424.00 ± 2791265.26

*SD = standard deviation

From Figure 4.2 and Table 4.2, it is clear that the analytical method for LY met the requirements for linearity as indicated by the correlation coefficient (R^2) of the standard curve.

The obtained R^2 of 0.9990 meets the requirement of ≥ 0.999 and shows that a linear relationship between the fluorescence values and concentration of LY exists, as measured by the SpectraMax[®] Paradigm[®] plate reader (Shabir 2004, Singh, 2013).

4.2.2 Precision

4.2.2.1 Intra-day precision

4.2.2.1.1 FITC-dextran 4000 (FD4) intra-day precision

Table 4.3 indicates the mean fluorescent values as well as the standard deviation (SD) and percentage relative standard deviation (%RSD) values that were calculated from the three FD4 concentrations (i.e. 3.125 $\mu\text{g/ml}$, 6.25 $\mu\text{g/ml}$ and 12.5 $\mu\text{g/ml}$) which were obtained by means of fluorometric analyses at three different time points on the same day for intra-day precision.

Table 4.3: Fluorescence values of FITC-dextran 4000 (FD4) obtained during the intra-day precision measurements, as well as standard deviation and percentage relative standard deviation (%RSD) values

Concentration FD4 ($\mu\text{g/ml}$)	Replicate	Mean fluorescent value	Standard deviation	%RSD
3.125	1	73866172.80	2 798 683.77	3.73
	2	74103493.60		
	3	76236593.78		
6.25	1	150775999.20	4620972.87	3.08
	2	150003508.00		
	3	148068618.40		
12.5	1	305664352.00	9620177.19	3.23
	2	296654374.40		
	3	296828076.80		

From Table 4.3 it is clear that the analytical method complied with the requirement for intra-day precision for FD4 as the %RSD values were < 5% (Shabir, 2004).

4.2.2.1.2 Lucifer Yellow (LY) intra-day precision

Table 4.4 indicates the mean fluorescent values as well as the standard deviation and percentage relative standard deviation (%RSD) values that were calculated from the three LY concentrations (i.e. 12.5 µg/ml, 25 µg/ml and 50 µg/ml) which were obtained by means of fluorometric analyses at three different time points on the same day for intra-day precision.

Table 4.4: Fluorescence values of Lucifer Yellow (LY) obtained during the intra-day precision measurements, as well as standard deviation and percentage relative standard deviation (%RSD) values

Concentration LY (µg/ml)	Repeat	Mean fluorescent value	Standard deviation	%RSD
12.5	1	34265730.40	16 939 662.90	4.79
	2	32503691.20		
	3	36913538.40		
25	1	67718754.80	3143145.51	4.55
	2	69301783.60		
	3	69744942.00		
50	1	133357143.20	209015.23	2.14
	2	139472195.20		
	3	131720249.60		

From Table 4.4 it is clear that the analytical method complied with the requirement for intra-day precision for Lucifer Yellow (LY), as the %RSD values were < 5% (Shabir, 2004).

4.2.2.2.1 FITC-dextran 4000 (FD4) inter-day precision

The fluorescence values of three different FD4 concentrations (i.e. 3.125 µg/ml, 6.25 µg/ml and 12.5 µg/ml) obtained, as well as the calculated standard deviation and %RSD values over a period of three days are illustrated in Table 4.5.

Table 4.5: Fluorescence values of FITC-dextran 4000 (FD4) obtained during the inter-day precision measurements, as well as standard deviation and percentage relative standard deviation (%RSD) values

Concentration FD4 ($\mu\text{g/ml}$)	Replicate	Mean fluorescent value	Standard deviation	%RSD
3.125	1	73866172.80	2708432.40	3.60
	2	76695143.11		
	3	74786018.40		
6.25	1	150775999.20	4447589.29	2.97
	2	149628360.89		
	3	147725850.40		
12.5	1	305664352.00	7817319.73	2.55
	2	307132761.60		
	3	302251526.40		

Table 4.5 illustrates that the analytical method for FD4 complied with the required %RSD of < 5% for inter-day precision (Shabir, 2004).

4.2.2.2.2 Lucifer Yellow (LY) inter-day precision

The fluorescence values of three different concentrations of LY (i.e. 12.5 $\mu\text{g/ml}$, 25 $\mu\text{g/ml}$ and 50 $\mu\text{g/ml}$) obtained, as well as the calculated standard deviation and %RSD values over a period of three days are illustrated in Table 4.6.

Table 4.6: Fluorescence values of Lucifer Yellow (LY) obtained during the inter-day precision measurements, as well as standard deviation and percentage relative standard deviation (%RSD) values

Concentration LY ($\mu\text{g/ml}$)	Replicate	Mean fluorescent value	Standard deviation	%RSD
12.5	1	34265730.40	1580953.86	4.65
	2	33705591.20		
	3	33952931.60		
25	1	67718754.80	2463755.02	3.62
	2	69340924.80		
	3	66676108.80		
50	1	133357143.20	2767824.85	2.03
	2	136219109.60		
	3	138301302.40		

Table 4.6 illustrates that the analytical method for LY complied with the required %RSD of < 5% for inter-day precision (Shabir, 2004).

4.2.3 Limit of detection and limit of quantification

The limit of detection (LOD) and the limit of quantification (LOQ) for FD4 and LY, respectively, were calculated by using the standard deviation (SD) of the fluorescence values of the blank (i.e. the background noise of the solvent (KRB)). Table 4.7 and Table 4.8 show the background noise of the KRB obtained and the SD used to calculate the LOD and LOQ for FD4 and LY, respectively.

Table 4.7: Background noise fluorescence values for FITC-dextran 4000 (FD4)

Background noise	Average	Standard deviation
230254	215425.38	8146.46
204637		
214750		
212336		
217168		
218732		
219476		
206050		

Using the values from Table 4.7, the LOD for FD4 was calculated to be 0.00111 µg/ml and the LOQ as 0.00338 µg/ml. The concentrations of all the FD4 samples determined in this study were higher than the values for LOD and LOQ.

Table 4.8: Background noise fluorescence values for Lucifer Yellow (LY)

Background noise	Average	Standard deviation
243985	224688.00	11722.84
207929		
236341		
221647		
228915		
216776		
226217		
215694		

Using the values from Table 4.8, the LOD for LY was calculated to be 0.0142 µg/ml and the LOQ as 0.0431 µg/ml. All the concentrations of LY determined in this study were higher than the LOD and LOQ values.

4.2.4 Specificity

In order to compensate for possible interferences of the various excipients including functional excipients (i.e. Ac-Di-Sol[®], Kollidon[®] VA 64, Pharmacel[®] 101, magnesium stearate, *Aloe vera* whole leaf extract, *Aloe vera* gel, *N*-trimethyl chitosan chloride and Avicel[®] PH 200) used in the preparation of the beads and subsequent mini-tablets, a standard curve was constructed for FD4 in the presence of these functional excipients (as illustrated by Figure 4.3).

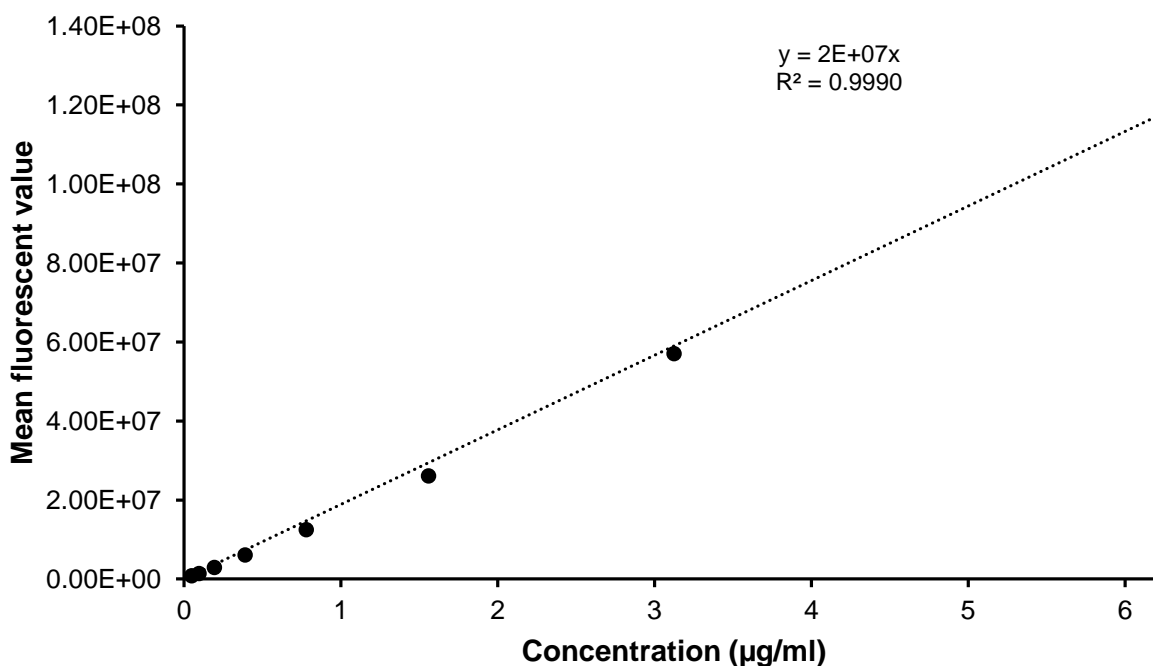


Figure 4.3: Calibration curve for FITC-dextran 4000 (FD4) in the presence of Ac-Di-Sol[®], Kollidon[®] VA 64, Pharmacel[®] 101, magnesium stearate, *Aloe vera* whole leaf extract, *Aloe vera* gel, *N*-trimethyl chitosan chloride and Avicel[®] PH 200

The calibration curve of FD4 in the presence of all these functional excipients presented with an R^2 of 0.9990, which complied with the requirement for linearity.

4.2.5 Accuracy

Accuracy can be defined as the closeness of the measured quantity to that of the theoretical value (Singh, 2013). The recovery of FD4 and LY, respectively, from the prepared solutions with specific concentrations should be between 98% and 102% in order for the analytical method to be deemed accurate. Table 4.9 shows the data obtained for FD4 accuracy, whilst Table 4.10 shows the data obtained for LY accuracy.

Table 4.9: Percentage recovery as an indication of the accuracy of the FITC-dextran 4000 (FD4) fluorometric analytical method

Theoretical concentration of FD4 (µg/ml)	Replicate	Measured concentration of FD4 (µg/ml)	% Recovery	% Mean recovery
3.125	1	3.06	98.07	99.73
	2	3.18	101.82	
	3	3.1	99.29	
6.25	1	6.25	100.09	99.16
	2	6.2	99.33	
	3	6.12	98.06	
12.5	1	12.68	101.45	101.24
	2	12.74	101.94	
	3	12.54	100.32	

The mean recovery values of all three concentrations used to determine the accuracy of FD4 were within the specified range of $100 \pm 2\%$, thus the analytical method for FD4 complied with the requirements for accuracy (Shabir, 2004).

Table 4.10: Percentage recovery as an indication of accuracy of the Lucifer Yellow (LY) fluorometric analytical method

Theoretical concentration (µg/ml)	Replicate	Measured concentration (µg/ml)	% Recovery	% Mean recovery
12.5	1	12.6	100.85	99.99
	2	12.4	99.2	
	3	12.49	99.93	
25	1	24.91	99.65	99.67
	2	25.31	101.24	
	3	24.53	98.12	
50	1	49.06	98.12	100.03
	2	50.11	100.22	
	3	50.88	101.76	

The mean recovery values of all three concentrations used to determine the accuracy of LY were within the specified range of $100 \pm 2\%$, thus the analytical method complied with the requirements for accuracy (Shabir, 2004).

4.2.6 Validation result summary

The fluorometric analytical methods for FD4 and LY using the SpectraMax® Paradigm® plate reader complied with all the required criteria for method validation, which included linearity, precision, LOD, LOQ, accuracy and specificity.

4.3 Bead evaluation

The beads prepared in this study were analysed and subjected to tests in order to verify the content of FD4, to determine and calculate the flow properties, to analyse the particle size distribution and to determine the outside bead morphology and inside structure of each respective bead formulation (0.5 mm, 0.75 mm, 1.0 mm and 1.5 mm diameter beads).

4.3.1 Assay

To determine the experimental quantity of FD4 present within each respective bead formulation, an assay was conducted on each of the four bead formulations. Table 4.11 shows the analysed quantity FD4 contained in each bead formulation (expressed as % of theoretical concentration).

Table 4.11: Average percentage of FITC-dextran 4000 (FD4) in each respective bead formulation

Bead formulation	% of theoretical concentration \pm SD*
0.5 mm	98.85 \pm 0.23
0.75 mm	99.07 \pm 0.18
1.0 mm	98.80 \pm 0.19
1.5 mm	98.73 \pm 0.20

*SD = standard deviation

4.3.2 Flow properties of the beads

In order to determine the flow properties of the prepared beads, a series of parameters or tests was determined, including bulk density, tapped density, Hausner ratio, Carr's index and flow rate. The results of the powder flow properties will be discussed in the following sub-sections.

4.3.2.1 Bulk and tapped density

The bulk and tapped density values for the four bead formulations with different particle sizes were calculated and are shown in Table 4.12.

Table 4.12: Bulk and tapped density values of the bead formulations

Bead formulation size	Bulk density (g/ml)	Tapped density (g/ml)
0.5 mm	0.337 ± 0.020	0.357 ± 0.005
0.75 mm	0.308 ± 0.019	0.322 ± 0.010
1.0 mm	0.240 ± 0.025	0.250 ± 0.007
1.5 mm	0.250 ± 0.030	0.263 ± 0.016

In general, an increase in the values of both bulk and tapped density can be observed with a decrease in bead size although the decrease in the density values seemed to have reached a threshold at a bead size of 1 mm, with only a relatively small change in density at 1.5 mm. The increase in the values of both the bulk and tapped density with a decrease in bead size can be attributed to the differences in packing geometry for the different bead sizes (Aulton, 2018). The smaller the bead diameter, the smaller the bed porosity and the denser the packing of the beads in the bed.

4.3.2.2 Carr's index and Hausner ratio

The bulk and tapped density values were used to calculate Carr's index and Hausner ratio for each bead formulation, respectively, as shown in Table 4.13.

Table 4.13: Carr's index and Hausner ratio of the bead formulations

Bead formulation size	Carr's index	Hausner Ratio
0.5 mm	5.602	1.059
0.75 mm	4.440	1.014
1.0 mm	4.000	1.041
1.5 mm	4.942	1.052

The four bead formulations exhibited a Hausner ratio value of ≤ 1.11 and a Carr's index value of ≤ 10 , which indicates excellent compressibility and flowability which can be attributed to the spherical or almost spherical nature of the beads as a result of the manufacturing method used (Aulton, 2018).

4.3.2.3 Flow rate

The flow rate (expressed as g/s) for each respective bead formulation was determined and the results are shown in Table 4.14.

Table 4.14: Flow rates of the bead formulations

Bead formulation	Flow rate (g/s)
0.5 mm	11.4
0.75 mm	9.6
1.0 mm	7.4
1.5 mm	6.8

The bead formulations exhibited a slower flow rate as the bead size increased, which may be attributed to the larger size beads having to move through the same restrictive opening, thus flowing more difficultly through the orifice although the flow rates could still be considered as adequate.

4.3.3 Particle size analysis

The particle size parameters and results obtained from the Malvern MasterSizer® 2000 of the different bead formulations are summarised in Table 4.17. The particle size parameters used to characterise the bead formulations are d(0.1), d(0.5), d(0.9), D(4,3) and span, which can briefly be explained as follow:

- d(0.1) is the value that indicates the tenth percentile of the particles smaller than this specific value,
- d(0.5) is the value that indicates the median of the particle size distribution,
- d(0.9) is the value that indicates the ninetieth percentile of the particles smaller than this value,
- D(4,3) is the average weighted volume of the particle size distribution, and
- span is an indication of the width of the particle size distribution.

Table 4.15: The particle size analysis results of the different bead formulations

Bead formulation	d(0.1) (μm)	d(0.5) (μm)	d(0.9) (μm)	D(4,3) (μm)	Span
0.5 mm	358.39	493.24	675.55	507.85	0.641
0.75 mm	536.03	743.53	1051.27	774.54	0.693
1.0 mm	714.89	977.74	1345.42	1008.85	0.645
1.5 mm	723.56	1085.99	1561.02	1117.45	0.771

In general, a relatively narrow particle size distribution as indicated by the span values of all the bead formulations is evident in Table 4.15, which can be attributed to the bead manufacturing technique of extrusion-spheronisation. This bead manufacturing method is known to produce uniform beads that have a narrow particle size distribution (Sinha *et al.*, 2009).

4.3.3.1 Beads (0.5 mm) containing FITC-dextran 4000

The results obtained from the particle size analysis on the Mastersizer[®] 2000 apparatus is shown in Figure 4.4. The bead particle size parameters for this bead formulation were as follows: 358.39 μm (d(0.1)) to 675.55 μm (d(0.9)), with a median distribution value (d(0.5)) of 493.24 μm . The average particle size (D(4,3)) of this bead formulation was 507.85 μm , which was close to the sieve size of 500 μm used during extrusion. The span of the distribution was 0.641, which is representative of a narrow particle size distribution.

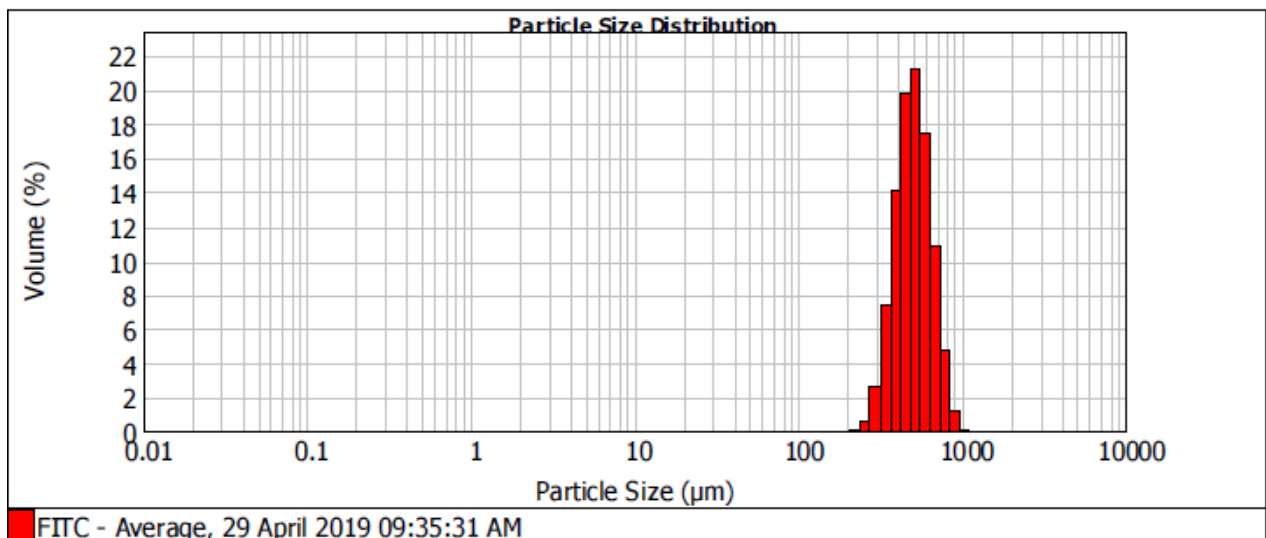


Figure 4.4: Typical percentage frequency distribution plot of the particle size distribution of the bead (0.5 mm) formulation containing FITC-dextran 4000

4.3.3.2 Beads (0.75 mm) containing FITC-dextran 4000

The results obtained from the particle size analysis on the Mastersizer[®] 2000 apparatus is shown in Figure 4.5. This indicates that the distribution parameters ranged from 536.03 μm ($d(0.1)$) to 1051.27 μm ($d(0.9)$) with a median distribution value ($d(0.5)$) of 743.53 μm . The average particle size value ($D(4,3)$) was 774.54 μm , which is relatively close to the intended bead size of 750 μm . The span of the distribution was 0.693, which is representative of a relatively narrow particle size distribution.

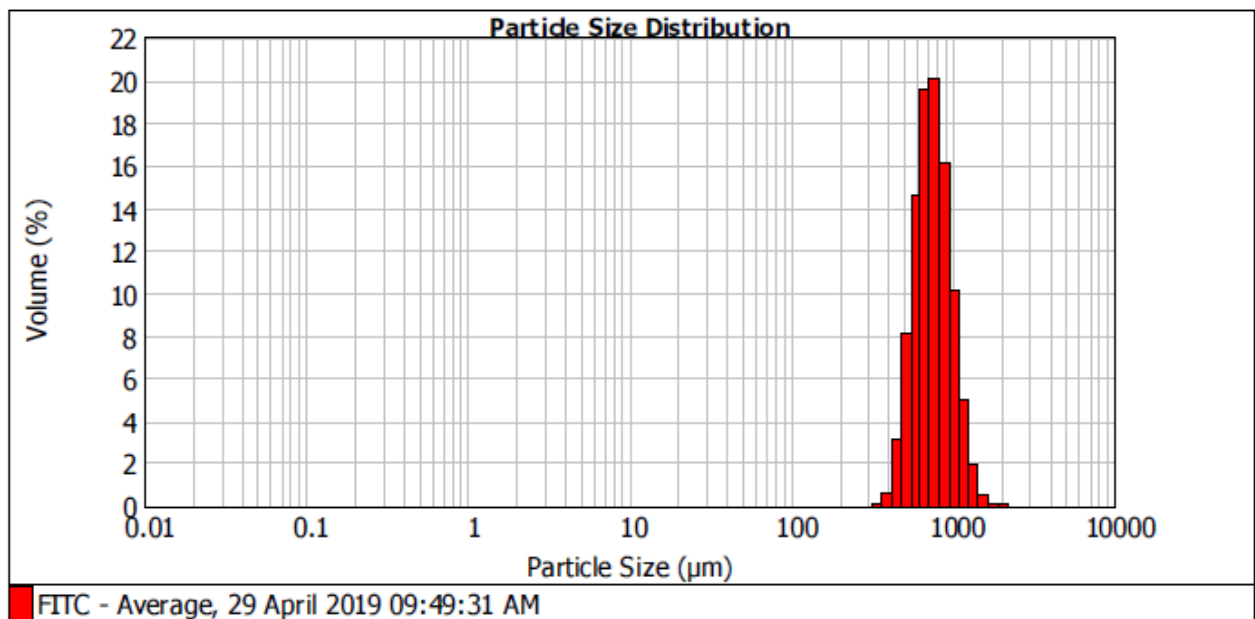


Figure 4.5: Typical percentage frequency distribution plot of the particle size distribution of the bead (0.75 mm) formulation containing FITC-dextran 4000

4.3.3.3 Beads (1.0 mm) containing FITC-dextran 4000

Figure 4.6 shows the percentage frequency distribution plot of the 1.0 mm bead formulation. The obtained results show that the distribution parameters ranged from 714.89 μm ($d(0.1)$) to 1345.42 μm ($d(0.9)$) with a median value ($d(0.5)$) of 977.74 μm . The average particle size value ($D(4,3)$) was 1008.85 μm , which is close to the intended bead size. The span of distribution was 0.645, which indicates a narrow particle size distribution.

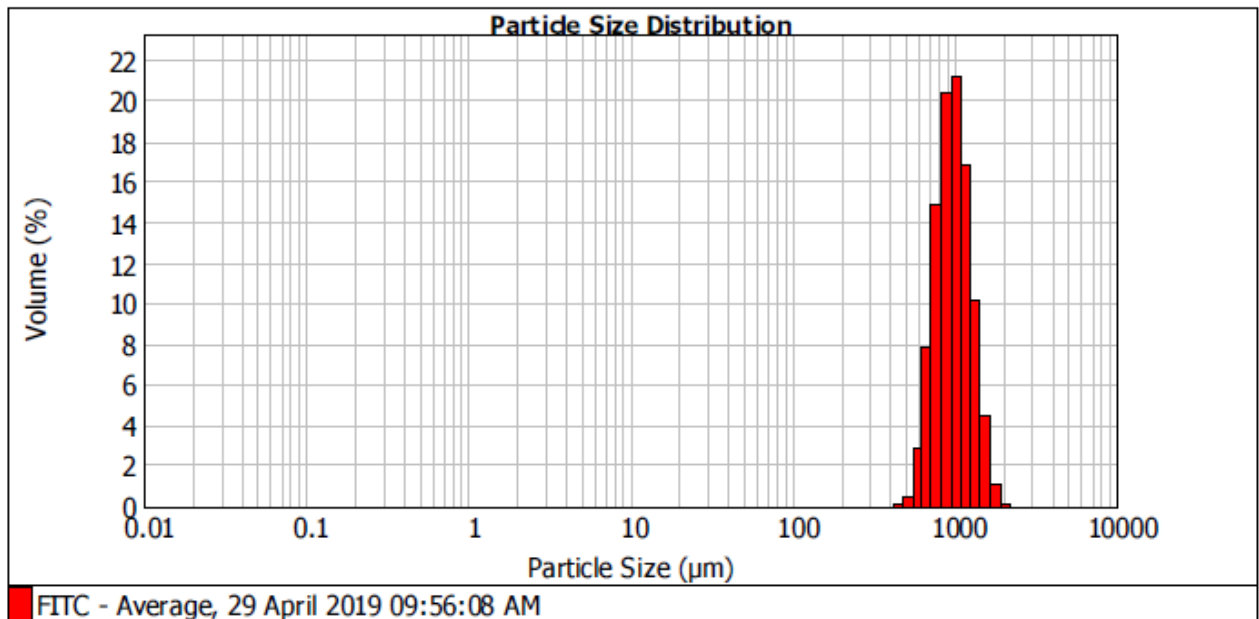


Figure 4.6: Typical percentage frequency distribution plot of the particle size distribution of the bead (1.0 mm) formulation containing FITC-dextran 4000

4.3.3.4 Beads (1.5 mm) containing FITC-dextran 4000

The percentage frequency distribution plot of the particle size distribution of the 1.5 mm beads is shown in Figure 4.7. The obtained results show that the distribution parameters ranged from 723.56 μm ($d(0.1)$) to 1561.02 μm ($d(0.9)$) with a median value ($d(0.5)$) of 1085.99 μm . The average particle size value ($D(4,3)$) was 1117.45 μm , which was not as close to the intended bead size in contrast to the other bead formulations. The span of the distribution was 0.771, which is indicative of a relatively narrow particle distribution although the span value for the distribution of this bead size was larger in comparison to the other bead sizes. The larger span value, in conjunction with the ($d(0.9)$) of 1561.02 μm , indicate that although the average particle size is not as close to the intended bead size as the other formulations, the particle size distribution was considered suitable for further experiments.

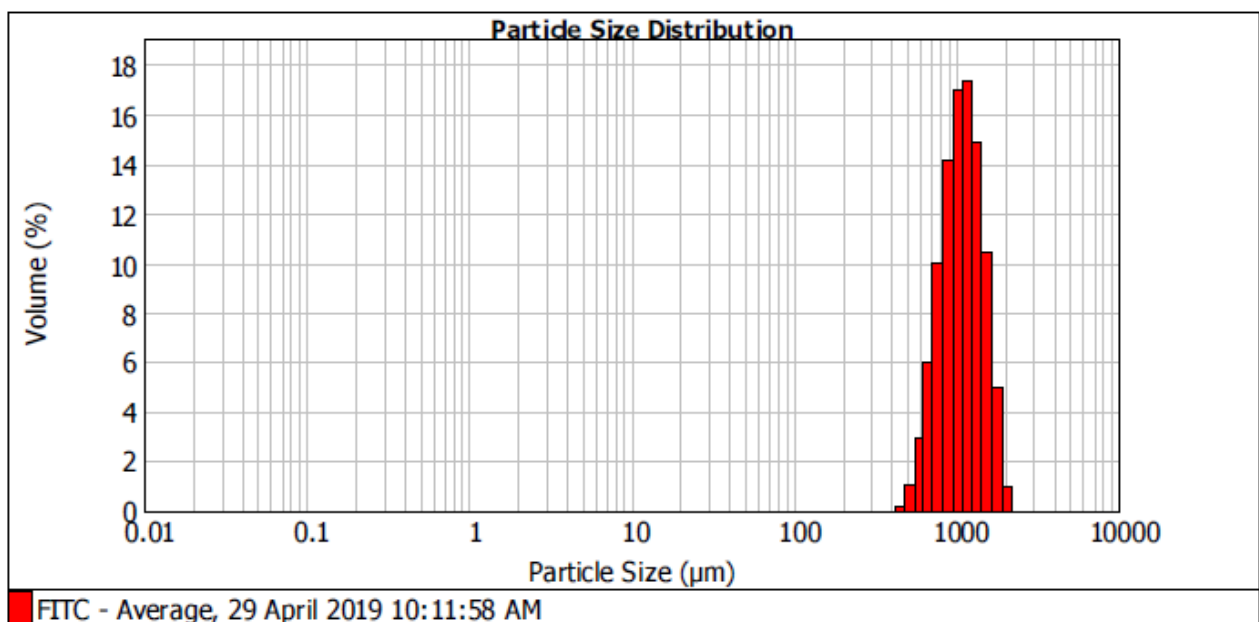


Figure 4.7: Typical percentage frequency distribution plot of the particle size distribution of the bead (1.5 mm) formulation containing FITC-dextran 4000

4.3.4 Bead morphology and internal structure

Figure 4.8 illustrates the bead morphology and internal structure of the various sized bead formulations, which all exhibited a spherical shape and smooth surface. The internal structures all exhibited a tightly packed core with a visible fibrous appearance.

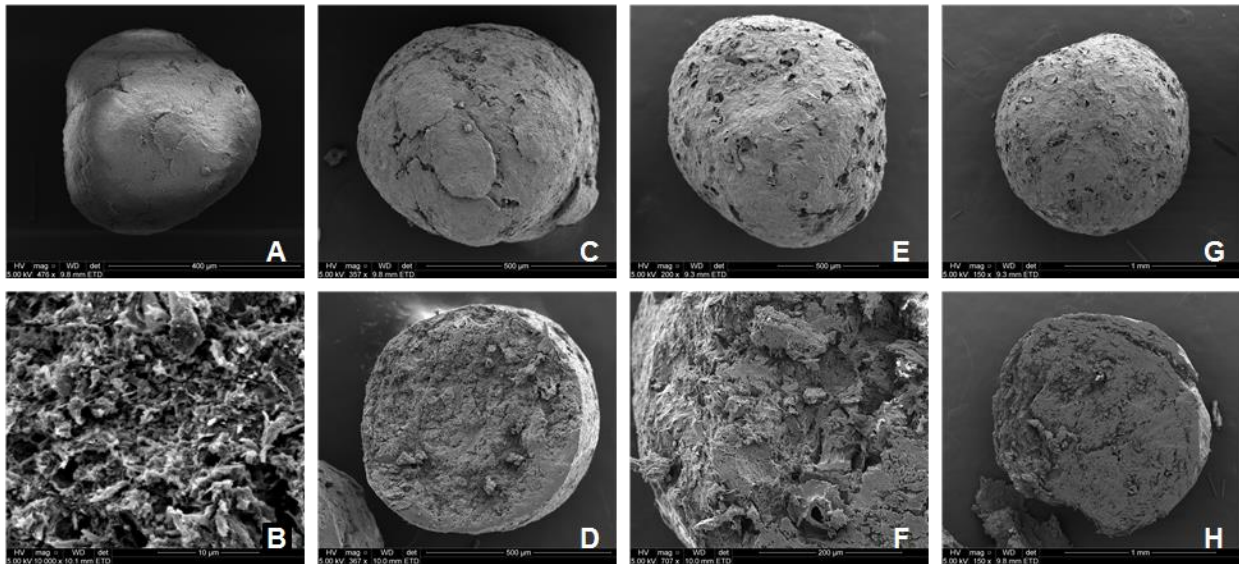


Figure 4.8: Micrographs illustrating the morphology and internal structures of the various bead formulations produced by means of extrusion-spheronisation; A) 0.5 mm bead morphology, B) 0.5 mm bead internal structure, C) 0.75 mm morphology, D) 0.75 mm internal structure, E) 1.0 mm bead morphology, F) 1.0 mm bead internal structure, G) 1.5 mm bead morphology and H) 1.5 mm bead internal structure

4.4 Chemical characterization of *N*-trimethyl chitosan chloride with proton nuclear magnetic resonance

Figure 4.9 shows the $^1\text{H-NMR}$ spectrum of *N*-trimethyl chitosan chloride (TMC).

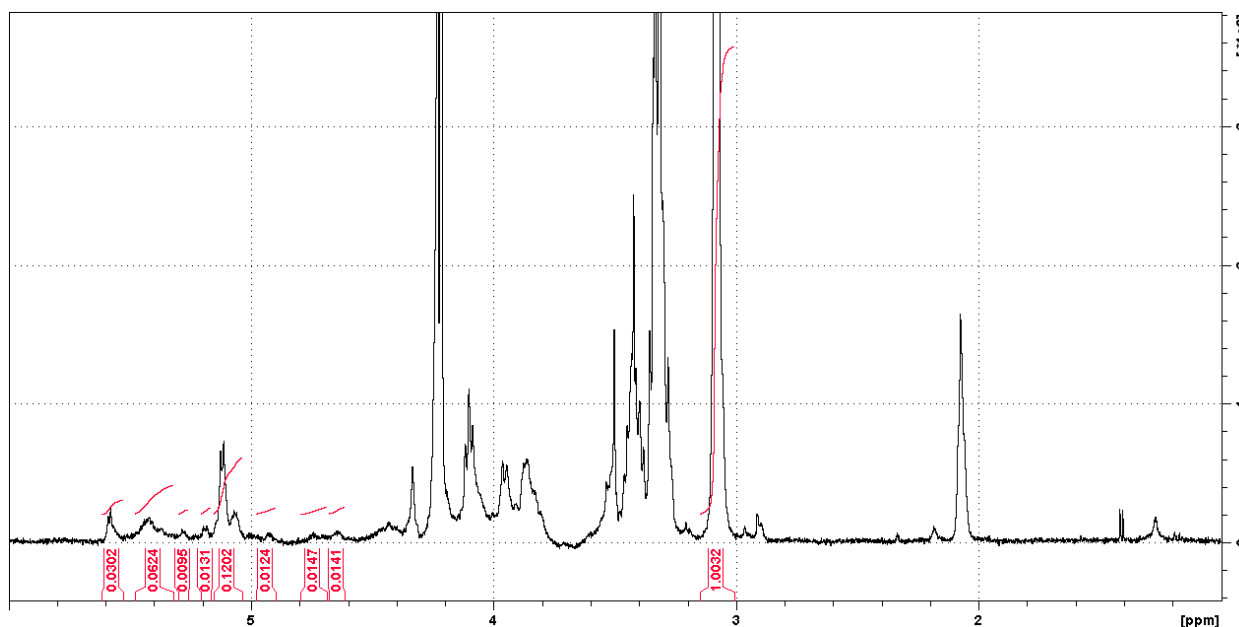


Figure 4.9: $^1\text{H-NMR}$ spectrum of *N*-trimethyl chitosan chloride

$$\begin{aligned}\text{Degree of Quaternisation} &= \left[\frac{[\text{N}(\text{CH}_3)_3]}{[\text{H-1}]} \times \frac{1}{9} \times 100 \right] \\ &= \left[\frac{1.0032}{0.2766} \times \frac{1}{9} \times 100 \right] \\ &= 40.298\% \approx 40.3\%\end{aligned}$$

The degree of quaternisation of the TMC used in this study as an absorption enhancer was calculated as 40.3%. According to studies conducted by Hamman *et al.* (2002), an increase in the degree of quaternisation increases the absorption enhancing capabilities of TMC, with the optimal degree of quaternisation being reached at 48% (Hamman *et al.*, 2002). Thus, the TMC used in this study as absorption enhancer was relatively close to the optimal degree of quaternisation for drug absorption enhancement.

4.5 Evaluation of mini-tablets

Mini-tablets (5 mm in diameter) were produced from the various bead formulations in combination with different absorption enhancers (i.e. *Aloe vera* gel and whole leaf materials and TMC). Avicel® PH 200 and magnesium stearate were incorporated as diluent and lubricant, respectively. These mini-tablets were subjected to evaluation testing and the results of this evaluation testing are presented and discussed in the following subsections.

4.5.1 Mass variation

Ten mini-tablets of each respective formulation were weighed and the weights were noted. The mini-tablets were produced at a formulated mass of 50 mg per mini-tablet and according to the BP (BP, 2019), if a tablet weighs less than 80 mg, the mass may not vary more than 10% of the original intended mass, thus in this case the parameters were 50 mg \pm 10% (not less than 45 mg and not more than 55 mg per tablet). In this case, 10 mini-tablets were taken at random to be weighed individually contrary to 20 tablets as specified in the BP. The rationale for this deviation was based on the design of the multiple-unit dosage form in this study (10 mini-tablets were used per hard gelatine capsule).

Table 4.16: Average mass and standard deviation of the different mini-tablet formulations containing FITC-dextran 4000 (FD4) and different absorption enhancers

Mini-tablet formulation	Average mass and standard deviations of the mini-tablets (mg)			
	Bead size			
	0.5 mm	0.75 mm	1.0 mm	1.5 mm
Control (FD4 alone)	51.86 \pm 0.88	53.91 \pm 0.35	51.2 \pm 0.72	50.12 \pm 0.56
<i>Aloe vera</i> gel (AVG)	51.01 \pm 0.56	53.92 \pm 0.43	52.02 \pm 0.73	48.75 \pm 1.27
<i>Aloe vera</i> whole leaf extract (AVW)	51.64 \pm 0.72	54.05 \pm 0.41	51.71 \pm 0.73	50.38 \pm 0.51
<i>N</i> -trimethyl chitosan chloride (TMC)	51.53 \pm 0.93	50.95 \pm 0.29	51.08 \pm 0.51	50.22 \pm 0.64

Table 4.16 illustrates the average mass of the mini-tablets prepared from the various sized bead formulations. It is clear that the mini-tablet formulations all complied with the parameters specified by the BP, as none of the formulations deviated by more than 10% from the average tablet mass.

4.5.2 Friability

The mini-tablets were subjected to the friability test as per BP specifications (BP, 2019). Ten mini-tablets were dusted, weighed and placed in the drum of the Erweka® friabilator, which rotated at 25 revolutions per minute for 4 min after which the mini-tablets were dusted and weighed again. This test was conducted for each formulation of mini-tablets. As seen in Table 4.17, all the mini-tablet formulations complied with the parameters for the friability test. It is important to note that none of the mini-tablets exhibited a percentage friability of more than 1.0%, thus complying with the specifications set by the BP.

Table 4.17: Percentage friability of the mini-tablet formulations

Mini-tablet formulation	Percentage friability of the mini-tablets			
	Bead size			
	0.5 mm	0.75 mm	1.0 mm	1.5 mm
Control	0.47	0.53	0.61	0.40
<i>Aloe vera</i> gel (AVG)	0.35	0.62	0.60	0.70
<i>Aloe vera</i> whole leaf extract (AVW)	0.49	0.54	0.27	0.62
<i>N</i> -trimethyl chitosan chloride (TMC)	0.28	0.55	0.53	0.56

4.5.3 Disintegration

The disintegration test was conducted on the mini-tablet-in-capsule dosage forms, which consisted of ten mini-tablets stacked inside a hard gelatine capsule (size 0). The BP (2019) specifies that there should be no debris left on the sieve of the disintegration apparatus chamber after 15 min have passed during the disintegration test. This test was conducted on all the mini-tablet-in-capsule formulations and the results are shown in Table 4.18. The results indicate that all the mini-tablet formulations disintegrated within the time parameter as specified by the BP, thus complying with the specifications for disintegration for solid oral dosage forms.

Table 4.18: Average disintegration time of the various mini-tablet-in-capsule formulations

Mini-tablet formulation	Average disintegration time and standard deviation of the mini-tablets (s)			
	Bead size			
	0.5 mm	0.75 mm	1.0 mm	1.5 mm
Control	521 ± 182	494 ± 68	338 ± 31	515 ± 213
<i>Aloe vera</i> gel (AVG)	482 ± 50	462 ± 70	473 ± 46	548 ± 122
<i>Aloe vera</i> whole leaf extract (AVW)	491 ± 47	459 ± 62	510 ± 146	553 ± 36
<i>N</i> -trimethyl chitosan chloride (TMC)	375 ± 18	394 ± 17	305 ± 31	338 ± 9

4.6 Dissolution studies

The dissolution tests were conducted on three mini-tablet-in-capsule systems from each formulation (i.e. in triplicate). The dissolution profiles of the different mini-tablet-in-capsule formulations are presented in Figure 4.10 – 4.14 in the sub-sections below. The area under the curve (AUC) values of the dissolution curves as well as mean dissolution time (MDT) values of the different formulations are presented in Table 4.19. A smaller MDT value indicates an overall faster dissolution rate over the entire dissolution period.

Table 4.19: Area under curve (AUC) and mean dissolution time (MDT) of all the mini-tablet-in-capsule systems

Bead size (mm)	Formulation	Average AUC₀₋₂₄₀ ($\mu\text{g/ml}\cdot\text{min}$)	MDT (min)
0.5	Control	339.70 \pm 1.78	34.49 \pm 0.69
	AVG	335.71 \pm 0.53	41.62 \pm 1.27
	AVW	327.98 \pm 2.69	44.70 \pm 1.62
	TMC	343.61 \pm 0.84	37.01 \pm 0.80
0.75	Control	352.13 \pm 1.03	36.31 \pm 0.09
	AVG	324.20 \pm 2.48	54.21 \pm 2.27
	AVW	325.20 \pm 2.12	55.89 \pm 1.03
	TMC	347.04 \pm 0.86	34.99 \pm 1.48
1.0	Control	353.62 \pm 0.40	27.51 \pm 0.21
	AVG	313.93 \pm 3.17	51.50 \pm 1.34
	AVW	315.80 \pm 2.67	57.65 \pm 3.03
	TMC	360.02 \pm 2.22	33.48 \pm 1.00
1.5	Control	335.96 \pm 2.02	33.58 \pm 0.55
	AVG	306.62 \pm 1.72	51.19 \pm 0.95
	AVW	308.39 \pm 2.07	50.81 \pm 2.39
	TMC	320.57 \pm 0.94	45.31 \pm 0.65

4.6.1 Dissolution studies conducted on the mini-tablet-in-capsule formulations containing 0.5 mm bead mini-tablets

Dissolution profiles of the different mini-tablet-in-capsule formulations prepared from the 0.5 mm diameter beads, containing the respective absorption enhancers, are depicted in Figure 4.10.

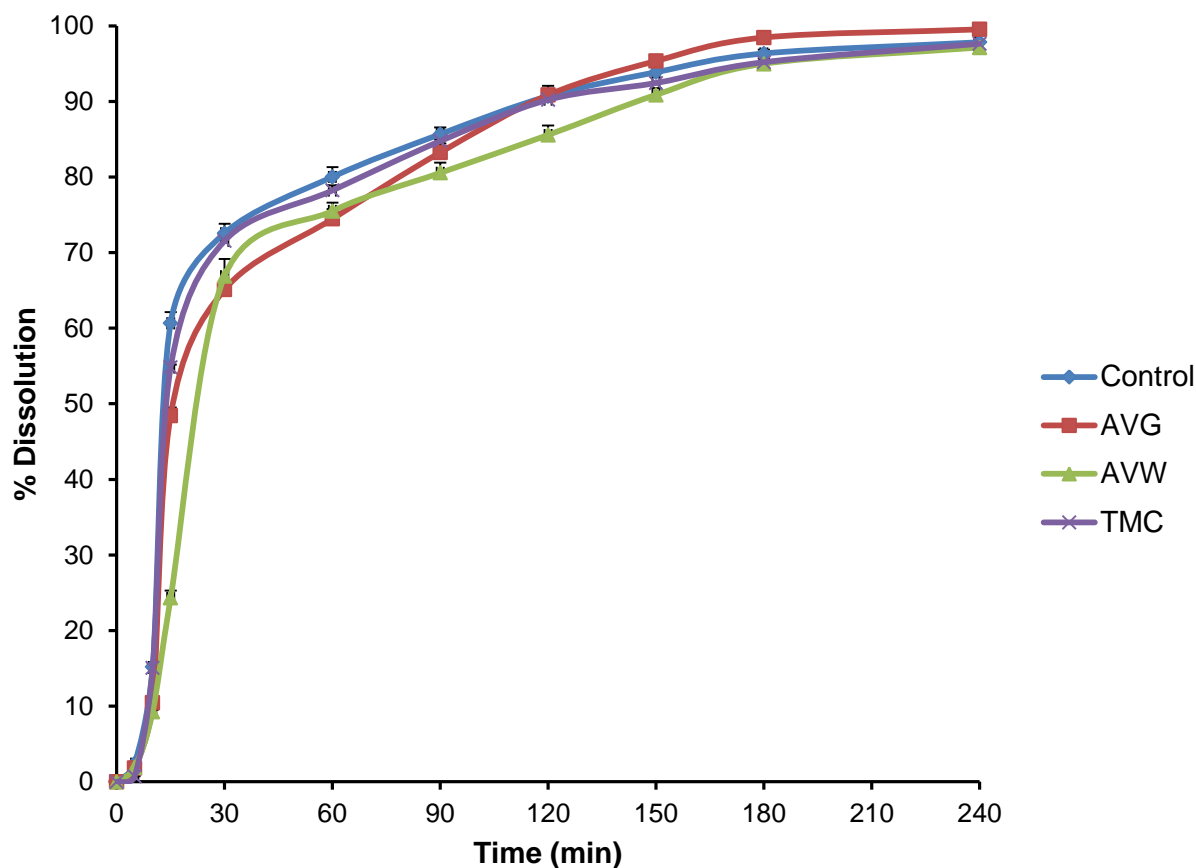


Figure 4.10: Percentage dissolution of FITC-dextran 4000 from the mini-tablet-in-capsule formulations containing 0.5 mm bead mini-tablets with no absorption enhancer (Control), *Aloe vera* gel (AVG), *Aloe vera* whole leaf extract (AVW) and *N*-trimethyl chitosan chloride (TMC)

All the mini-tablet-in-capsule formulations prepared from the 0.5 mm diameter beads, irrespective of the absorption enhancer it contains, exhibited > 80% FD4 release within 120 min. Furthermore, the extent of FD4 release for the different formulations as indicated by the AUC values (AUC_{0-240}) varied within a relatively small range, which varied from 327.98 ± 2.69 $\mu\text{g/ml}\cdot\text{min}$ to 343.61 ± 0.84 $\mu\text{g/ml}\cdot\text{min}$.

It is clear from the different profiles seen in Figure 4.10 that the AVW-containing formulation followed by the AVG-containing formulation exhibited the slowest FD4 release as indicated by the higher MDT values. The AVW-containing formulation and AVG-containing formulation had MDT values of 44.70 ± 1.62 min and 41.62 ± 1.27 min, respectively, as opposed to 34.49 ± 0.69 min for the control formulation. This can be explained by the fact that *A. vera* gel increased the viscosity of the aqueous pores in the matrices of the FD4 containing beads as a consequence of its gelling behaviour due to the presence of large polysaccharides molecules (de Bruyn *et al.*, 2018; Hamman, 2008).

The formation of a gel layer surrounding solid particles such as beads as well as in the aqueous pores in the bead matrices result in a decreased diffusion rate of dissolved FD4 molecules and therefore a slower dissolution rate and release from the formulations containing AVG, which resulted in higher MDT values. The control formulation exhibited the fastest drug release from the mini-tablet-in-capsule formulation as there is no polymer in this formulation that can contribute to an increase in the viscosity of the diffusion layer surrounding the solid particles. The TMC-containing mini-tablet-in-capsule formulation exhibited a dissolution profile similar to that of the control formulation. Although TMC (a polysaccharide) also has the ability to increase viscosity due to its polymeric nature, it is evident that this effect did not occur to the same extent as the MDT value of the TMC-containing formulation was similar to the MDT value of the control formulation (37.01 ± 0.80 min and 34.49 ± 0.69 min respectively). This may be explained by a decrease in molecular size of chitosan during the synthesis of TMC and the effect of TMC on viscosity seemed not pronounced at the concentration investigated in this study.

4.6.2 Dissolution studies conducted on the mini-tablet-in-capsule formulations containing 0.75 mm bead mini-tablets

Dissolution profiles of the different mini-tablet-in-capsule formulations prepared from the 0.75 mm diameter beads, containing the respective absorption enhancers, are depicted in Figure 4.11.

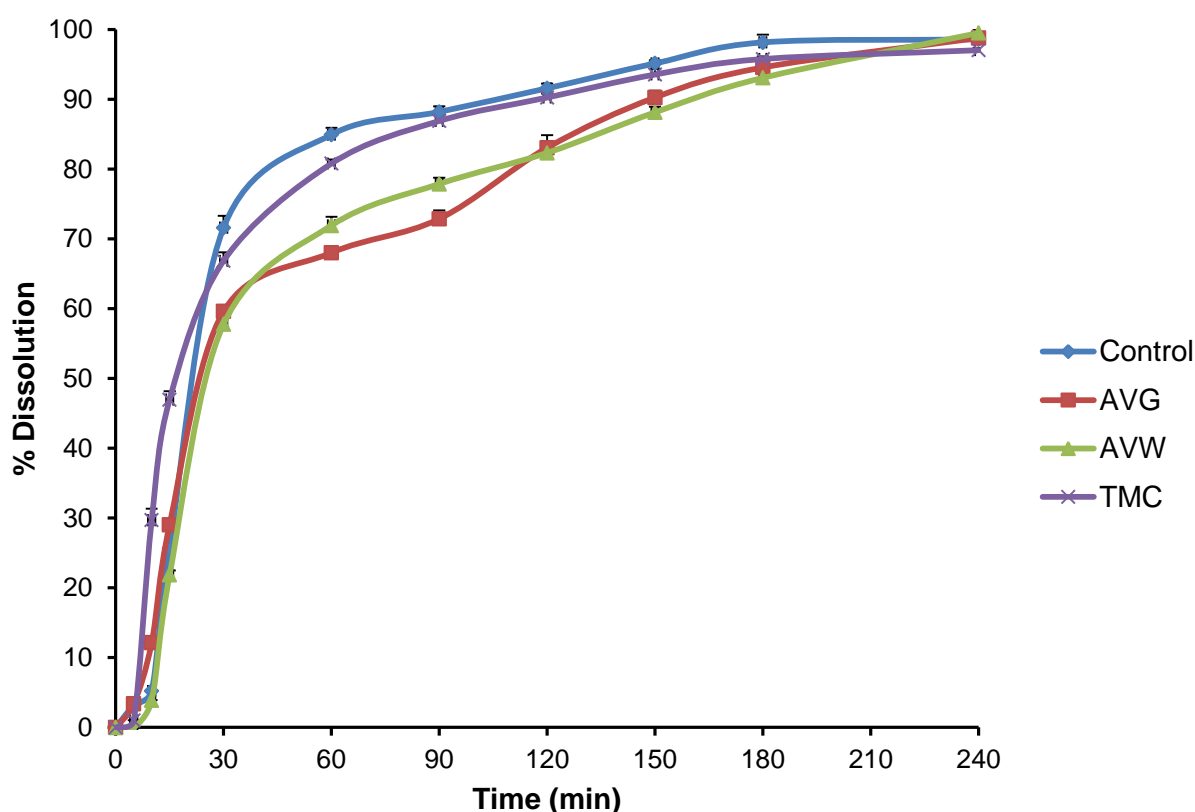


Figure 4.11: Percentage dissolution of FITC-dextran 4000 from the multiple unit dosage forms containing 0.75 mm bead mini-tablets with no absorption enhancer (Control), *Aloe vera* gel (AVG), *Aloe vera* whole leaf extract (AVW) and *N*-trimethyl chitosan chloride (TMC)

In general, similar dissolution trends were obtained for the mini-tablet-in-capsule formulations prepared from the 0.75 mm diameter bead formulations to those observed for the 0.5 mm bead formulations. Once again, it is evident that the *A. vera* gel and whole leaf containing formulations exhibited the slowest dissolution rate for the mini-tablet-in-capsule formulations prepared from the 0.75 mm diameter formulations. This is evident from the higher MDT values of the AVW and AVG formulations (55.89 ± 1.03 min and 54.21 ± 2.27 min, respectively) in comparison to the MDT value of 36.31 ± 0.09 min for the control formulation.

However, the difference in dissolution rate between the *A. vera* gel and whole leaf formulations was not pronounced. The control and TMC-containing mini-tablet-in-capsule formulations exhibited comparable dissolution rates as indicated by MDT values of 36.31 ± 0.09 min and 34.99 ± 1.48 min, respectively. With regard to the extent of FD4 release, all the formulations rendered AUC values within a relatively small range, which stretched from 324.40 ± 2.48 $\mu\text{g/ml}\cdot\text{min}$ to 352.13 $\mu\text{g/ml}\cdot\text{min}$. However, the extent of the FD4 release (AUC_{0-240}) for the *A. vera*-containing formulations was slightly lower in comparison to the control. Albeit, this difference was less than 10% between both *A. vera*-containing formulations and the control formulation.

4.6.3 Dissolution studies conducted on the mini-tablet-in-capsule formulations containing 1.0 mm bead mini-tablets

Dissolution profiles of the different mini-tablet-in-capsule formulations prepared from the 1.0 mm diameter beads, containing the respective absorption enhancers, are depicted in Figure 4.12.

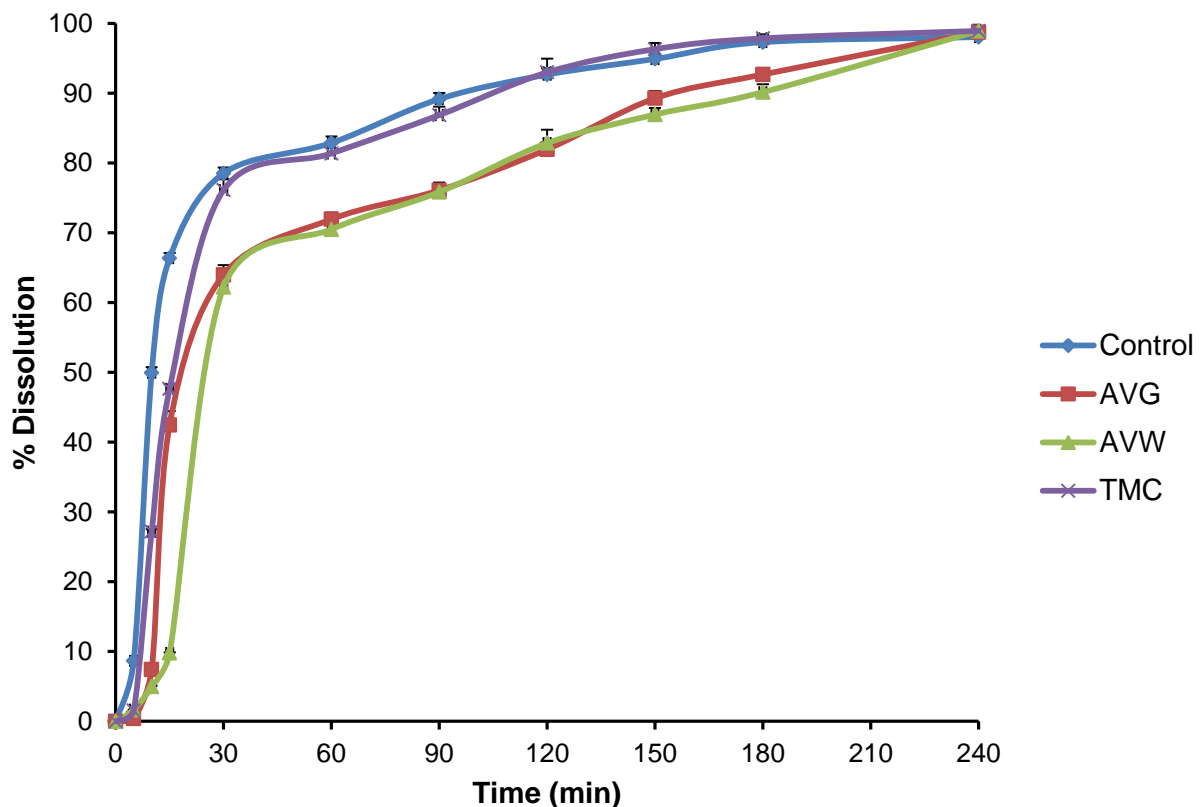


Figure 4.12: Percentage dissolution of FITC-dextran 4000 from the multiple unit dosage forms containing 1.0 mm bead mini-tablets with no absorption enhancer (Control), *Aloe vera* gel (AVG), *Aloe vera* whole leaf extract (AVW) and *N*-trimethyl chitosan chloride (TMC)

It is evident from Figure 4.12 that, similar to the formulations prepared from the 0.5 mm and 0.75 mm diameter beads, the control and TMC formulations prepared from the 1.0 mm beads exhibited faster FD4 release in comparison to the *A. vera* gel and whole leaf containing formulations. Once again the MDT values for the control and TMC-containing formulations were relatively close with MDT values of 27.51 ± 0.21 min and 33.48 ± 1.00 min, respectively. Furthermore, similar to the 0.5 mm and 0.75 mm diameter bead formulations, the release of FD4 from the *A. vera* gel and whole leaf containing mini-tablet-in-capsule formulations was notably slower with MDT values of 57.65 ± 3.03 min and 51.50 ± 1.34 min, respectively.

As indicated previously, this is most probably due to the gelling behaviour of the *A. vera* materials incorporated into the formulations. This can be explained by a decrease in the diffusion coefficient as a result of increased viscosity, which decreases the initial FD4 release from the mini-tablet-in-capsule formulations. With regard to the extent of FD4 release, AUC_{0-240} values ranged from 313.93 ± 3.17 $\mu\text{g/ml}\cdot\text{min}$ to 360.02 ± 2.22 $\mu\text{g/ml}\cdot\text{min}$. Similar to the mini-tablet-in-capsule formulations prepared from 0.75 mm diameter beads; the extent of the FD4 release (AUC_{0-240}) for the *A. vera*-containing formulations was lower in comparison to the control. This difference was approximately 11% for both *A. vera*-containing formulations from that of the control formulation.

4.6.4 Dissolution studies conducted on the mini-tablet-in-capsule formulations containing 1.5 mm bead mini-tablets

Dissolution profiles of the different mini-tablet-in-capsule formulations prepared from the 1.5 mm diameter beads, containing the respective absorption enhancers, are depicted in Figure 4.13.

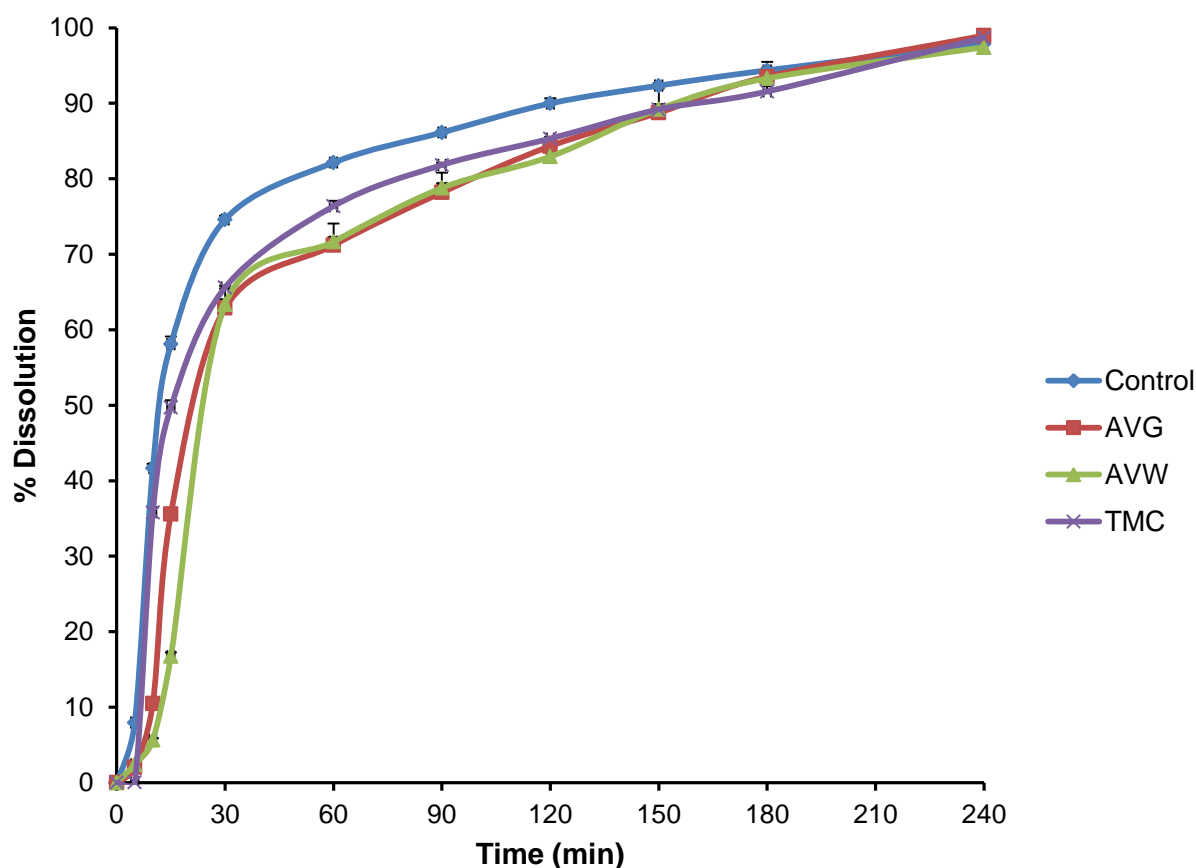


Figure 4.13: Percentage dissolution of FITC-dextran 4000 from the multiple unit dosage forms containing 1.5 mm bead mini-tablets with no absorption enhancer (Control), *Aloe vera* gel (AVG), *Aloe vera* whole leaf extract (AVW) and *N*-trimethyl chitosan chloride (TMC)

In agreement with the dissolution results observed with the mini-tablet-in-capsule formulations prepared from the three other diameter sized beads, *A. vera*-containing formulations prepared with 1.5 mm beads exhibited higher MDT values than that of the control. The MDT value of the AVG and AVW formulations (51.19 ± 0.95 min and 50.81 ± 2.39 min, respectively) were approximately 1.5 times higher than that of the control indicating a marked difference in dissolution rate between the *A. vera*-containing formulations and the control formulation for the 1.5 mm bead formulations.

With regard to the extent of FD4 release, all formulations containing absorption enhancers exhibited AUC_{0-240} values ranging from $306.62 \pm 1.72 \mu\text{g/ml.min}$ to $320.57 \pm 0.94 \mu\text{g/ml.min}$ compared to that of the control ($335.96 \pm 2.02 \mu\text{g/ml.min}$).

4.6.5 Effect of bead size on dissolution

In general it is evident that for the *A. vera* material-containing formulations an increase in bead size resulted in an increase in dissolution time as indicated by the higher MDT values (Table 4.19). This effect was observed for both AVG and AVW containing mini-tablet-in-capsule formulations. This may be attributed to both the surface area of the bead exposed to the dissolution medium as well as the effect of *A. vera* on the viscosity of the diffusion layer and aqueous pores in the matrices. The smaller a bead, the larger the area available for dissolution as illustrated by a modified equation of Noyes and Whitney. The larger the area available for dissolution, the faster the dissolution rate as there exists a direct proportionality between surface area and dissolution rate (Dukić-Ott *et al.*, 2009; Patadia *et al.*, 2013). The effect of bead size on the dissolution rate of FD4 was more pronounced for the *A. vera*-containing formulations but less pronounced for the differently sized control formulations and TMC-containing formulations. This may to some extent be explained by the viscosity enhancing properties of the *A. vera* materials, which is less pronounced in the smaller beads due to the smaller volume of their matrices. The larger beads have larger volume matrices and a viscosity enhancing effect will delay diffusion and therefore release of the FD4 more pronouncedly due to the longer distance of FD4 molecule diffusion through the matrices of the larger particles.

The effect of bead size on the dissolution rate of FD4 was not clearly seen in the control mini-tablet-in-capsule formulations and to a much lesser extent on the TMC-containing formulations. This can possibly partially be explained by the high solubility properties of FD4. FD4 is freely soluble in water and it is well known that the effect of particle size and therefore bead size on dissolution rate is usually of higher consequence for poorly soluble compounds (Florence & Attwood, 1988). Therefore, the relatively low influence of bead size on the dissolution rate of FD4 in the control formulations may be attributed to the excellent solubility of FD4 in water (TdB Consultancy, 2016). It is also evident that the influence of bead size on the dissolution rate of FD4 from the *A. vera*-containing formulations reached a threshold in mini-tablet-in-capsule formulations prepared with beads at a diameter of 1.0 mm. This means a difference in dissolution rate was only evident for bead sizes smaller than 1.0 mm in diameter. This is in agreement with results obtained with multiple-unit pellet system (MUPS) tablets prepared from different sized beads in a previous study (Hamman *et al.*, 2019).

4.6.6 Dissolution study conclusion

The control formulation showed the highest FD4 release, irrespective of bead size, when compared to the formulations containing drug absorption enhancers. The differences in FD4 release can possibly be attributed to the viscosity enhancing effects of the *A. vera* gel and whole leaf materials, which not only increased the diffusion layer around the beads but also within the bead matrices.

4.7 Ex vivo transport studies

Ex vivo transport studies were conducted on excised pig intestinal tissue obtained from the local abattoir. Membrane integrity of the excised tissues was determined under the conditions that were used for the transport studies before the transport studies on the mini-tablets commenced.

4.7.1 Determination of membrane integrity by means of Lucifer Yellow

The transport of the exclusion marker molecule, Lucifer Yellow (LY), across the excised pig intestinal tissue as a function of time is given in Figure 4.14. The results indicate that the average transport of LY over 120 min was 1.928%, which is below the recommended maximum value of 3% transport to indicate intact membranes (Sigma-Aldrich, 2013). This indicates that the membrane integrity was maintained over the period of the transport studies of 120 min. The average P_{app} value was $3.397 \times 10^{-7} \pm 4.60803 \times 10^{-7}$ cm/s, which is below the maximum accepted range of $8.2 - 9.1 \times 10^{-7}$ cm/s to indicate intact membranes (Bhushani *et al.*, 2016).

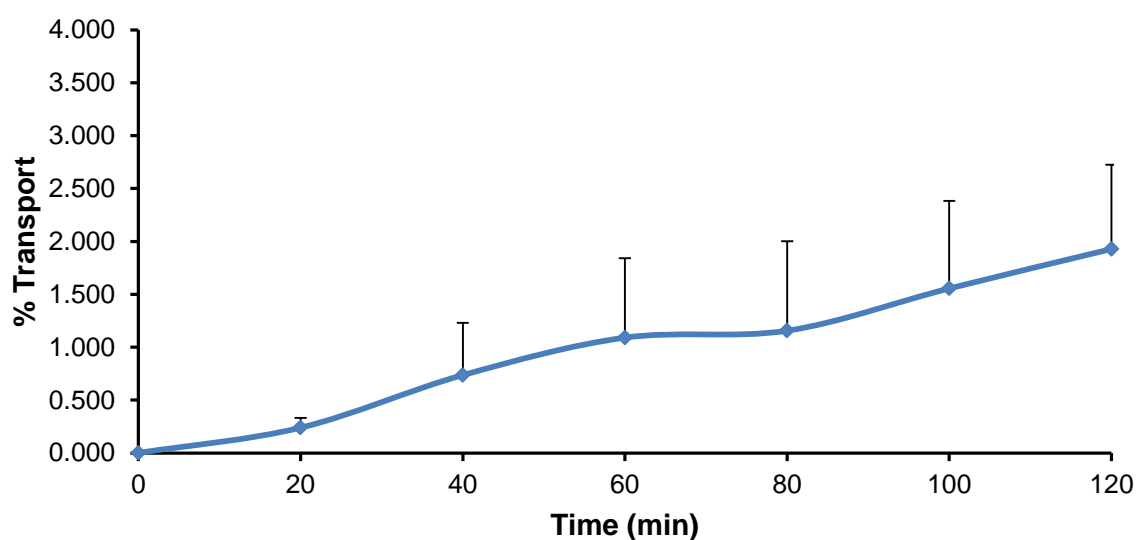


Figure 4.14: Average percentage Lucifer Yellow transport across excised pig intestinal tissues mounted in a Sweetana-Grass diffusion chamber apparatus

4.7.2 Comparison of FITC-dextran 4000 delivery (FD4) across excised pig intestinal tissues from the mini-tablet formulations

Amongst other objectives, this study aimed to investigate the influence of bead size and absorption enhancer types on the delivery of a macromolecular drug (i.e. FD4) across pig intestinal tissues formulated into mini-tablet drug delivery systems.

4.7.2.1 Mini-tablets containing FITC-dextran 4000 (FD4) with no absorption enhancers (Control)

Figure 4.15 shows the percentage cumulative FD4 transport across excised pig intestinal tissues obtained from the different mini-tablet formulations without absorption enhancers (control), after being applied to the donor chambers (i.e. apical side) of Sweetana-Grass diffusion apparatus over a period of 120 min.

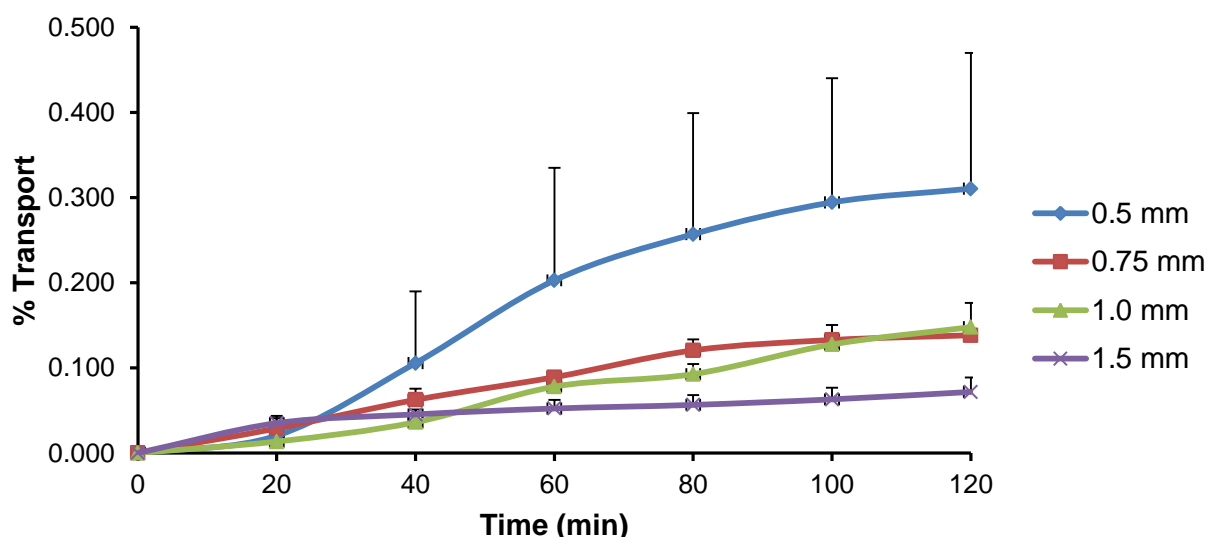


Figure 4.15: Cumulative percentage FITC-dextran 4000 transport from the mini-tablets without absorption enhancers (control) prepared from different sized beads

It is evident from Figure 4.15 that the cumulative amount of FD4 transported from all the control mini-tablet formulations was less than 0.4% of the applied dose. However, it is clear that the extent of FD4 transported depended on the size of the beads used to prepare the mini-tablets. The 0.5 mm mini-tablets exhibited the fastest initial FD4 delivery ($0.106 \pm 0.084\%$ cumulative FD4 transport at 40 min) as well as the highest cumulative transport at 120 min ($0.310 \pm 0.159\%$ transport of the applied dosage at 120 min).

The faster and higher transport obtained with the mini-tablets prepared from the smaller bead sizes (especially 0.5 mm and 0.75 mm) can be attributed to the larger surface area exposed to the KRB buffer and to the membrane. The smaller the beads, the higher the contact surface between the beads and the excised pig intestinal tissue membrane for direct delivery of FD4.

The fact that differences in the percentage transport of FD4 across pig intestinal tissues was observed while no marked difference during the dissolution studies may further be explained by the type of agitation applied. Agitation decreases the thickness of the diffusion layer around particles and thereby increases the dissolution rate (Korjamo *et al.*, 2009). The mild agitation during the transport studies with bubbling of medical air through the chambers was probably lower than during the dissolution studies. It is therefore possible that the higher agitation forces during the dissolution studies overshadowed the effect of bead size on the dissolution rate of the highly soluble FD4. Other factors such as transport medium volume and surface area available to form contact with the membrane probably also played a role in FD4 delivery across the excised pig intestinal tissues.

4.7.2.2 Mini-tablets containing *Aloe vera* gel

Figure 4.16 illustrates the cumulative percentage FD4 transport data of the various mini-tablet formulations prepared from the different sized beads with *A. vera* gel as absorption enhancer in the mini-tablet matrix after being applied to the apical side of a Sweetana-Grass diffusion chamber over a period of 120 min.

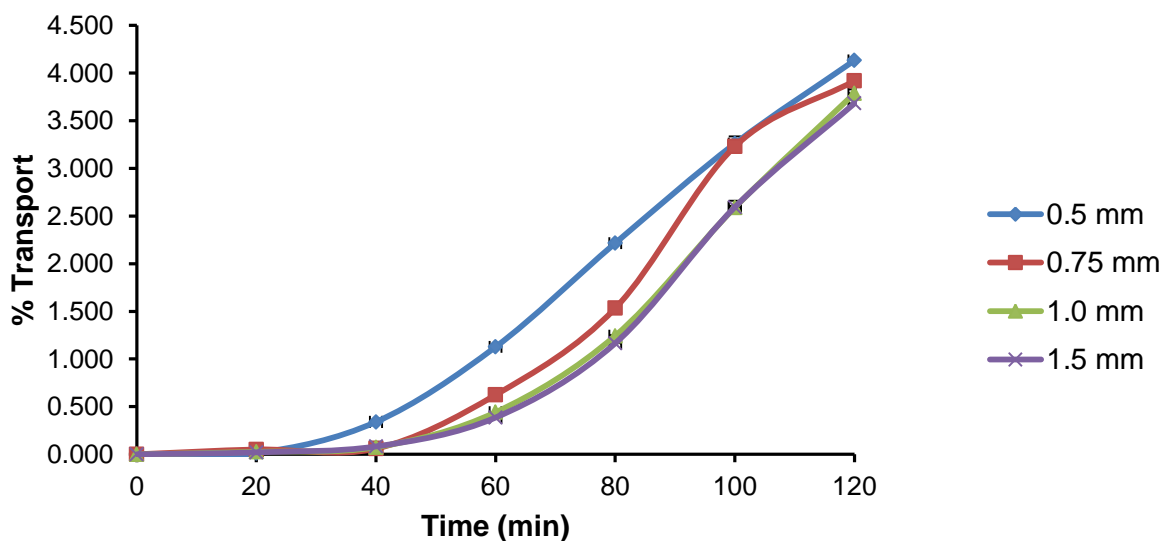


Figure 4.16: Cumulative percentage FITC-dextran 4000 transport from the mini-tablets prepared from the different sized beads containing *A. vera* gel

Figure 4.16 illustrates that, as expected, FD4 transport across excised pig intestinal tissue was obtained that inversely correlated with the bead size in the mini-tablet formulations. The FD4 transport and extent clearly increased with a decrease in bead size. In the case of the mini-tablets prepared from the 0.5 mm beads, FD4 was detected in the basolateral chamber after 20 min (0.013% of the applied dose) indicating relatively fast FD4 transport from this formulation, while FD4 could only be detected after 40 min from the other mini-tablet formulations. At a time of 40 min after application of the mini-tablets, the FD4 transport was 4-fold higher from the mini-tablets prepared with 0.5 mm beads than from those prepared with the 1.5 mm beads. The trend continued over the complete transport period of 120 min since the mini-tablets prepared with 0.5 mm beads exhibited a cumulative FD4 transport of $4.1 \pm 0.029\%$, which is approximately 10% higher than the $3.7 \pm 0.036\%$ of the mini-tablets prepared with the 1.5 mm beads. It is thus clear that bead size influenced both the rate and extent of FD4 transport across pig intestinal tissue for the formulations containing *A. vera* gel as absorption enhancer. This can be explained by the higher surface area of the smaller beads for increased contact with the membrane and thereby allowing increased FD4 delivery after interaction of the *A. vera* gel with the membrane to modulate tight junctions for paracellular delivery (Haasbroek *et al.*, 2019)

It is important to note that the inclusion of *A. vera* gel in the different sized bead formulations have led to a statistically significant ($p < 0.05$) increase in the percentage FD4 transport when compared to the control formulations. It has previously been shown in several *in vitro* studies that *A. vera* gel can enhance macromolecular drug transport across intestinal epithelia when applied in solution (Chen *et al.*, 2009; Lebitsa *et al.*, 2011; Beneke *et al.*, 2012) or formulated into beads (De Bruyn *et al.*, 2018). This is due to the enhanced paracellular absorption caused by the opening of tight junctions between adjacent epithelial cells by the *A. vera* gel (Chen *et al.*, 2009; Lemmer & Hamman, 2013; Haasbroek *et al.*, 2019).

4.7.2.3 Mini-tablets containing *Aloe vera* whole leaf materials

Figure 4.17 shows the data for the cumulative percentage FD4 transport obtained from the various sized bead containing mini-tablet formulations with *A. vera* whole leaf extract as absorption enhancer as part of the mini-tablet matrix system.

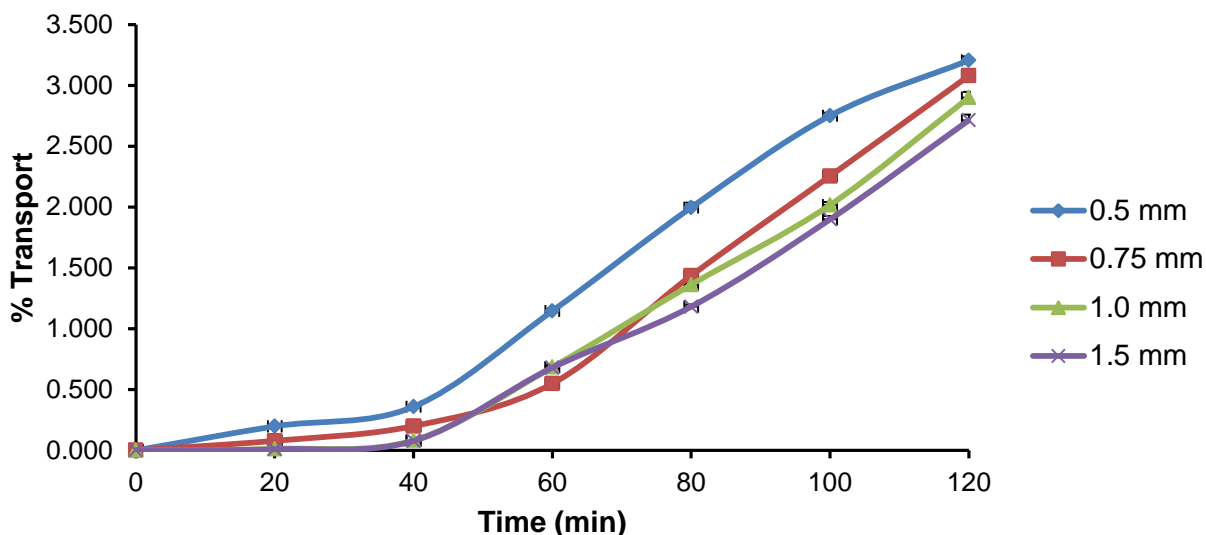


Figure 4.17: Cumulative percentage FITC-dextran 4000 transport from the mini-tablets prepared from the different sized beads containing *A. vera* whole leaf extract

In general, the same trend in terms of FD4 transport across pig intestinal tissue that was observed for the mini-tablet formulations containing *A. vera* gel was also observed for the mini-tablet formulations containing *A. vera* whole leaf extract. From Figure 4.17, it is clear that the 0.5 mm bead containing mini-tablets exhibited a higher initial percentage ($0.198 \pm 0.003\%$ at 20 min) and cumulative percentage FD4 transport ($3.206 \pm 0.034\%$ after a time period of 120 min) when compared to the 1.5 mm bead containing mini-tablets, which exhibited only $0.009 \pm 0.0003\%$ transport at 20 min and $2.713 \pm 0.047\%$ cumulative transport after a period of 120 min. As indicated, the 0.5 mm bead size formulations exhibited a notably faster transport in comparison to the other formulations. Besides the faster transport of FD4, this mini-tablet formulation as well as the 0.75 mm bead containing mini-tablet formulation exhibited a notably higher extent of FD4 transport in comparison to the two bigger bead size containing mini-tablet formulations (1.0 mm and 1.5 mm respectively) formulations. The mini-tablets containing 0.5 mm diameter beads produced the highest cumulative FD4 transport of $3.206 \pm 0.034\%$ followed by $3.079 \pm 0.018\%$ for the 0.75 mm bead formulation. The 1.0 mm and 1.5 mm bead formulations both exhibited cumulative percentage transport below 3% with respective values of $2.9 \pm 0.0469\%$ and $2.7 \pm 0.0474\%$. *A. vera* whole leaf extract significantly ($p < 0.05$) enhanced FD4 transport across excised pig intestinal tissues when compared to the control. *A. vera* whole leaf materials has previously been shown to increase drug transport across excised intestinal epithelia when applied in solution (Chen *et al.*, 2009; Lebitsa *et al.*, 2011; Beneke *et al.*, 2012). The mechanism of action is similar to that of *A. vera* gel in that it opens the tight junctions to allow paracellular transport of macromolecular drugs (Chen *et al.*, 2009; Lemmer & Hamman, 2013; Haasbroek *et al.*, 2019).

This study therefore proved that *A. vera* whole leaf extract, when incorporated into a mini-tablet formulation as part of the matrix system, can significantly improve the delivery of macromolecular drugs across pig intestinal epithelia.

4.7.2.4 Mini-tablets containing *N*-trimethyl chitosan chloride

Figure 4.18 shows the cumulative percentage FD4 transport from the various sized bead containing mini-tablets with TMC as absorption enhancer as part of the mini-tablet matrix system.

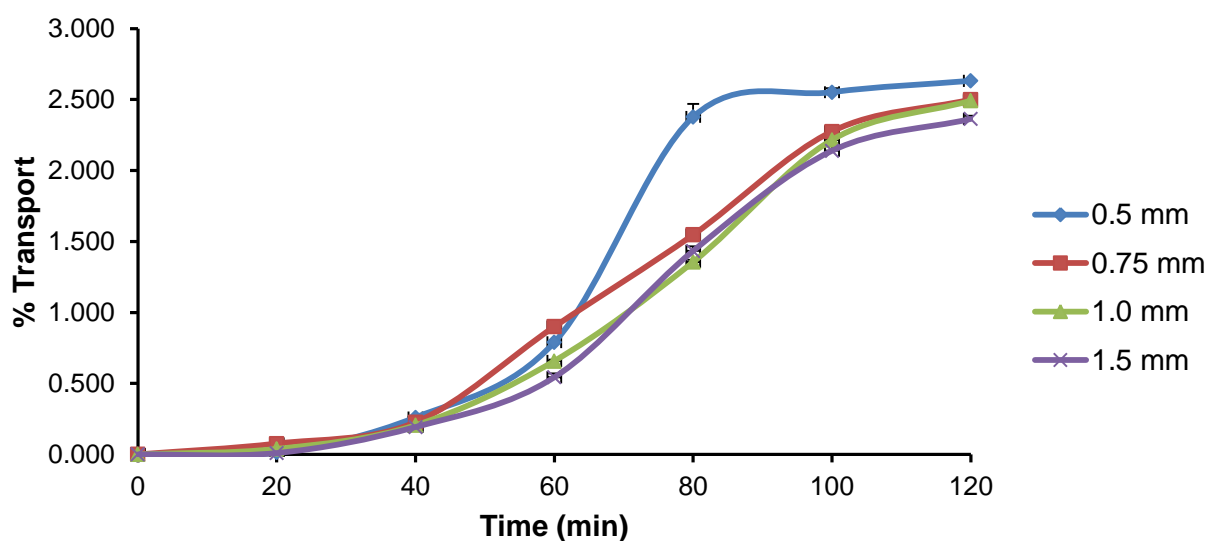


Figure 4.18: Cumulative percentage FITC-dextran 4000 transport from the mini-tablets prepared from the different sized beads containing *N*-trimethyl chitosan chloride

Figure 4.18 shows the cumulative percentage FD4 transport of the different bead sized mini-tablet formulations after a time period of 120 min. As with the other mini-tablet formulations (containing *A. vera*), bead size also influenced the FD4 transport from the TMC-containing formulations. It is evident, however, that the influence of bead size on FD4 transport became apparent only after 40 min. Initially the mini-tablet formulations exhibited similar FD4 transport behaviour across the excised pig intestinal tissues, although this similarity seemed to disappear after 40 min. The 0.5 mm bead containing mini-tablets exhibited a cumulative FD4 transport of $2.632 \pm 0.013\%$, which was higher than that of the 1.5 mm bead containing mini-tablet formulation, which exhibited a cumulative FD4 transport of $2.364 \pm 0.023\%$. TMC is a partially quaternised derivative of chitosan with improved solubility in neutral and alkaline environments.

Furthermore, confocal laser scanning microscopy revealed that TMC is capable of opening tight junctions to allow the passage of hydrophilic, macromolecular drugs through the intestinal epithelium (Thanou *et al.*, 2000). This study showed that TMC, as part of a mini-tablet matrix system, is capable of enhancing permeation of macromolecular compound (i.e. FD4) across excised pig intestinal tissues.

4.7.2.5 Apparent permeability coefficient (P_{app}) values for the different formulations

In Figure 4.19, the apparent permeability coefficient (P_{app}) values for the different mini-tablet formulations containing the different absorption enhancers are presented.

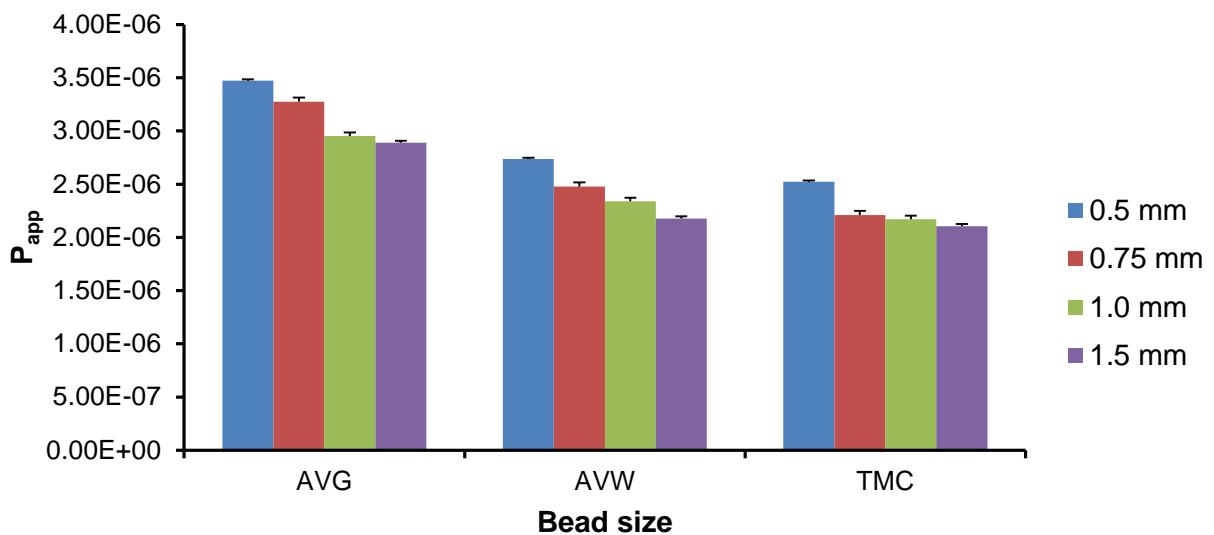


Figure 4.19: Apparent permeability (P_{app}) values for the different multiple-unit dosage forms (MUDFs)

The P_{app} values clearly indicate that the transport of FD4 across pig intestinal tissue was dependent on the size of the beads used to prepare the mini-tablets. For all formulations, irrespective of the absorption enhancer used in the matrix system, the 0.5 mm bead formulations rendered the highest transport of FD4 across pig intestinal tissue. In general, the 0.5 mm and 0.75 mm bead formulations exhibited notably higher P_{app} values than the 1.0 mm and 1.5 mm bead formulations. The P_{app} values for the 1.0 mm and 1.5 mm bead formulations were fairly similar for all absorption enhancers indicating that the effect of bead size started to decrease as the bead size increased beyond 1.0 mm. Table 4.20 shows the specific P_{app} values for each different bead sized formulation with regard to the different absorption enhancers.

Table 4.20: Apparent permeability (P_{app}) values for the different multiple-unit dosage forms (MUDFs)

Bead size (mm)	P_{app} values for the respective absorption enhancers (cm/s)		
	AVG	AVW	TMC
0.5	$3.47 \times 10^{-6} \pm 1.11 \times 10^{-8}$	$2.74 \times 10^{-6} \pm 1.88 \times 10^{-8}$	$2.52 \times 10^{-6} \pm 2.27 \times 10^{-8}$
0.75	$3.28 \times 10^{-6} \pm 3.80 \times 10^{-8}$	$2.48 \times 10^{-6} \pm 2.05 \times 10^{-8}$	$2.21 \times 10^{-6} \pm 5.68 \times 10^{-9}$
1.0	$2.95 \times 10^{-6} \pm 3.43 \times 10^{-8}$	$2.34 \times 10^{-6} \pm 3.09 \times 10^{-8}$	$2.17 \times 10^{-6} \pm 5.19 \times 10^{-9}$
1.5	$2.89 \times 10^{-6} \pm 2.01 \times 10^{-8}$	$2.18 \times 10^{-6} \pm 3.57 \times 10^{-8}$	$2.11 \times 10^{-6} \pm 2.92 \times 10^{-8}$

With regards to the different absorption enhancers, *A. vera* gel formulations rendered the highest P_{app} values for all the bead sizes used in comparison to the other two absorption enhancers (*A. vera* whole leaf material and TMC), as seen in Table 4.20.

4.8 Conclusion

The mini-tablet-in-capsule drug delivery systems that were successfully prepared in this study differed with regard to the type of absorption enhancer included as well as the size of the beads used to prepare these mini-tablets. Four different sized beads (0.5 mm, 0.75 mm, 1.0 mm and 1.5 mm in diameter) containing FD4 were prepared. These beads were then mixed with each of the three selected absorption enhancers (*A. vera* gel, *A. vera* whole leaf extract and TMC) and compressed into mini-tablets that were filled into size 0 hard gelatine capsules. A fluorescence spectrophotometric analytical method was validated to quantify samples for FD4 and LY content in terms of linearity, limit of detection, limit of quantification, precision, specificity and accuracy.

The mini-tablet formulations were evaluated with respect to mass variation, disintegration, crushing strength, friability, dissolution behaviour and transport of the model compound across pig intestinal tissue. Dissolution studies indicated that the mini-tablet-in-capsule formulations released their FD4 content to different rates and extents. The dissolution profiles of the various sized bead mini-tablet-in-capsule formulations indicated immediate drug release behaviour (i.e. not controlled drug release behaviour). The dissolution results indicated that dissolution rate was dependent on the absorption enhancer included in the formulation. Both *A. vera* gel and *A. vera* whole leaf materials notably decreased the dissolution rate of FD4 as indicated by higher MDT values probably due to viscosity enhancement of the diffusion layer and pores in the matrices of the beads.

Transport results clearly indicated that the bead size had a definite influence on the transport of FD4 across pig intestinal tissue. The influence of the different sizes of beads were clearly observed as the 0.5 mm and 0.75 mm bead containing mini-tablets showed a statistically significant increase in FD4 transport across the excised pig intestinal tissues across the whole range of absorption enhancers ($p < 0.05$) when compared to the 1.0 mm and 1.5 mm bead formulations. The AVG containing mini-tablets, irrespective of bead size, also exhibited a statistical significant increase in FD4 transport when compared to the AVW and TMC mini-tablets ($p < 0.05$). Membrane integrity was upheld throughout all transport experiments as shown by the LY transport studies. The results of this study confirmed that macromolecular drug (i.e. FD4) delivery is possible by means of absorption enhancers used as part of a mini-tablet matrix system. However, to confirm the clinical significance of these drug absorption enhancing results, *in vivo* testing must be conducted.

CHAPTER 5

CONCLUSIONS AND RECOMMENDATIONS

5.1 Final conclusions

The oral route remains the preferred route of drug delivery due to the ease of use and the advantage of self-administration by the patient (Renukuntla *et al.*, 2013). However, the oral route is usually excluded from the administration of peptide and protein drugs (e.g. insulin) due to poor absorption from the gastrointestinal tract as a result of their unfavourable physicochemical properties (Crowley & Martini, 2004). These unfavourable properties include the hydrophilic nature and large molecular weight of peptide drugs (Beneke *et al.*, 2012), which cause an oral bioavailability of peptide and protein drugs of only 1 – 2% (Renukuntla *et al.*, 2013).

The aim of this study was to develop mini-tablet-in-capsule dosage forms capable of successfully delivering a macromolecular model compound (FD4) across excised pig intestinal tissues. Objectives to attain this aim included to investigate the influence of different bead sizes and different drug absorption enhancers on the delivery of FD4 from mini-tablet-in-capsule delivery systems delivery. The FD4 was incorporated into four different sizes of beads (i.e. 0.5 mm, 0.75 mm, 1.0mm and 1.5 mm respectively) that were prepared by means of extrusion-spheronisation. The beads were evaluated in terms of size, size distribution, morphology and assayed to determine the actual concentration of FD4 in each respective bead formulation. Images of the different beads batches were then taken with an electron microscope to provide information on the surface morphology, form and internal structures. All the beads were found to be relatively spherical in shape, which exhibited FD4 content of $100 \pm 2\%$ based on the assay done on each formulation.

Upon successful preparation of the different bead formulations containing FD4 as model compound, they were then used to produce mini-tablets (5 mm in diameter) which were subsequently evaluated in terms of mass variation, friability, disintegration, crushing strength, drug release by means of drug dissolution studies and transport of FD4 across excised pig intestinal tissues. The dissolution studies revealed that the mini-tablets prepared from the two smallest bead sizes (0.5 mm and 0.75 mm), released the FD4 at a slightly faster rate than the mini-tablets containing the two bigger bead sizes (1.0 mm and 1.5 mm).

Although the drug release profiles varied from the different mini-tablet-in-capsule formulations, it was clear that those containing TMC inclined to release the FD4 faster than those that contained *A. vera* gel and whole leaf extract. This was explained by the gelling characteristics of *A. vera* gel and whole leaf extracts that slowed down the diffusion of the FD4 molecules from the beads, while the TMC did not affect the dissolution behaviour of FD4 at the concentration used in the beads in this study. The dissolution rate of FD4 was inversely proportional to bead size when *A. vera* gel was included as drug absorption enhancer in the mini-tablets.

The *ex vivo* transport data of LY showed that membrane integrity was maintained throughout (120 min) the transport experiments. The *ex vivo* transport data clearly showed that all the mini-tablet formulations, which contained absorption enhancers, significantly ($p < 0.05$) improved the transport of FD4 across the excised pig intestinal tissues when compared to the control group. The mini-tablet formulations that contained *A. vera* gel showed the highest increase in the cumulative percentage transport of FD4 when compared to the control groups. The cumulative percentage transport of FD4 from the mini-tablet formulation containing *A. vera* gel as absorption enhancer after 120 min was $4.1 \pm 0.029\%$ for the 0.5 mm bead containing mini-tablet formulation and $3.7 \pm 0.036\%$ for the 1.5 mm bead containing mini-tablet formulation. This represented a statistical significant ($p < 0.05$) increase in the amount of FD4 transported across the pig intestinal tissue in comparison to the control formulations (which was less than 0.4% cumulative transport after 120 min). Across the range of mini-tablets produced, those containing *A. vera* gel were statistically significant when compared to the other groups.

Previous studies focussed on enhancing macromolecular drug transport by means of applying solutions or combining different absorption enhancers into the beads itself. This study has proven that intestinal transport of macromolecular drugs can be enhanced by incorporating absorption enhancers in the matrix system of mini-tablet formulations prepared from beads. The rationale for this is to cause a biphasic release pattern with the first phase of release being the absorption enhancer to allow the opening of the tight junctions to enable paracellular transport followed by the release of FD4 (macromolecular compound representing peptide or protein drugs) in the second phase of release. The efficacy of the respective absorption enhancers investigated in this study can be ranked as follows: *A. vera* gel > *A. vera* whole leaf extract > TMC > control (FD4 alone without absorption enhancer). It is notable that the smaller beads (0.5 mm and 0.75 mm respectively) in general exhibited faster FD4 transport across the excised pig intestinal tissues. The larger sized beads (1.0 mm and 1.5 mm respectively) exhibited relatively slower FD4 transport percentages across excised pig intestinal tissues.

5.2 Future recommendations

During this study, the multiple-unit dosage form comprising of mini-tablets produced from beads showed promise with regards to macromolecular drug delivery. It proved in concept that enhanced intestinal absorption of macromolecular drugs is a promising field. Further studies are, however, required as follows:

- Formulation of a multiple-unit dosage form with small sized beads (0.5 mm in diameter) with a well-known peptide drug as active (e.g. insulin) and *A. vera* gel as absorption enhancer in the matrix system and *in vitro* evaluation of this dosage form,
- *In vivo* evaluation of the proof of concept of this study (e.g. mini-tablets prepared from beads in capsule) in an animal model,
- Investigations into the mechanism of action of absorption enhancers such as *A. vera* gel and whole leaf extract in slowing the dissolution of a model compound down from the beads,
- Comparison of dissolution and drug delivery performance of mini-tablet-in-capsule drug delivery systems prepared from powders and beads, and
- Investigation of a multiple-unit delivery system containing *A. vera* as absorption enhancer in a matrix system via other delivery routes such as the nasal, buccal and rectal routes.

REFERENCES

- Anderson, M.A. & Van Itallie, C.M. 2009. Physiology and function of the tight junction. *Cold Spring Harbor Perspectives in Biology*, 1: 1 – 16.
- Artursson, P., Palm, K. & Luthman, K. 2001. Caco-2 monolayers in experimental and theoretical predictions of drug transport. *Advanced Drug Delivery Reviews*, 46: 27 – 43.
- Ashford, M. 2018. Gastrointestinal tract - physiology and drug absorption. (In Aulton, M.E. & Taylor, K.M.G. eds. *Aulton's pharmaceuticals: the design and manufacture of medicines*. 5th ed. Elsevier. London. p. 300 – 318.)
- Aulton, M.E. 2018. Powder flow. (In Aulton, M.E. & Taylor, K.M.G. eds. *Aulton's pharmaceuticals: the design and manufacture of medicines*. 5th ed. Elsevier. London. p. 189 – 201.)
- Aungst, B.J. 2012. Absorption enhancers: applications and advances. *The AAPS journal*, 14: 10 – 18.
- Banga, A.K. 2006. Therapeutic peptides and proteins: formulation, processing and delivery system. 3rd ed. London: Taylor & Francis.
- Banting, F.G., Best, C.H., Campbell, W.R., Collip, J.B. & Fletcher, A.A. 1921. Pancreatic extracts in the treatment of diabetes mellitus. *The Canadian Medical Association Journal*, 141 – 146.
- Beneke, C., Viljoen, A. & Hamman, J.H. 2012. *In vitro* drug absorption enhancements effects of *Aloe vera* and *Aloe ferox*. *Scientia Pharmaceutica*, 80: 475 – 486.
- Berg, J.M., Stryer, L. & Tymoczko, J.L. 2015. The biosynthesis of amino acids. (In: Berg, J.M., Tymoczko, J.L., Gatto, G.J. & Stryer, L. eds. *Biochemistry*. 8th ed. New York: W.H. Freeman. p. 713 – 742.)
- Bhushani, J.A., Karthik, P. & Anandharamakrishnan, C. 2016. Nanoemulsion based delivery system for improved bioaccessibility and Caco-2 cell monolayer permeability of green tea catechins. *Food Hydrocolloids*, 56: 372 – 382.
- BP (British Pharmacopoeia). 2019. London: HMSO.

Bruno, B.J., Miller, G.D. & Lim, C.S. 2013. Basics and recent advances in peptide and protein drug delivery. *Therapeutic Delivery*, 4: 1443 – 1467.

Buckley, S.T., Hubálek, F. & Rahbek, U.L. 2016. Chemically modified peptides and proteins - critical considerations for oral delivery. *Tissue Barriers*, 4: e1156805-1 – e1156805-11.

Chan, L.M.S., Lowes, S. & Hirst, B.H. 2004. The ABCs of drug transport in intestine and liver efflux proteins limiting drug absorption and bioavailability. *European Journal of Pharmaceutical Sciences*, 21: 25 – 51.

Cheboyina, S., Chambliss, W.G. & Wyandt, C.M. 2004. A novel freeze pelletization technique for preparing matrix pellets. *Pharmaceutical Technology*, 98 – 110.

Chen, W., Lu, Z., Viljoen, A. & Hamman, J.H. 2009. Intestinal drug transport enhancement by *Aloe vera*. *Planta Medica*, 75: 587 – 595.

Chen, Y., Yuan, L., Zhou, L., Zhang, Z. & Wu, Q. 2012. Effect of cell-penetrating peptide-coated nanostructured lipid carriers on the oral absorption of tripterine. *International Journal of Nanomedicine*, 7: 4581 – 4591.

Choonara, B.F., Choonara, Y.E., Kumar, P., Bijukumar, D., du Toit, L.C. & Pillay, V. 2014. A review of advanced oral drug delivery technologies facilitating the protection and absorption of protein and peptide molecules. *Biotechnology Advances*, 32: 1269 – 1282.

Crowley, P.J. & Martini, L.G. 2004. Formulation design: new drugs from old. *Drug Discovery Today: Therapeutic Strategies*, 4: 537 – 542.

Dane, S. & Hänninen, O. 2015. Enzymes of digestion. (In Encyclopedia of life support systems. 2nd ed.: 45 – 50). <http://www.eolss.net/sample-chapters/c03/e6-54-02-04.pdf>. Date of access: 8 Feb 2019.

Daugherty, A.L. & Mrsny, R.J. 1999. Transcellular uptake mechanisms of the intestinal epithelial barrier: part one. *Pharmaceutical Science and Technology Today*, 2: 144 – 151.

Derakhshankhah, H. & Jafari, S. 2018. Cell penetrating peptides: A concise review with emphasis on biomedical applications. *Biomedicine & Pharmacotherapy*, 108: 1090 – 1096.

De Bruyn, S., Willers, C., Steyn, J.D., Steenekamp, J.H & Hamman, J.H. 2018. Development and evaluation of a double-phase multiple-unit dosage form for enhanced insulin intestinal delivery. *Drug Delivery Letters*, 8, 52 – 60.

- Di Pasquale, G. & Chiorini, J.A. 2005. AAV Transcytosis through barrier epithelia and endothelium. *Molecular Therapy*, 13: 506 – 516.
- Dukić-Ott, A., Thommes, M., Remon, J.P., Kleinebudde, P. and Vervaet, C. 2009. Production of pellets via extrusion-spheronisation without the incorporation of microcrystalline cellulose: a critical review. *European Journal of Pharmaceutics and Biopharmaceutics*, 71: 38 – 46.
- Dulal, P. 2010. Protein or peptide drugs: applications, problems and solutions. *Biotechnology Society of Nepal*, 2: 1 – 5.
- Du Toit, T., Malan, M.M., Lemmer, H.J.R., Gouws, C., Aucamp, M.E., Breytenbach, W.J. & Hamman, J.H. 2016. Combining chemical permeation enhancers for synergistic effects. *European Journal of Drug Metabolism and Pharmacokinetics*, 41: 575 – 586.
- Florence, A.T. & Attwood, D. 1988. Physicochemical principals of pharmacy. 2nd ed. Macmillan. London. p. 1 – 484.
- Fonte, P., Araújo, F., Silva, C., Pereira, C., Reis, S., Santos, H.A. & Sarmiento, B. 2015. Polymer-based nanoparticles for oral insulin delivery: revisited approaches. *Biotechnology Advances*, 33: 1342 – 1354.
- Friend, D.R. 2005. New oral delivery systems for treatment of inflammatory bowel disease. *Advanced Drug Delivery Reviews*, 57: 247 – 265.
- Gaber, D.M., Nafee, N. & Abdallah, O.Y. 2015. Mini-tablets versus pellets as promising multiparticulate modified release delivery systems for highly soluble drugs. *International Journal of Pharmaceutics*, 488, 86 – 94.
- Grass, G.M. & Sweetana, S.A. 1988. *In vitro* measurement of gastrointestinal tissue permeability using a new diffusion cell. *Pharmaceutical Research*, 5: 372 – 376.
- Green, J.M. 1996. A practical guide to analytical method validation. *American Chemical Society*, 305A – 309A.
- Gupta, A.M., Shivhare, U.D. & Suruse, P.B. 2015. Different aspects of pellets formulation and their evaluation. *International Journal of Pharmaceutical and Phytopharmacological Research*, 6: 331 – 336.

Haasbroek, A., Willers, C., Glyn, M., du Plessis, L. & Hamman, J.H. 2019. Intestinal drug absorption enhancement by *Aloe vera* gel and whole leaf extracts: *In vitro* investigations into the mechanisms of action. *Pharmaceutics*, 11: 1 – 17.

Hamman, H., Hamman, J.H. & Steenekamp, J.H. 2017. Multiple-unit pellet systems (MUPS): production and applications as advanced drug delivery systems. *Drug Delivery Letters*, 7: 1 – 10.

Hamman, H., Hamman, J., Wessels, A., Scholtz, J. & Steenekamp, J. 2019. Development of multiple-unit pellet system tablets by employing the SeDeM expert diagram system II: pellets containing different active pharmaceutical ingredients. *Pharmaceutical Development and Technology*, 24: 145 – 156.

Hamman, J.H., Enslin, G.M. & Kotzé, A.F. 2005. Oral delivery of peptide drugs. *Biodrugs*, 3: 165 – 174.

Hamman, J.H. & Kotzé, A.F. 2001. Effect of the type of base and number of reaction steps on the degree of quarterisation and molecular weight of *N*-trimethyl chitosan chloride. *Drug Development and Industrial Pharmacy*, 27: 373 – 380.

Hamman, J.H. & Steenekamp, J.H. 2011. Oral peptide drug delivery: strategies to overcome challenges. (In Castanho, M. & Santos, N.C. eds. Peptide drug discovery and development: translational research in academia and industry. 1st ed. WILEY-VCH. Weinheim. p. 71 – 91.)

Hellum, B.H. & Nilsen, O.G. 2008. *In vitro* inhibition of CYP3A4 Metabolism and P-glycoprotein-mediated transport by trade herbal products. *Basic & Clinical Pharmacology & Toxicology*, 102: 466 – 475.

Hirjau, M., Nicoara, A.C., Hirjau, V. & Lupuleasa, D. 2011. Pelletization techniques used in pharmaceutical fields. *Practica Farmaceutică*, 4, 206 – 211.

Jalali, A., Moghimipour, E. & Akhagari, A. 2014. Enhancing effects of bile salts on gastrointestinal absorption of insulin. *Tropical Journal of Pharmaceutical Research*, 13: 1797 – 1802.

Korjamo, T., Heikkinen, A.T. & Mönkkönen, J. 2009. Analysis of unstirred water layer in *In Vitro* permeability experiments. *Journal of Pharmaceutical Sciences*, 98: 4469 – 4479.

Lancaster, C.E., Ho, C.Y., Hipolito, V.E.B., Botelho, R.J. & Terebiznik, M.R. 2018. Phagocytosis: what's on the menu?. *Biochemistry and Cell Biology*, 97: 1 – 40.

- Lebitsa, T., Viljoen, A., Lu, Z. & Hamman, J.H. 2012. *In vitro* drug permeation enhancement potential of aloe gel materials. *Current Drug Delivery*, 9: 297 – 304.
- Lemmer, H.J.R. & Hamman J.H. 2013. Paracellular drug absorption enhancement through tight junction modulation. *Expert Opinion on Drug Delivery*, 10: 103 – 114.
- Lennernäs, H. 1998. Human intestinal permeability. *Journal of Pharmaceutical Sciences*, 87: 403 – 410.
- Lueßen, H.L., de Leeuw, D.P., Pérard, D., Lehr, C., de Boer, A.G., Verhoef, J.C. & Junginger, H.E. 1996. Mucoadhesive polymers in peroral peptide drug delivery: influence of mucoadhesive excipients on the proteolytic activity of intestinal enzymes. *European Journal of Pharmaceutical Sciences*, 4: 117 – 128.
- Lundquist, P. & Artursson, P. 2016. Oral absorption of peptides and nanoparticles across the human intestine: opportunities, limitations and studies in human tissues. *Advanced Drug Delivery Reviews*, 106: 256 – 276.
- Mahajan, A., Rawat, A.S., Bhatt, N. & Chauhan, M.K. 2014. Structural modification of proteins and peptides. *Indian Journal of Pharmaceutical Education and Research*, 3: 34 – 46.
- Mahato, R.I., Narang, A.J., Thoma, L. & Miller, D.D. 2003. Emerging trends in oral delivery of peptide and protein drugs. *Critical Reviews in Therapeutic Drug Carrier Systems*, 20: 153 – 214.
- Mansuri, S., Kesharwani, P., Jain, K., Tekade, R.K. & Jain, N.K. 2016. Mucoadhesion: a promising approach in drug delivery system. *Reactive and Functional Polymers*, 100: 151 – 172.
- Maroni, A., Zema, L., Del Curto, M.D., Foppoli, A. & Gazzaniga, A. 2012. Oral colon delivery of insulin with the aid of functional adjuvants. *Advanced Drug Delivery Reviews*, 64: 540 – 556.
- Mitchell, M.D. & Thompson, D.C. 2013. The role of intestinal efflux transporters in drug absorption. *Biofiles*, 8: 1012 – 1013.
- Morishita, M. & Peppas, N.A. 2006. Is the oral route possible for peptide and protein drug delivery?. *Drug Discovery Today*, 11: 905 – 910.
- Mourya, V.K. & Inamdar, N.N. 2009. Trimethyl chitosan and its applications in drug delivery. *Journal of Materials Science: Materials in Medicine*, 20: 1057 – 1079.

Niu, M., Tan, T., Gua, P., Hovgaard, L., Lu, Y., Qi, J., Lian, R., Li, X. & Wu, W. 2014. Enhanced oral absorption of insulin-loaded liposomes containing bile salts: a mechanistic study. *International Journal of Pharmaceutics*, 460: 119 – 130.

Pandey, P., Saini, M. 2017. Mucoadhesive drug delivery system: an overview. *Pharmaceutical and Biological Evaluations*, 4: 183 – 187.

Park, J.W., Kim, S.K., Al-Hilal, T.A., Jeon, O.C., Moon, H.T. & Byun, Y. 2010. Strategies for Oral Delivery of macromolecule drugs. *Biotechnology and Bioprocess Engineering*, 15: 66 – 75.

Patadia, R., Vora, C., Mittal, K. & Mashru, R. 2013. Dissolution criticality in developing solid oral formulations: from inception to perception. *Critical Reviews™ in Therapeutic Carrier Systems*, 30: 495 – 534.

Patterson, J.K., Lei, X.G. & Miller, D.D. 2008. The pig as an experimental model for elucidating the mechanisms governing dietary influence on mineral absorption. *Experimental Biology and Medicine*, 233: 651 – 664.

Pfister, D. & Morbidelli, M. 2014. Process for protein PEGylation. *Journal of Controlled Release*, 180: 134 – 149.

Ranjit, K. & Baquee, A.A. 2013. Nanoparticle: an overview of preparation, characterization and application. *International Research Journal of Pharmacy*, 4: 47 – 57.

Ranjith, K. & Mahalaxmi, R. 2015. Pharmaceutical Mini Tablets. *International Journal of PharmTech Research*, 7, 507 – 515.

Rautio, J., Kumpulainen, H., Heimbach, T., Oliyai, R., Oh, D., Järvinen, T. & Savolainen, J. 2008. Prodrugs: design and clinical applications. *Nature Reviews Drug Discovery*, 7: 255 – 270.

Renkuntla, J., Vadlapudi, A.D., Patel, A., Boddu, S.H.S. & Mitra, A.K. 2013. Approaches for enhancing oral bioavailability of peptides and proteins. *International Journal of Pharmaceutics*, 447: 75 – 93.

Rúnarsson, Ö.V., Holappa, J., Nevalainen, T., Hjálmsdóttir, M., Järvinen, T., Loftsson, T., Einarsson, J.M., Jónsdóttir, S., Valdimarsdóttir, M. & Másson, M. 2007. Antibacterial activity of methylated chitosan and chitooligomer derivatives: synthesis and structure activity relationships. *European Polymer Journal*, 43: 2660 – 2671.

- Salama, N.N., Eddington, N.D. & Fasano, A. 2006. Tight junction modulation and its relationship to drug delivery. *Advanced Drug Delivery Reviews*, 58: 15 – 28.
- Salamat-Miller, N. & Johnston, T.P. 2005. Current strategies used to enhance the paracellular transport of therapeutic polypeptides across the intestinal epithelium. *International Journal of Pharmaceutics*, 294: 201 – 216.
- Schneeberger, E.E. & Lynch, R.D. 2004. The tight junction: a multifunctional complex. *American Journal of Physiology-Cell Physiology*, 286: C1213 – C1228.
- Shabir, G.A. 2004. A practical approach to validation of HPLC methods under current good manufacturing practices. *Journal of Validation Technology*, 10: 29 – 37.
- Shaji, J. & Patole, V. 2008. Protein and peptide drug delivery: oral approaches. *Indian Journal of Pharmaceutical Sciences*, 70: 269 – 277.
- Sigma-Aldrich. 2013. Product information: CompoZr[®] ADME/Tox cell lines C2BBE1 BCRP knockout and wild type cell lines 24 well assay ready plates (technical bulletin). 1 – 6. <https://www.sigmaaldrich.com/content/dam/sigma-aldrich/docs/Sigma/Bulletin/1/mtox1002pc24bul.pdf>
- Singh, R. 2013. HPLC method development and validation- an overview. *Journal of Pharmaceutical Education and Research*, 4: 26 – 33.
- Sinha, V.R., Agrawal, M.K., Agrawal, A., Singh, G. & Ghai, D. 2009. Extrusion-spheronization: process variables and characterization. *Critical Reviews™ in Therapeutic Carrier Systems*, 26: 275 – 331.
- Sirisha, V.R.K., Vijaya Sri, K., Suresh, K., Kamalakar Reddy, G. & Devanna, N. 2013. A review of pellets and pelletization process - a multiparticulate drug delivery system. *International Journal of Pharmaceutical Sciences and Research*, 4: 2145 – 2158.
- Srivastava, S. & Mishra, G. 2010. Fluid bed technology: overview and parameters for process selection. *International Journal of Pharmaceutical Sciences and Drug Research*, 2: 236 – 246.
- Su, F., Lin, K., Sonaje, K., Wey, S., Yen, T., Ho, Y., Panda, N., Chuang, E., Maiti, B. & Sung, H. 2012. Protease inhibition and absorption enhancement by functional nanoparticles for effective oral insulin delivery. *Biomaterials*, 33: 2801 – 2811.
- Tabachnick, B.G. & Fidell, L.S. 2001. Using multivariate statistics. 4th ed. Allyn & Bacon, Boston. p 966.

- Tang, V.W. & Goodenough, D.A. 2003. Paracellular ion channel at the tight junction. *Biophysical Journal*, 8: 1660 – 1673.
- TdB Consultancy. 2016. FITC-dextran. 1 – 5. https://tdbcons.com/images/FITC-Dextran_11-2016.pdf. Date of access: 7 Feb 2018.
- Tegos, G.P., Haynes, M., Strouse, J.J., Khan, M.M.T., Bologna, C.G., Oprea, T.I. & Sklar, L.A. 2011. Microbial efflux pump inhibition: tactics and strategies. *Current Pharmaceutical Design*, 17: 1291 – 1302.
- Thanou, M.M., Verhoef, J.C., Romeijn, S.G., Nagelkerke, J.F., Merkus, F.W.H.M & Junginger, H.E. 1999. Effects of *N*-trimethyl chitosan chloride, a novel absorption enhancer, on Caco-2 intestinal epithelia and the ciliary beat frequency of chicken embryo trachea. *International Journal of Pharmaceutics*, 185: 73 – 82.
- Trabulo, S., Cardoso, A.L., Mano, M. & Pedroso de Lima, M.C. 2010. Cell-penetrating peptides - mechanisms of cellular uptake and generation of delivery systems. *Pharmaceutics*, 3: 961 – 993.
- Vasir, J.K., Tambwekar, K. & Garg, S. 2003. Bioadhesive microspheres as a controlled drug delivery system. *International Journal of Pharmaceutics*, 255, 13 – 32.
- Vertzoni, M., Augustijns, P., Grimm, M., Koziolk, M., Lemmens, G., Parrott, N., Pentafragka, C., Reppas, C., Rubbens, J., Van Den Abeele, J., Vanuytsel, T., Weitschies, W. & Wilson, C.G. 2019. Impact of regional differences along the gastrointestinal tract of healthy adults on oral drug absorption: An UNGAP review. *European Journal of Pharmaceutical Sciences*, 134, 153 – 175.
- Vervaet, C., Baert, L. & Remon, J.P. 1995. Extrusion-spheronisation: a literature review. *International Journal of Pharmaceutics*, 116: 131 – 146.
- Vikash, K., Kumar, M.S., Vikas, L.A. & Ranjit, S. 2011. Multiple unit dosage form: pellet and pelletization techniques: an overview. *International Journal of Research in Ayurveda and Pharmacy*, 1: 121 – 125.
- Vinson, J.A., Al Kharrat, H. & Andreoli, L. 2005. Effect of *Aloe vera* preparations on the human bioavailability of vitamins C and E. *Phytomedicine*, 12: 760 – 765.

Wallis, L., Malan, M.M., Gouws, C., Steyn, J.D., Ellis, S., Abay, E., Wiesner, L., Otto, D.P. & Hamman, J.H. 2016. Evaluation of isolated fractions of *Aloe vera* gel materials on indinavir pharmacokinetics: *in vitro* and *in vivo* studies. *Current Drug Delivery*, 13, 471 – 480.

World Health Organization 1999. WHO monographs on selected medicinal plants. Geneva.

Wileman, T., Harding, C. & Stahl, P. 1985. Receptor-mediated endocytosis. *Biochemical Journal*, 232: 1 – 14.

Yamamoto, A., Taniguchi, T., Rikyuu, K., Tsuji, T., Fujita, T., Murakami, M. & Muranishi, S. 1994. Effects of various protease inhibitors on the intestinal absorption and degradation of insulin in rats. *Pharmaceutical Research*, 11: 1496 – 1501.


Yin, N., Brimble, M.A., Harris, P.W.R. & Wen, J. 2014. Enhancing the oral bioavailability of peptides drugs by using chemical modification and other approaches. *Medicinal Chemistry*, 4: 763 – 769.

Zawilska, J.B., Wojcieszak, J. & Olenjniczak, A.B. 2013. Prodrugs: a challenge for the drug development. *Pharmacological Reports*, 65: 1 – 14.

Zhu, L., Lu, L., Wang, S., Wu, J., Shi, J., Yan, T., Xie, C., Li, Q., Hu, M. & Liu, Z. 2017. Oral absorption basics: pathways and physiochemical and biological factors affecting absorption. (*In* Qiu, Y., Chen, Y., Zhang, G.G.Z., Yu, L. & Mantri, R.V. eds. *Developing solid oral dosage forms: pharmaceutical practice and theory*. 2nd ed. Elsevier. London. p 297 – 330.)

ADDENDUM A

STANDARD OPERATING PROCEDURE: BIOLOGICAL WASTE MANAGEMENT

 Centre of Excellence for Pharmaceutical Sciences Document type: Standard Operating Procedure (SOP)	Section: Research laboratories in building G2; G16 and G20	
Title: [Title]	Date issued: 30 June 2016	
	Review Date:	
	Compiled by: Leroux	
SOP No: [Subject]	Version o[Status]	No: Page 104 of 12

1. Definitions

The following definitions are applicable to this SOP:

Waste (according to the Waste Amendment Act, 2014 (Act No 26 of 2014)): “Any substance, material or object, that is unwanted, rejected, abandoned, discarded or disposed of, by the holder of the substance, material or object, whether or not such substance, material or object can be re-used, recycled or recovered and includes all wastes as defined in Schedule 3 to this Act”.

Hazardous waste (Act No 26 of 2014): “Any waste that contains organic or inorganic elements of compounds that may, owing to the inherent physical, chemical or toxicological characteristics of that waste, have a detrimental impact on health and the environment”.

Biological waste: Waste containing mostly natural organic materials such as cell cultures, animal/human tissues or blood, animal excrements, microbiological cultures etc.

2. Purpose

To manage radioactive waste in the research laboratory of Building G20 (Room G14) on the Potchefstroom campus of the North-West University to ensure the safety and health of the researchers (both staff and students) as well as to ensure that the environment is not contaminated by waste materials of a potential hazardous nature. This ensures compliance with the policy regarding the use of unsealed radioactive nuclides, which is subject to regulatory control in terms of the Hazardous Substance Act, 1973 (Act 15 of 1973).

3. Objective

To ensure safe handling, storage and removal of liquid and/or solid biological waste materials as well as needles and sharp waste generated in the research laboratories of Buildings G2, G16 and G20.

4. Scope

This SOP is applicable to the all research laboratories in buildings G2, G11 and G20 generating potentially hazardous liquid and/or solid biological and sharp waste waste materials.

5. Responsibilities

All staff and students working inside the research laboratories of buildings G2, G16 and G20 are responsible to follow the procedures outlined in this SOP. The safety officers are responsible for completion of documentation such as disposal request form, treatment request form, communication with the medical waste company (currently Oricol), as well as reporting any incidents to the Occupational Health and Safety Committee.

6. Apparatus and equipment

Apparatus/equipment	Location (Room No.)	Check points	Criteria for approval/rejection
Autoclave	LAMB (G14)	Preheat until jacket pressure and temperature reach minimum level to start an autoclave cycle	Autoclave must be serviced once a year, and Sterikon+ bio-indicator for check on autoclaving quality must be done quarterly
Hazardous waste containers	All research laboratories	Appropriately labelled	Correct label and container for waste type

7. List of other SOPs relevant to this SOP

None.

8. Safety measures

The following general safety measures should always be followed:

- All staff and students working in the research laboratories of buildings G2, G16 and G20 should familiarise themselves with the potential hazardousness and other safety aspects such as incompatibilities between chemicals or potential presence of pathogens in biological material before handling them.
- All staff and students must be appropriately trained in handling hazardous waste materials.
- Adherence to dress code: always wear a laboratory coat, gloves and, if the need arise, eye protective goggles or a face mask during handling of biological materials.
- All biological materials should be regarded as potentially hazardous and therefore be handled with care.

- Emergency post for eye washing should be available in all laboratories.
- Disinfect all needles, blades, loops and slides by autoclaving before discarding.
- Keep large enough bins for broken glass in the laboratory (store room).

9. Procedures

9.1 Waste containers

- 9.1.1 Only use waste containers supplied by the removal company that is compatible with the type of waste material.
- 9.1.2 Different types of waste containers shall be available for different types of waste as prescribed by the waste company which may include: biological waste – sharps/needles (plastic bucket with lid), biological waste – solids (box with red

liner), biological waste – liquid (plastic drum with screw lid), medical waste – solids, liquids and sludge (plastic drum with screw lid) (Please refer to Addendum A).

- 9.1.3 Containers shall be labeled correctly with all appropriate information: Site information include campus name, building number, room number and date, Waste information include full names and class of biological material as prescribed by the waste removal company before removal.
- 9.1.4 Containers must remain closed at all times (except when waste is added) and be sealed appropriately.
- 9.1.5 Containers must be kept clean and dry.
- 9.1.6 Containers for liquids must never be filled to the top to allow space for expansion (only fill to about 90% of container volume). Incompatible liquids are not allowed to be mixed in any waste container.

9.2 Contaminated sharps and needles

- 9.2.1 Place the sharps and needles in the designated waste bins provided by the waste removal company (yellow buckets).
- 9.2.2 No waste other than the sharps and needles shall be placed in these containers.
- 9.2.3 When the need arises for removal of the waste (e.g. container is full), the safety officer should be informed to complete a disposal request form and to notify the medical waste company (currently Oricol) according to the procedure described in Addendum A.

9.3 Biological materials and contaminated disposable items

- 9.3.1 Biological materials (e.g. tissue and blood) and contaminated disposable items (other than sharps and needles) are placed in the disposable red plastic bag that is placed inside the appropriate waste container and stored in the refrigerator in Room G14, Building G20.
- 9.3.2 When the need arises for removal of the waste (e.g. container is full), the safety officer should be informed to complete a disposal request form and to notify the medical waste company (currently Oricol) according to the procedure described in Addendum A.

9.4 Contaminated broken glassware

- 9.4.1 Place the broken glassware (after it has been decontaminated by autoclaving) in the designated bins for broken glass.
- 9.4.2 No other waste should be placed in this container.

10. Records and data sheets

There should be material safety data sheets (MSDS) available on all chemicals used in the specified laboratories.

Record the type and volume of waste disposed on record books placed next to the waste container.

All records (including copies of disposal request forms and treatment request forms) must be kept for 5 years at the North-West University by the safety officer.

11. Scheme of SOP development

Action	Designated person	Signature	Date
Compile	H. Netsimbupfe		2015/09/03
Compile	C. Gouws		2016/06/30

Addendum A:

ADDENDUM A: "Chemical, pharmaceutical and medical waste procedure"

Chemical, pharmaceutical and medical waste procedure

Aim

To control and manage the booking, collecting, handling and disposal of all chemical, pharmaceutical and medical waste originating from clients. To prevent incompatible chemicals being stored and transported together.

Scope

This procedure applies to all Oricol and client personnel requesting the assistance of Oricol staff in the disposal of chemical, pharmaceutical and medical waste.

Responsibility

- Oricol contract manager and/or sales representative
- Oricol drivers and assistants
- Client
- Booking clerk
- Hazardous waste clerk
- Logistics management

Method

Client responsibility

Chemical waste

- When the need to dispose of chemical waste arises, a TRF (treatment request form) must be completed and sent to the Oricol contract manager or sales representative. An example of a TRF can be seen in Appendix A and should be in Word format where possible.
- Campus name, Building number, building name and room number and date must be completed in full in order to ensure that the waste is collected from the right site.
- Chemical names must be written out in full on the TRF and the storage containers and no abbreviations or chemical formulas may be used (i.e. "Ether" instead of "Et2O and "Dimethylphosphinoethane" instead of "DMPE").
- A separate TRF must be completed for the following chemicals and/or their compounds as the incinerator is not permitted to accept and incinerate them. These will be collected and disposed of separately at the hazardous waste landfill:
 - Arsenic (As)
 - Astatine (At)
 - Cadmium (Cd)
 - Chromium (Cr)
 - Cesium (Cs)
 - Cyanide(CN)
 - Francium (Fr)
 - Iodine (I)
 - Krypton (Kr)
 - Lead (Pb)
 - Mercury (Hg)
 - Nickel (Ni)
 - Phosphorous (P)
 - Rubidium (Rb)
 - Selenium (Se)

Last printed	Date	Document Writer	Authorised By	Doc Rev No	Page No.
12/06/2014 3:31 PM	03/01/2012	Paul Eloff	Peter Allen	6	1 of 7

Once printed this document is an uncontrolled version and should be checked against the electronic version for validity.
 Document: Procedure

Chemical, pharmaceutical and medical waste procedure

- The UN number and class of the chemicals must also be completed. The chemicals must then be grouped together in the following classes. Should the container be a mixture of chemicals, the highest concentration constituent applies:
 - Class 3 (Flammable Liquids); 4.1 (Flammable Solids); 4.2 (Spontaneously Combustible material); 4.3 (Dangerous when Wet material); 8.2 (Alkalis) and 9. (Miscellaneous materials not classified). A **GREEN** sticker must be placed on the box or container.
Examples: Acetone, Magnesium, white phosphorous, sodium hydroxide, calcium
 - Class 6.1 (Toxic Substances). A **RED** sticker must be placed on the box or container
Examples: Potassium cyanide, mercuric chloride
 - Class 5.1 (Oxidizing Agents) and 8.1. (Acids). A **ORANGE** sticker must be placed on the box or container
Examples: Calcium hypochlorite, ammonium nitrate, hydrogen peroxide
 - Class 5.2 (Organic Peroxides) must be grouped separately and a **BLUE** sticker must be placed on the box or container. These chemicals will be transported with Class 5.1(Oxidizing Agents) and 8.1. (Acids).
Examples: benzoyl peroxides, cumene hydroperoxide, hydrochloric acid.

(Note: no collection will take place if chemicals aren't identified by means of a colour coded sticker & class)

- Each grouped class will be collected on different days/loads to ensure legal compliance.
- All chemical containers must be properly sealed. The bottle or jar must have a cap that fits tightly. If the chemical is a liquid, there must be at least 3 cm of room at the top of the container. The outside of the container must be clean and dry.
(Note: Chemicals shall not be removed if they are in leaking or otherwise inappropriate containers)
- The chemical, pharmaceutical and medical waste that needs to be disposed of, must be kept until your TRF or DRF has been returned by Oricol indicating service date and reference number.
- When the need to dispose of medical or pharmaceutical waste, a DRF (disposal request form) must be completed and sent to the Oricol contract manager or sales representative. An example of a DRF can be seen in Appendix B and should be in Word format where possible.
- On the day of collection, all chemical, pharmaceutical and medical waste needs to be at a centralised area at the collection point. A customer copy of the TRF/DRF must be placed with the waste. This TRF/DRF will have a unique number. A TRF/DRF that has not got a unique number on that matches Oricol's TRF/DRF will not be collected
- This is important as the collection staff will use this TRF/DRF to match up the TRF/DRF that was received to ensure the correct waste is removed.

Last printed	Date	Document Writer	Authorised By	Doc Rev No	Page No.
12/06/2014 3:31 PM	03/01/2012	Paul Eloff	Peter Allen	6	2 of 7

Once printed this document is an uncontrolled version and should be checked against the electronic version for validity.
Document: Procedure

Chemical, pharmaceutical and medical waste procedure

- Medical waste containers must be properly sealed. Bio-hazardous tape must be used in the case of medical waste boxes.
- The maximum weights for containers are shown below. Under no circumstances must the weight of the containers exceed the maximum weight.

<i>Container</i>	<i>Maximum allowed weight in kg</i>
5L Sharps and Lids (Needles Ect)	2.5
10L Sharps and Lids (Needles Ect)	3.5
20L Sharps and Lids (Needles Ect)	8
5L Anatomical Waste	2.5
10L Anatomical Waste	5
20L Anatomical Waste	12
20L Pharmaceutical waste	12
50L Box & Liner	9
142L Box & Liner	15

Bookings (For Oricol ES use only)

- The sales representative or Oricol contract manager will forward the TRF/DRF received from the client to the Hazardous Waste Clerk to generate a unique number.
- In the case of TRF's, a quote will be requested from the disposal site by the hazardous waste clerk.
- Once the disposal site sent the quote, the Hazardous waste clerk will reply with an acceptance form to the disposal site.
- The Hazardous waste clerk will make a booking with the Booking clerk. More than one booking shall be made if the TRF contains more than one group of classes. The Booking Clerk will complete the booking ref number and service date on the TRF/DRF and send it to the Hazardous waste Clerk.
- The Hazardous waste clerk will print out the TRF/DRF with the reference number and service date and prepare the stock.
- The Hazardous waste clerk will request delivery notes on daily basis from the logistics department which he will then use to match up with the TRF's/DRF's. Special care must be taken to ensure the waste type is correct and reflects the classes for collection.
- The Bookings waste clerk will then communicate the service date and reference number to the sales representative or Oricol contract manager which in turn needs to communicate this information with the client.

Collection and Handling (For Oricol ES use only)

- The collection staff will take the crates and a trolley with to ease loading and offloading of the waste
- When arriving at the site, the collection staff will confirm the TRF/DRF corresponds to the client's DRF/TRF. They will only check that the TRF/DRF is the same and not check each chemical item for item. It is still the client's responsibility to supply them with the correct waste.
- The collections staff will confirm containers are labelled sealed and have no residue.
- Oricol staff will not remove any waste that does not conform.

Last printed	Date	Document Writer	Authorised By	Doc Rev No	Page No.
12/06/2014 3:31 PM	03/01/2012	Paul Eloff	Peter Allen	6	3 of 7

Once printed this document is an uncontrolled version and should be checked against the electronic version for validity.
 Document: Procedure

Chemical, pharmaceutical and medical waste procedure

- In the case of chemical waste, collection staff will collect chemicals as per the delivery note instruction of which colour to collect
- The client will then sign the delivery note to confirm collection. Should there be no one to sign for the collection; the waste will not be removed.
- The crate must then be sealed and the trolley used to transport the waste to the vehicle. When arriving at the vehicle, the boxes will be offloaded and placed inside the vehicle for chemical waste.
- In the case of medical waste, the trolley must be used to transport the containers or boxes to the vehicle.
- The waste will then be transported and disposed of at the appropriate disposal site.

Last printed	Date	Document Writer	Authorised By	Doc Rev No	Page No.
12/06/2014 3:31 PM	03/01/2012	Paul Eloff	Peter Allen	6	4 of 7

Once printed this document is an uncontrolled version and should be checked against the electronic version for validity.
Document: Procedure



**Chemical, pharmaceutical and medical waste procedure
Disposal Request Form (DRF) for medical and pharmaceutical waste**

Generator Details				Waste Management Details		
Company Name	Account Number			Oricol environmental Services		
Contact Person	Department			JUAN-MARI DAVIES		
Cell Number	Campus, Building Name, Room No:			083 305 4526		
Tel Number				011 9225900		
Fax Number				011 922 5901		
Email Address				Juan-Marimari.davies@oricol.co.za		
*Booking can only be made once this form has been completed in full.				16 Vuurstag, Spartan ext7, Kempton park		
Date booking made (Completed by Client):				Service date: (Completed by booking clerk):		
Booking Reference number (Completed by booking clerk):						

Item No.	Product Name, Container Capacity and Type	Number of Containers	PLEASE TICK ✓			Estimated Quantity
			EXCHANGE	REMOVE	PLACEMENT	

Last printed	Date	Document Writer	Authorised By	Doc Rev No	Page No.
12/06/2014 3:31 PM	03/01/2012	Paul Eloff	Peter Allen	6	6 of 7

Once printed this document is an uncontrolled version and should be checked against the electronic version for validity.
Document: Procedure

Chemical, pharmaceutical and medical waste procedure

Revision Notes		
Date	Rev: No	Notes
26 January 2012	02	Added dangerous good load compatibility chart
24 September 2012	03	Added medical waste to procedure
9 October 2012	04	Added Account number and Site
31 January 2013	05	Update TRF document in landscape mode
23 May 2013	06	Update of collecting and packing of chemicals
22 October 2013	07	Update of classifying and packing
11 June 2014	08	Update checking of TRF/DRF

Last printed	Date	Document Writer	Authorised By	Doc Rev No	Page No.
12/06/2014 3:31 PM	03/01/2012	Paul Eloff	Peter Allen	6	7 of 7

Once printed this document is an uncontrolled version and should be checked against the electronic version for validity.
Document: Procedure

ADDENDUM B

ETHICS APPROVAL



Private Bag X1290, Potchefstroom
South Africa 2520

Tel: 086 016 9698
Web: <http://www.nwu.ac.za/>

North-West University Animal Care, Health and Safety Research Ethics Committee (NWU-AnimCareREC)

Tel: 018 299-1208
Email: Ethics-AnimCare@nwu.ac.za (for animal studies)

27 October 2019

ETHICS APPROVAL LETTER OF STUDY

Based on approval by the North-West University Animal Care, Health and Safety Research Ethics Committee (NWU-AnimCareREC) on 27/10/2019, the NWU-AnimCareREC hereby approves your study as indicated below. This implies that the NWU-AnimCareREC grants its permission that, provided the general conditions specified below are met and pending any other authorisation that may be necessary, the study may be initiated, using the ethics number below.

Study title: Development of a mini-tablet-in-capsule dosage form for macromolecular drug delivery																															
Principal Investigator/Study Supervisor/Researcher: Prof JH Steenekamp																															
Student: L Bodenstein - 22784136																															
Ethics number:	<table border="1"><tr><td>N</td><td>W</td><td>U</td><td>-</td><td>0</td><td>0</td><td>5</td><td>7</td><td>9</td><td>-</td><td>1</td><td>9</td><td>-</td><td>A</td><td>5</td></tr><tr><td colspan="3">Institution</td><td colspan="5">Study Number</td><td colspan="2">Year</td><td colspan="5">Status</td></tr></table>	N	W	U	-	0	0	5	7	9	-	1	9	-	A	5	Institution			Study Number					Year		Status				
N	W	U	-	0	0	5	7	9	-	1	9	-	A	5																	
Institution			Study Number					Year		Status																					
<i>Status:</i> S = Submission; R = Re-Submission; P = Provisional Authorisation; A = Authorisation																															
Application Type: Single study	Risk: <table border="1"><tr><td>Category 0</td></tr></table>	Category 0																													
Category 0																															
Commencement date: 27/10/2019																															
Expiry date: 30/10/2020																															
Approval of the study is provided for a year, after which continuation of the study is dependent on receipt and review of an annual monitoring report and the concomitant issuing of a letter of continuation. A monitoring report is due at the end of October annually until completion.																															

General conditions:
<i>While this ethics approval is subject to all declarations, undertakings and agreements incorporated and signed in the application form, the following general terms and conditions will apply:</i>
<ul style="list-style-type: none">• <i>The principal investigator/study supervisor/researcher must report in the prescribed format to the NWU-AnimCareREC:</i><ul style="list-style-type: none">– <i>Annually on the monitoring of the study, whereby a letter of continuation will be provided annually, and upon completion of the study; and</i>– <i>without any delay in case of any adverse event or incident (or any matter that interrupts sound ethical principles) during the course of the study.</i>• <i>The approval applies strictly to the proposal as stipulated in the application form. Should any amendments to the proposal be deemed necessary during the course of the study, the principal investigator/study supervisor/researcher must apply for approval of these amendments at the NWU-AnimCareREC, prior to implementation. Should there be any deviations from the study proposal without the necessary approval of such amendments, the ethics approval is immediately and automatically forfeited.</i>

- *Annually a number of studies may be randomly selected for active monitoring.*
- *The date of approval indicates the first date that the study may be started.*
- *In the interest of ethical responsibility, the NWU-AnimCareREC reserves the right to:*
 - *request access to any information or data at any time during the course or after completion of the study;*
 - *to ask further questions, seek additional information, require further modification or monitor the conduct of your research or the informed consent process;*
 - *withdraw or postpone approval if:*
 - *any unethical principles or practices of the study are revealed or suspected;*
 - *it becomes apparent that any relevant information was withheld from the NWU-AnimCareREC or that information has been false or misrepresented;*
 - *submission of the annual monitoring report, the required amendments, or reporting of adverse events or incidents was not done in a timely manner and accurately; and/or*
 - *new institutional rules, national legislation or international conventions deem it necessary.*
- *NWU-AnimCareREC can be contacted for further information via Ethics-AnimCare@nwu.ac.za or 018 299 1208*

NWU-AnimCareREC would like to remain at your service and wishes you well with your study. Please do not hesitate to contact the NWU-AnimCareREC for any further enquiries or requests for assistance.

Yours sincerely,

Chairperson: NWU-AnimCareREC

Current details:(23239522) G:\My Drive\9. Research and Postgraduate Education\9.1.5.4 Templates\9.1.5.4.2_NWU-AC_EAL.docm
20 August 2019

File Reference: 9.1.5.4.2

ADDENDUM C

ALOE VERA LEAF MATERIALS $^1\text{H-NMR}$ SPECTRA

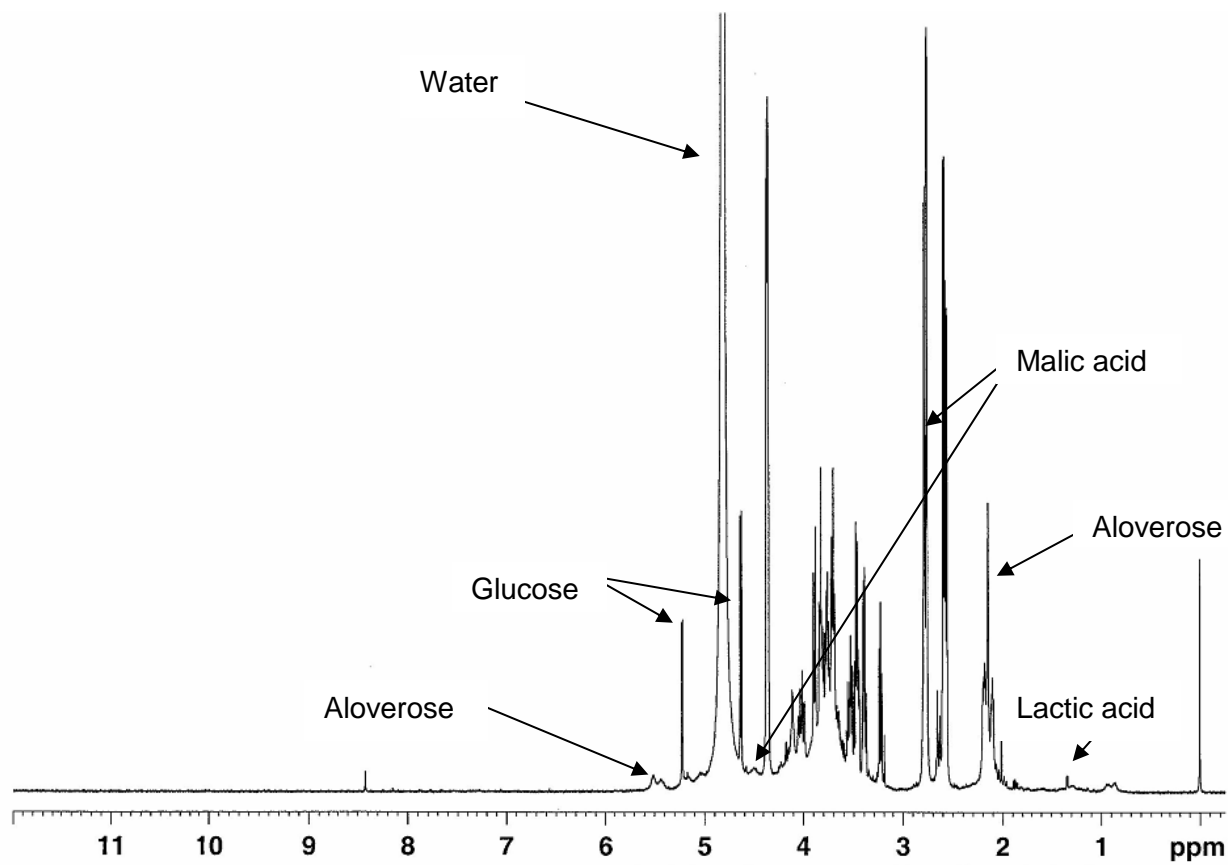


Figure C1: $^1\text{H-NMR}$ spectrum of *Aloe vera* gel (Daltonmax)

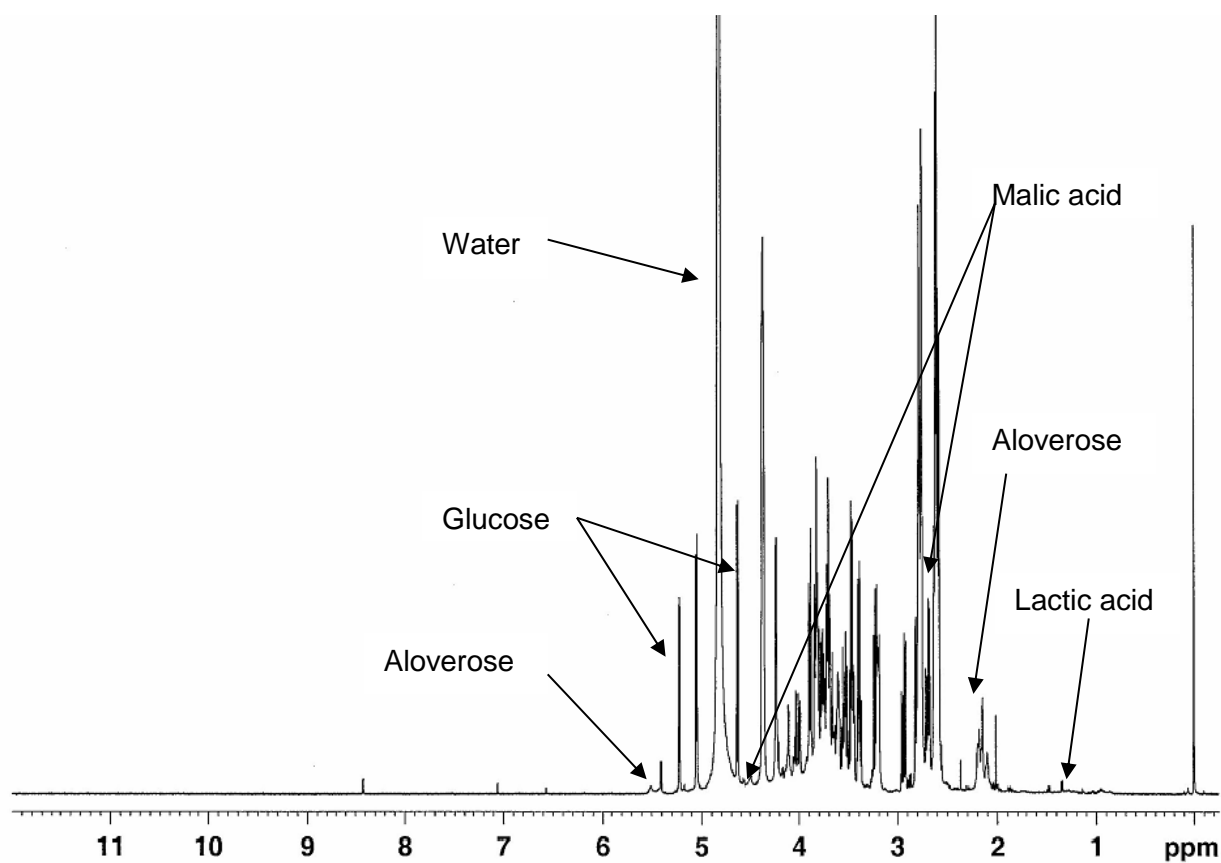


Figure C2: ¹H-NMR spectrum of *Aloe vera* whole leaf (Daltonmax)

ADDENDUM D

TMC $^1\text{H-NMR}$ SPECTRUM

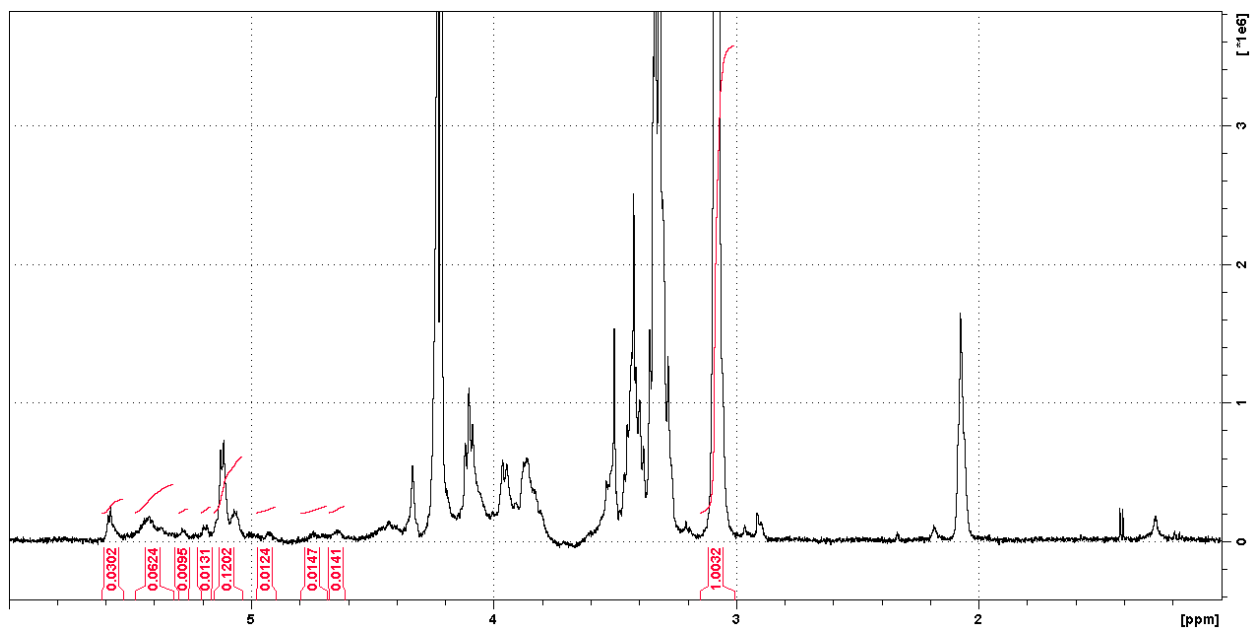


Figure D1: $^1\text{H-NMR}$ spectrum of TMC (Daltonmax)

ADDENDUM E

SPHERONISATION PROCESS



Figure E1: Side view of extruder pushing the wetted powder mass through the sieve



Figure E2: Spaghetti-like extrudate



Figure E3: Front view of the extruder producing spaghetti like extrudate

ADDENDUM F

EXPERIMENTAL DATA

Validation: Specificity

Table F1: Table showing the experimental data from the specificity test. The specificity suspension contains FD4, Pharmacel[®] 101, Kollidon[®] VA 64, Ac-di-sol[®], Avicel[®] PH 200, magnesium stearate, *Aloe vera* gel and whole leaf extract and TMC.

Specificity suspension	
Concentration (µg/ml)	Fluorescence - Background noise
6.25	120198332.00
3.125	57062490.00
1.56	26084754.50
0.781	12472029.00
0.39	6051044.75
0.195	2947736.50
0.097	1396611.25
0.0488	835794.00

Dissolution studies

Table F2: Dissolution of mini-tablet-in-capsule formulations containing 0.5 mm beads with FITC-dextran 4000 (control)

Time (min)	% Dissolution			Average	STDEV
	1	2	3		
0	0	0	0	0	0
5	2.35	2.46	2.42	2.41	0.054
10	15.12	15.23	15.25	15.20	0.069
15	59.33	60.35	62.27	60.65	1.492
30	71.42	72.35	73.91	72.56	1.256
60	78.99	79.57	81.48	80.02	1.304
90	84.78	85.70	86.54	85.67	0.882
120	89.91	90.45	91.75	90.70	0.945
150	93.51	93.36	94.74	93.87	0.758
180	96.08	96.00	96.95	96.34	0.528
240	97.43	97.41	98.64	97.83	0.707

Table F3: Dissolution of mini-tablet-in-capsule formulations containing 0.5 mm beads with FITC-dextran 4000 and *Aloe vera* gel (AVG)

Time (min)	% Dissolution			Average	STDEV
	1	2	3		
0	0	0	0	0	0
5	1.78	1.80	1.79	1.79	0.010
10	10.28	10.71	10.35	10.44	0.230
15	48.31	49.56	47.46	48.44	1.060
30	65.57	64.15	65.61	65.11	0.830
60	73.14	74.50	75.74	74.46	1.300
90	82.56	82.57	84.63	83.25	1.190
120	89.64	90.84	92.08	90.85	1.220
150	95.04	95.25	95.76	95.35	0.370
180	98.66	98.45	98.26	98.46	0.200
240	99.55	99.65	99.39	99.53	0.130

Table F4: Dissolution of mini-tablet-in-capsule formulations containing 0.5 mm beads with FITC-dextran 4000 and *Aloe vera* whole leaf extract (AVW)

Time (min)	% Dissolution			Average	STDEV
	1	2	3		
0	0	0	0	0	0
5	1.94	1.92	1.88	1.91	0.027
10	9.03	9.44	9.38	9.28	0.219
15	24.51	25.19	23.30	24.33	0.960
30	65.14	66.07	69.44	66.88	2.264
60	74.54	75.26	76.71	75.50	1.108
90	79.35	80.28	82.02	80.55	1.358
120	84.20	85.80	86.70	85.57	1.262
150	90.06	90.72	91.85	90.88	0.904
180	95.53	93.67	95.75	94.98	1.140
240	97.34	96.06	98.00	97.13	0.985

Table F5: Dissolution of mini-tablet-in-capsule formulations containing 0.5 mm beads with FITC-dextran 4000 and *N*-trimethyl chitosan chloride (TMC)

Time (min)	% Dissolution			Average	STDEV
	1	2	3		
0	0	0	0	0	0
5	0.68	0.75	0.71	0.71	0.034
10	15.47	15.31	14.40	15.06	0.577
15	54.94	55.09	54.39	54.81	0.373
30	72.46	71.19	71.01	71.55	0.792
60	77.50	78.34	78.84	78.23	0.677
90	84.77	84.54	84.95	84.76	0.206
120	89.64	89.67	91.35	90.22	0.979
150	92.52	92.44	92.36	92.44	0.078
180	95.66	94.71	95.20	95.19	0.474
240	97.22	97.40	98.29	97.63	0.573

Table F6: Dissolution of mini-tablet-in-capsule formulations containing 0.75 mm beads with FITC-dextran 4000 (control)

Time (min)	% Dissolution			Average	STDEV
	1	2	3		
0	0	0	0	0	0
5	3.19	3.15	3.14	3.16	0.026
10	5.25	5.20	5.23	5.23	0.023
15	25.57	25.45	25.98	25.67	0.279
30	72.95	72.13	69.69	71.59	1.695
60	86.04	84.39	84.32	84.92	0.975
90	89.02	87.43	88.12	88.19	0.796
120	92.32	91.21	91.18	91.57	0.648
150	95.64	94.99	94.76	95.13	0.456
180	99.43	97.54	97.46	98.14	1.113
240	99.58	98.21	97.92	98.57	0.886

Table F7: Dissolution of mini-tablet-in-capsule formulations containing 0.75 mm beads with FITC-dextran 4000 and *Aloe vera* gel (AVG)

Time (min)	% Dissolution			Average	STDEV
	1	2	3		
0	0	0	0	0	0
5	3.36	3.36	3.38	3.37	0.014
10	12.00	12.11	12.30	12.14	0.154
15	28.89	28.96	29.26	29.04	0.200
30	58.98	59.20	60.63	59.60	0.894
60	67.29	67.72	69.01	68.01	0.899
90	71.83	72.53	74.22	72.86	1.229
120	81.33	82.94	84.89	83.05	1.781
150	89.64	89.73	91.37	90.25	0.976
180	94.17	94.18	95.30	94.55	0.645
240	99.10	98.59	98.65	98.78	0.278

Table F8: Dissolution of mini-tablet-in-capsule formulations containing 0.75 mm beads with FITC-dextran 4000 and *Aloe vera* whole leaf extract (AVW)

Time (min)	% Dissolution			Average	STDEV
	1	2	3		
0	0	0	0	0	0
5	0.00	0.00	0.00	0.00	0.000
10	3.82	3.93	3.86	3.87	0.059
15	21.27	21.73	22.54	21.85	0.642
30	56.18	57.98	59.11	57.76	1.475
60	70.88	71.58	73.27	71.91	1.228
90	77.09	77.70	78.81	77.87	0.871
120	81.39	82.83	82.75	82.32	0.810
150	87.22	88.71	88.44	88.12	0.796
180	92.06	93.35	93.78	93.06	0.893
240	98.78	99.87	99.80	99.48	0.612

Table F9: Dissolution of mini-tablet-in-capsule formulations containing 0.75 mm beads with FITC-dextran 4000 and *N*-trimethyl chitosan chloride (TMC)

Time (min)	% Dissolution			Average	STDEV
	1	2	3		
0	0	0	0	0	0
5	1.01	0.99	0.97	0.99	0.016
10	29.07	28.47	31.53	29.69	1.624
15	47.16	45.69	48.06	46.97	1.194
30	67.56	65.47	67.53	66.85	1.199
60	81.32	80.17	80.86	80.78	0.578
90	86.62	86.13	87.92	86.89	0.923
120	89.94	89.88	90.89	90.24	0.566
150	94.21	92.74	93.66	93.54	0.741
180	95.81	96.09	95.37	95.76	0.361
240	97.16	97.25	96.67	97.02	0.312

Table F10: Dissolution of mini-tablet-in-capsule formulations containing 1.0 mm beads with FITC-dextran 4000 (control)

Time (min)	% Dissolution			Average	STDEV
	1	2	3		
0	0	0	0	0	0
5	8.90	8.49	8.62	8.67	0.211
10	50.55	50.24	49.04	49.95	0.798
15	66.52	67.02	65.50	66.35	0.774
30	78.40	79.40	77.73	78.51	0.837
60	83.00	83.73	81.87	82.87	0.934
90	88.42	90.11	88.93	89.15	0.867
120	91.90	93.65	92.42	92.65	0.896
150	94.41	95.71	94.57	94.90	0.712
180	96.66	98.51	96.74	97.30	1.044
240	97.47	99.17	97.45	98.03	0.987

Table F11: Dissolution of mini-tablet-in-capsule formulations containing 1.0 mm beads with FITC-dextran 4000 and *Aloe vera* gel (AVG)

Time (min)	% Dissolution			Average	STDEV
	1	2	3		
0	0	0	0	0	0
5	0.40	0.40	0.42	0.40	0.010
10	7.39	7.22	7.66	7.42	0.224
15	41.18	41.45	44.73	42.45	1.980
30	62.83	63.52	65.55	63.97	1.414
60	71.50	71.28	73.01	71.93	0.942
90	75.70	75.22	77.32	76.08	1.101
120	81.46	81.34	83.06	81.95	0.959
150	88.54	88.79	90.45	89.26	1.039
180	92.57	91.80	93.67	92.68	0.940
240	98.94	97.82	99.45	98.74	0.833

Table F12: Dissolution of mini-tablet-in-capsule formulations containing 1.0 mm beads with FITC-dextran 4000 and *Aloe vera* whole leaf extract (AVW)

Time (min)	% Dissolution			Average	STDEV
	1	2	3		
0	0	0	0	0	0
5	1.66	1.69	1.65	1.67	0.022
10	4.89	5.06	5.07	5.01	0.099
15	9.68	9.85	9.85	9.79	0.101
30	61.26	62.45	62.90	62.20	0.845
60	69.37	71.11	70.98	70.48	0.968
90	75.21	75.84	76.43	75.82	0.613
120	80.69	84.31	83.52	82.84	1.904
150	85.86	87.68	87.26	86.93	0.954
180	88.94	91.16	90.32	90.14	1.120
240	99.66	99.14	97.97	98.92	0.869

Table F13: Dissolution of mini-tablet-in-capsule formulations containing 1.0 mm beads with FITC-dextran 4000 and *N*-trimethyl chitosan chloride (TMC)

Time (min)	% Dissolution			Average	STDEV
	1	2	3		
0	0	0	0	0	0
5	1.58	1.57	1.57	1.57	0.005
10	27.56	27.02	26.94	27.17	0.337
15	46.99	48.25	47.65	47.63	0.627
30	77.48	74.43	76.42	76.11	1.550
60	81.35	79.84	82.91	81.37	1.534
90	86.04	86.32	88.21	86.86	1.181
120	94.21	90.69	94.03	92.97	1.983
150	97.03	95.30	96.58	96.30	0.894
180	98.41	97.21	97.90	97.84	0.602
240	99.09	98.31	99.34	98.91	0.540

Table F14: Dissolution of mini-tablet-in-capsule formulations containing 1.5 mm beads with FITC-dextran 4000 (control)

Time (min)	% Dissolution			Average	STDEV
	1	2	3		
0	0	0	0	0	0
5	8.08	7.88	7.94	7.97	0.106
10	41.94	40.96	42.05	41.65	0.599
15	58.48	58.84	56.97	58.10	0.992
30	75.11	74.16	74.54	74.60	0.476
60	81.96	82.16	82.33	82.15	0.184
90	86.10	86.41	85.90	86.14	0.254
120	89.50	89.70	90.76	89.99	0.680
150	92.10	92.21	92.74	92.35	0.342
180	94.72	94.04	94.37	94.38	0.342
240	98.28	97.55	97.89	97.91	0.366

Table F15: Dissolution of mini-tablet-in-capsule formulations containing 1.5 mm beads with FITC-dextran 4000 and *Aloe vera* gel (AVG)

Time (min)	% Dissolution			Average	STDEV
	1	2	3		
0	0	0	0	0	0
5	2.01	2.06	2.04	2.04	0.024
10	10.28	10.54	10.71	10.51	0.217
15	34.98	36.30	35.49	35.59	0.665
30	62.08	62.43	64.20	62.90	1.137
60	70.14	71.26	72.24	71.21	1.047
90	76.96	78.30	79.33	78.20	1.187
120	83.84	84.25	84.90	84.33	0.534
150	88.17	88.07	90.03	88.76	1.104
180	92.71	93.42	94.47	93.53	0.886
240	98.34	99.08	99.49	98.97	0.584

Table F16: Dissolution of mini-tablet-in-capsule formulations containing 1.5 mm beads with FITC-dextran 4000 and *Aloe vera* whole leaf extract (AVW)

Time (min)	% Dissolution			Average	STDEV
	1	2	3		
0	0	0	0	0	0
5	2.39	2.37	2.47	2.41	0.053
10	5.47	5.58	5.90	5.65	0.226
15	16.35	16.62	17.30	16.76	0.492
30	61.36	63.13	65.58	63.36	2.121
60	70.45	70.10	74.43	71.66	2.405
90	77.26	78.03	81.08	78.79	2.020
120	81.62	81.85	85.37	82.95	2.101
150	87.28	88.08	92.34	89.23	2.722
180	91.94	92.16	95.83	93.31	2.185
240	96.60	96.88	98.80	97.42	1.198

Table F17: Dissolution of mini-tablet-in-capsule formulations containing 1.5 mm beads with FITC-dextran 4000 and *N*-trimethyl chitosan chloride (TMC)

Time (min)	% Dissolution			Average	STDEV
	1	2	3		
0	0	0	0	0	0
5	0.04	0.04	0.04	0.04	0.001
10	36.39	35.12	35.95	35.82	0.643
15	48.68	50.50	50.01	49.73	0.938
30	65.74	65.77	65.34	65.62	0.242
60	75.58	76.89	76.66	76.37	0.702
90	81.61	82.17	81.71	81.83	0.295
120	85.57	85.13	85.29	85.33	0.224
150	89.24	89.43	88.93	89.20	0.254
180	90.78	92.07	91.86	91.57	0.689
240	97.88	99.22	99.01	98.70	0.722

Ex vivo transport data

Table F18: Apical to basolateral transport of mini-tablet formulations containing 0.5 mm beads with FITC-dextran 4000 (control)

Time (min)	% Transport			Average	STDEV
	1	2	3		
0	0	0	0	0	0
20	0.03	0.03	0.00	0.02039	0.01513
40	0.20	0.08	0.04	0.10556	0.08419
60	0.35	0.18	0.09	0.2027	0.13221
80	0.40	0.25	0.12	0.25699	0.14226
100	0.45	0.28	0.16	0.29429	0.14599
120	0.47	0.30	0.16	0.3104	0.15931

Table F19: Apical to basolateral transport of mini-tablet formulations containing 0.5 mm beads with FITC-dextran 4000 and *Aloe vera* gel (AVG)

Time (min)	% Transport			Average	STDEV
	1	2	3		
0	0	0	0	0	0
20	0.01	0.01	0.01	0.01257	0.00026
40	0.34	0.34	0.34	0.33998	0.00365
60	1.10	1.14	1.14	1.12703	0.02192
80	2.21	2.20	2.23	2.21542	0.01469
100	3.17	3.29	3.31	3.25969	0.07497
120	4.17	4.12	4.11	4.13253	0.02948

Table F20: Apical to basolateral transport of mini-tablet formulations containing 0.5 mm beads with FITC-dextran 4000 and *Aloe vera* whole leaf extract (AVW)

Time (min)	% Transport			Average	STDEV
	1	2	3		
0	0	0	0	0	0
20	0.20	0.20	0.20	0.19753	0.00257
40	0.36	0.36	0.36	0.35882	0.00451
60	1.14	1.13	1.17	1.14601	0.01850
80	2.01	2.03	1.95	1.99617	0.04135
100	2.74	2.73	2.78	2.75069	0.02593
120	3.20	3.18	3.24	3.20607	0.03366

Table F21: Apical to basolateral transport of mini-tablet formulations containing 0.5 mm beads with FITC-dextran 4000 and *N*-trimethyl chitosan chloride (TMC)

Time (min)	% Transport			Average	STDEV
	1	2	3		
0	0	0	0	0	0
20	0.01	0.01	0.01	0.01379	0.00029
40	0.26	0.26	0.26	0.26078	0.00293
60	0.79	0.79	0.80	0.79012	0.00466
80	2.43	2.43	2.27	2.3778	0.09261
100	2.55	2.58	2.52	2.55193	0.02894
120	2.62	2.64	2.64	2.63215	0.01346

Table F22: Apical to basolateral transport of mini-tablet formulations containing 0.75 mm beads with FITC-dextran 4000 (control)

Time (min)	% Transport			Average	STDEV
	1	2	3		
0	0	0	0	0	0
20	0.03	0.01	0.02	0.02088	0.01222
40	0.05	0.07	0.05	0.05713	0.01327
60	0.08	0.08	0.08	0.08047	0.00190
80	0.11	0.13	0.11	0.11712	0.01274
100	0.13	0.13	0.13	0.13242	0.00151
120	0.13	0.14	0.14	0.13829	0.00426

Table F23: Apical to basolateral transport of mini-tablet formulations containing 0.75 mm beads with FITC-dextran 4000 and *Aloe vera* gel (AVG)

Time (min)	% Transport			Average	STDEV
	1	2	3		
0	0	0	0	0	0
20	0.05	0.05	0.05	0.05069	0.00403
40	0.13	0.03	0.02	0.05997	0.05733
60	0.62	0.61	0.64	0.6231	0.01493
80	1.55	1.53	1.51	1.53232	0.01905
100	3.29	3.16	3.24	3.23046	0.06587
120	3.98	3.89	3.89	3.91883	0.05297

Table F24: Apical to basolateral transport of mini-tablet formulations containing 0.75 mm beads with FITC-dextran 4000 and *Aloe vera* whole leaf extract (AVW)

Time (min)	% Transport			Average	STDEV
	1	2	3		
0	0	0	0	0	0
20	0.07	0.08	0.08	0.07838	0.00735
40	0.20	0.20	0.20	0.19963	0.00312
60	0.54	0.54	0.57	0.54879	0.01566
80	1.43	1.44	1.43	1.4358	0.00354
100	2.22	2.24	2.30	2.25446	0.04154
120	3.07	3.07	3.10	3.07865	0.01772

Table F25: Apical to basolateral transport of mini-tablet formulations containing 0.75 mm beads with FITC-dextran 4000 and *N*-trimethyl chitosan chloride (TMC)

Time (min)	% Transport			Average	STDEV
	1	2	3		
0	0	0	0	0	0
20	0.07	0.08	0.08	0.07651	0.00210
40	0.23	0.22	0.22	0.22673	0.00571
60	0.90	0.90	0.90	0.90013	0.00224
80	1.56	1.55	1.52	1.54725	0.02046
100	2.27	2.25	2.31	2.2753	0.02853
120	2.49	2.52	2.49	2.50024	0.02082

Table F26: Apical to basolateral transport of mini-tablet formulations containing 1.0 mm beads with FITC-dextran 4000 (control)

Time (min)	% Transport			Average	STDEV
	1	2	3		
0	0	0	0	0	0
20	0.01	0.02	0.02	0.01351	0.00507
40	0.03	0.04	0.04	0.03616	0.00744
60	0.09	0.07	0.07	0.07793	0.00662
80	0.11	0.09	0.08	0.09265	0.01174
100	0.15	0.12	0.11	0.12746	0.02295
120	0.18	0.13	0.13	0.14778	0.02855

Table F27: Apical to basolateral transport of mini-tablet formulations containing 1.0 mm beads with FITC-dextran 4000 and *Aloe vera* gel (AVG)

Time (min)	% Transport			Average	STDEV
	1	2	3		
0	0	0	0	0	0
20	0.03	0.03	0.03	0.02586	0.00054
40	0.11	0.10	0.01	0.0744	0.05618
60	0.44	0.44	0.44	0.44115	0.00047
80	1.24	1.24	1.25	1.24326	0.00759
100	2.63	2.63	2.51	2.58938	0.07094
120	3.81	3.81	3.74	3.7864	0.04246

Table F28: Apical to basolateral transport of mini-tablet formulations containing 1.0 mm beads with FITC-dextran 4000 and *Aloe vera* whole leaf extract (AVW)

Time (min)	% Transport			Average	STDEV
	1	2	3		
0	0	0	0	0	0
20	0.01	0.01	0.01	0.01249	0.00065
40	0.08	0.08	0.08	0.08168	0.00180
60	0.70	0.68	0.67	0.68427	0.01642
80	1.37	1.35	1.37	1.36196	0.00868
100	1.99	2.03	2.03	2.01663	0.02365
120	2.85	2.93	2.92	2.89964	0.04698

Table F29: Apical to basolateral transport of mini-tablet formulations containing 1.0 mm beads with FITC-dextran 4000 and *N*-trimethyl chitosan chloride (TMC)

Time (min)	% Transport			Average	STDEV
	1	2	3		
0	0	0	0	0	0
20	0.04	0.04	0.04	0.03862	0.00084
40	0.20	0.21	0.20	0.20547	0.00476
60	0.67	0.66	0.65	0.65824	0.00933
80	1.37	1.36	1.34	1.35591	0.01483
100	2.22	2.22	2.21	2.21579	0.00135
120	2.50	2.49	2.49	2.4923	0.00421

Table F30: Apical to basolateral transport of mini-tablet formulations containing 1.5 mm beads with FITC-dextran 4000 (control)

Time (min)	% Transport			Average	STDEV
	1	2	3		
0	0	0	0	0	0
20	0.03	0.04	0.04	0.03506	0.00871
40	0.04	0.04	0.05	0.04535	0.00587
60	0.06	0.04	0.06	0.05227	0.01024
80	0.06	0.04	0.06	0.05649	0.01164
100	0.07	0.05	0.07	0.06303	0.01372
120	0.09	0.05	0.07	0.07172	0.01710

Table F31: Apical to basolateral transport of mini-tablet formulations containing 1.5 mm beads with FITC-dextran 4000 and *Aloe vera* gel (AVG)

Time (min)	% Transport			Average	STDEV
	1	2	3		
0	0	0	0	0	0
20	0.02	0.02	0.02	0.02083	0.00097
40	0.08	0.08	0.08	0.08258	0.00065
60	0.40	0.38	0.38	0.38577	0.00927
80	1.16	1.17	1.17	1.16499	0.00776
100	2.59	2.61	2.58	2.59332	0.01304
120	3.71	3.69	3.64	3.68201	0.03591

Table F32: Apical to basolateral transport of mini-tablet formulations containing 1.5 mm beads with FITC-dextran 4000 and *Aloe vera* whole leaf extract (AVW)

Time (min)	% Transport			Average	STDEV
	1	2	3		
0	0	0	0	0	0
20	0.01	0.01	0.01	0.00931	0.00036
40	0.08	0.08	0.08	0.07767	0.00102
60	0.69	0.68	0.66	0.67963	0.01455
80	1.19	1.19	1.16	1.18098	0.01968
100	1.92	1.90	1.87	1.89829	0.02669
120	2.76	2.72	2.66	2.71326	0.04740

Table F33: Apical to basolateral transport of mini-tablet formulations containing 1.5 mm beads with FITC-dextran 4000 and *N*-trimethyl chitosan chloride (TMC)

Time (min)	% Transport			Average	STDEV
	1	2	3		
0	0	0	0	0	0
20	0.01	0.01	0.01	0.00964	0.00052
40	0.20	0.19	0.19	0.19292	0.00222
60	0.57	0.53	0.53	0.54374	0.02652
80	1.42	1.47	1.41	1.43377	0.03172
100	2.10	2.19	2.13	2.13927	0.05006
120	2.34	2.37	2.38	2.36351	0.02277

ADDENDUM G

STATISTICAL ANALYSIS DATA

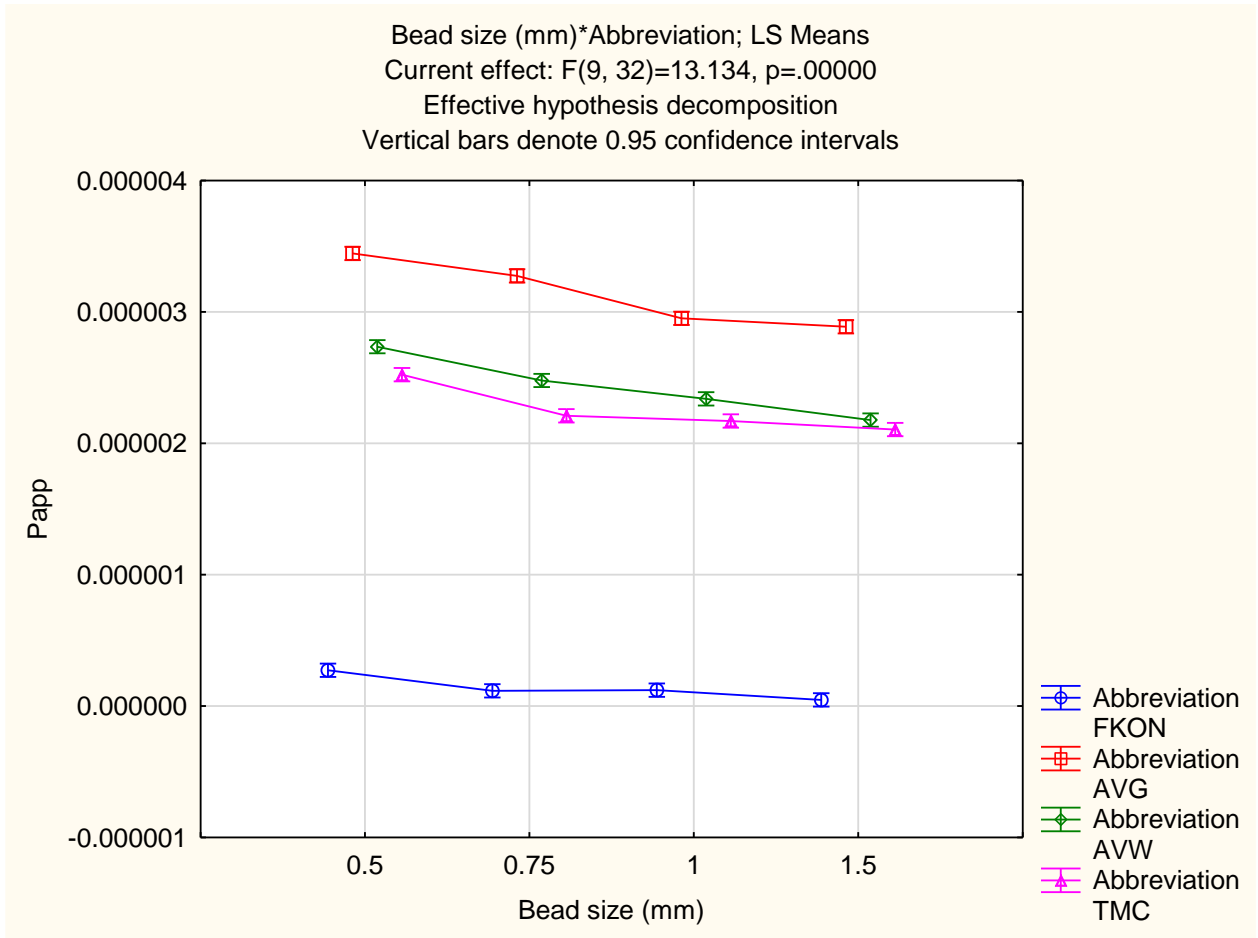


Figure G1: Statistical significance of different sized bead containing mini-tablets

Effect	Univariate Tests of Significance for Papp (L.Bodenstein_Stats_1) Sigma-restricted parameterization Effective hypothesis decomposition				
	SS	Degr. of Freedom	MS	F	p
Intercept	0.000000	1	0.000000	102126.2	0.000000
Bead size (mm)	0.000000	3	0.000000	233.6	0.000000
Abbreviation	0.000000	3	0.000000	10758.1	0.000000
Bead size (mm)*Abbreviation	0.000000	9	0.000000	13.1	0.000000
Error	0.000000	32	0.000000		

Cell No.	Bead size (mm)*Abbreviation; LS Means (L.Bodenstein_Stats_1) Current effect: F(9, 32)=13.134, p=.00000 Effective hypothesis decomposition						
	Bead size (mm)	Abbreviation	Papp Mean	Papp Std.Err.	Papp -95.00%	Papp +95.00%	N
1	0.5	FKON	0.000000	0.000000	0.000000	0.000000	3
2	0.5	AVG	0.000003	0.000000	0.000003	0.000003	3
3	0.5	AVW	0.000003	0.000000	0.000003	0.000003	3
4	0.5	TMC	0.000003	0.000000	0.000002	0.000003	3
5	0.75	FKON	0.000000	0.000000	0.000000	0.000000	3
6	0.75	AVG	0.000003	0.000000	0.000003	0.000003	3
7	0.75	AVW	0.000002	0.000000	0.000002	0.000003	3
8	0.75	TMC	0.000002	0.000000	0.000002	0.000002	3
9	1	FKON	0.000000	0.000000	0.000000	0.000000	3
10	1	AVG	0.000003	0.000000	0.000003	0.000003	3
11	1	AVW	0.000002	0.000000	0.000002	0.000002	3
12	1	TMC	0.000002	0.000000	0.000002	0.000002	3
13	1.5	FKON	0.000000	0.000000	-0.000000	0.000000	3
14	1.5	AVG	0.000003	0.000000	0.000003	0.000003	3
15	1.5	AVW	0.000002	0.000000	0.000002	0.000002	3
16	1.5	TMC	0.000002	0.000000	0.000002	0.000002	3

Cell No.	Tukey HSD test; variable Papp (L.Bodenstein_Stats_1) Homogenous Groups, alpha = .05000 (Non-Exhaustive Search) Error: Between MS = .00000, df = 32.000									
	Bead size (mm)	Abbreviation	Papp Mean	1	2	3	4	5	6	7
13	1.5	FKON	0.000000	****						
5	0.75	FKON	0.000000	****						
9	1	FKON	0.000000	****						
1	0.5	FKON	0.000000		****					
16	1.5	TMC	0.000002			****				
12	1	TMC	0.000002			****				
15	1.5	AVW	0.000002			****				
8	0.75	TMC	0.000002			****	****			
11	1	AVW	0.000002				****			
7	0.75	AVW	0.000002					****		
4	0.5	TMC	0.000003					****		
3	0.5	AVW	0.000003						****	
14	1.5	AVG	0.000003							****
10	1	AVG	0.000003							****
6	0.75	AVG	0.000003							
2	0.5	AVG	0.000003							

Cell No.	Tukey HSD test; variable Papp (L.Bodenstein_Stats_1) Homogenous Groups, alpha = .05000 (Non-Exhaustive Search) Error: Between MS = .00000, df = 32.000	
	8	9
13		
5		
9		
1		
16		
12		
15		
8		
11		
7		
4		
3		
14		
10		
6	****	
2		****